2009-07-22

Respiratory Syncytial Virus (RSV) Induces Innate Immunity through Toll-Like Receptors and Acquired Immunity via the RSV G Protein: A Dissertation

Matthew R. Murawski
University of Massachusetts Medical School

Respiratory Syncytial Virus (RSV) induces innate immunity through Toll-like Receptors and acquired immunity via the RSV G protein

A Dissertation Presented

By

Matthew R. Murawski

Submitted to the Faculty of the

University of Massachusetts Graduate School of Biomedical Sciences, Worcester

in partial fulfillment of the requirements for the degree of

DOCTOR OF PHILOSOPHY

July 22nd, 2009

Immunology and Virology Program

Respiratory Syncytial Virus (RSV) induces innate immunity through Toll-like Receptors and acquired immunity via the RSV G protein

A Dissertation Presented
By

Matthew R. Murawski

The signatures of the Dissertation Defense Committee signifies completion and approval as to style and content of the Dissertation

Robert Finberg, M.D., Thesis Advisor

Evelyn Kurt-Jones, Ph.D, Member of Committee

Egil Lien, Ph.D., Member of Committee

Stefanie Vogel, Ph.D., Member of Committee

Raymond Welsh, Ph.D., Member of Committee

The signature of the Chair of the Committee signifies that the written dissertation meets the requirements of the Dissertation Committee

Dale Greiner, Ph.D., Chair of Committee

The signature of the Dean of the Graduate School of Biomedical Sciences signifies that the student has met all graduation requirements of the school.

Anthony Carruthers, Ph.D.,
Dean of the Graduate School of Biomedical Sciences

Immunology and Virology Program
July 22nd, 2009

Copyright Information

The chapters of this dissertation have appeared in the following publications/manuscripts:

Matthew R. Murawski, Glennice N. Bowen, Anna M. Cerny, Larry J. Anderson, Lia M. Haynes, Ralph A. Tripp, Evelyn A. Kurt-Jones, and Robert W. Finberg. 2009. *Respiratory Syncytial Virus Activates Innate Immunity through Toll-Like Receptor 2*. J. Virol. Feb; 83 (3): 1492-1500.

Matthew R. Murawski*, Lori W. McGinnes*, Robert W. Finberg, Evelyn A. Kurt-Jones, Michael J. Massare, Gale Smith, Penny M. Heaton, Armando E. Fraire, and Trudy G. Morrison. * These authors contributed equally. Newcastle Disease Virus-Like Particles Containing Respiratory Syncytial Virus (RSV) G protein Induced Protection in BALB/c Mice With No Evidence of Immunopathology. J. Virol. In revision.

Upregulation of Foxp3 expression in mouse and human Treg is IL-2/STAT5 dependent: implications for the NOD STAT5B mutation in diabetes pathogenesis. MATTHEW R. MURAWSKI, SALLY A. LITHERLAND, MICHAEL J. CLARE-SALZLER, AND ABDOREZA DAVOODI-SEMIROMI. 2006. Ann. N.Y. Acad. Sci. 1079: 198-204.

Acknowledgements

At the beginning, I naively thought graduate school was going to be a test of my own ability to accomplish a very lofty goal. I quickly realized, however, that without the constant support of many different individuals, achievement of this goal would be, simply stated, impossible. Therefore, I have many people to thank because without you, this goal could not have been achieved.

I would like to thank my mentor, Dr. Robert Finberg, for supporting my research throughout my time here at UMass. Thank you in particular for accepting me into your lab following my transfer from the University of Florida. I have truly appreciated your candid advice and guidance throughout this graduate process. I would also like to thank Dr. Evelyn Kurt-Jones for your suggestions and guidance during my time in the Finberg Lab.

I would like to thank the University of Massachusetts and all of the support staff that have provided me with assistance in various capacities. These range from core facilities performing different scientific functions to the graduate school of biomedical sciences administrative staff who helped integrate me into the UMass community, and who helped me finalize the requirements for graduation. I'd like to thank two people in particular, Michael Cole and Gaile Arcouette, both members of the GSBS administrative staff, for all of your assistance. Thank you.

I would like to thank the members and former members of the Finberg Lab. Thank you Shenghua, Jennifer, Melvin, Anna, Glennice, Mike, Jessica, Damon, Jing,

Frank, and Joe. Thank you Ryan and Christine, fellow graduate students, for your help and advice, and for the many uplifting conversations we have had during my time here.

I'd like to thank Dr. Trudy Morrison and her lab, Lori and Cathy, for all of your help and guidance. Thank you for making the VLP vaccine study a very fruitful collaboration. I have very much enjoyed working with all of you. I'd also like to thank my Thesis Research Advisory Committee for guiding me towards completion of my graduate studies. Thank you to Dr. Dale Greiner, Dr. Evelyn Kurt-Jones, Dr. Shan Lu, and Dr. Raymond Welsh. Thank you to my previous graduate school mentor, Dr. Michael Clare-Salzler for your help and guidance during my tenure at the University of Florida. Thank you for the opportunity to work in your lab and for all of your help during my transfer to UMass.

Importantly, I would like to thank all of my family and friends for listening to me talk about my work even though you probably had little idea what I was talking about most of the time, and more importantly, for your continued support during my graduate career. In particular I'd like to thank my siblings John, Christina, and Anthony, and my wife's entire family: her father, Robert, mother, Claudia, brothers, Robert, David, Jim, and John, and sister, Christine.

I'd like to say a special thank you to my parents for your endless support and encouragement throughout this long process. There were probably more times than I can even remember when your words kept me going even when I didn't think I could or wanted to. Additionally, I'd like to thank my grandparents who, despite no longer being

here on this earth, have never ceased to play an instrumental role in my life. Your contributions to my success and more importantly, my life, could never be overstated.

Lastly, and most important of all, I'd like to thank my rock, my wife, Dr. Mary Murawski. Your insatiable desire to better yourself is infectious and I feel honored and blessed to constantly benefit from your endlessly optimistic spirit. We have talked so frequently during this journey about how great it will be when we've both completed our graduate studies. All I can say at this point is, I'm so excited to discover what the future holds for us now.

Abstract

Respiratory syncytial virus (RSV) causes a common infection that is associated with a range of respiratory illnesses from common cold-like symptoms to serious lower respiratory tract illnesses such as pneumonia and bronchiolitis. RSV is the single most important cause of serious lower respiratory tract illness in children < 1 year of age. Host innate and acquired immune responses activated following RSV infection have been suspected as contributing to RSV disease. Toll-like receptors (TLRs) activate innate and acquired immunity and are candidates for playing key roles in the host immune response to RSV. Leukocytes express TLRs including TLR2, TLR6, TLR3, TLR4, and TLR7 that can potentially interact with RSV and promote immune responses following infection. Using knockout mice, we have demonstrated that TLR2 and TLR6 signaling in leukocytes can activate innate immunity against RSV by promoting TNF-α, IL-6, CCL2 (MCP-1), and CCL5 (RANTES) production. As previously noted, TLR4 also contributed to cytokine activation (71, 90). Furthermore, we demonstrated that signals generated following TLR2 and TLR6 activation were important for controlling viral replication *in vivo*. Additionally, TLR2 interactions with RSV promoted neutrophil migration and dendritic cell activation within the lung. Collectively, these studies indicate that TLR2 is involved in RSV recognition and subsequent innate immune activation and may play a role in modulating acquired immune responses through DCs.

Despite the fact that RSV is the single most important cause of infant upper respiratory tract disease, there are no licensed vaccines available to prevent RSV disease.

We have developed a virus-like particle (VLP) vaccine candidate for RSV. The VLP is composed of the NP and M proteins of Newcastle disease virus (NDV) and a chimera protein containing the cytoplasmic and transmembrane domains of the NDV HN protein and the ectodomain of the human RSV G protein (H/G). BALB/c mice immunized with 10 or 40 μg total VLP-H/G protein by intraperitoneal or intramuscular inoculation stimulated antibody responses to G protein as good as or better than comparable amounts of UV-inactivated RSV. Furthermore, VLP-H/G induced robust CTL responses in vaccinated animals. Immunization with two or even a single dose of these particles resulted in the complete protection of BALB/c mice from RSV replication in the lungs. Upon RSV challenge of VLP-H/G immunized mice, no enhanced pathology in the lungs was observed, although lungs of mice immunized in parallel with formalin-inactivated RSV (FI-RSV) showed the significant pathology that has been previously observed with FI-RSV vaccination. Thus, the VLP-H/G candidate vaccine was immunogenic in BALB/c mice and prevented replication of RSV in murine lungs with no evidence of immunopathology. These data support further development of virus-like particle vaccine candidates for RSV.

Table of Contents

List of Figures

Chapter I

Chapter II

Chapter III

Chapter IV

List of Tables

Chapter II

List of Abbreviations

RSV: respiratory syncytial virus
FI-RSV: formalin-inactivated respiratory syncytial virus
UV-RSV: ultraviolet irradiated respiratory syncytial virus
MMTV: mouse mammalliary tumor virus
HCMV: human cytomegalovirus
HCV: hepatitis C virus
I.N.: intranasal
I.P.: intraperitoneal
I.M.: intramuscular
Th1: T cell helper 1
Th2: T cell helper 2
IFN: interferon
IL-6: interleukin 6
IFNb: interferon beta
TNF-α: tumor necrosis factor-alpha
MCP-1: monocyte chemoattractant protein-1
IRF: interferon regulatory factor
NF-κB: nuclear factor kappa B
RANTES: regulation upon activation, normal T cell expressed, and secreted
IFN-γ: interferon gamma
MIP-1α: macrophage inflammatory protein-1alpha
DC: dendritic cell
MHC: major histocompabibility complex
PBMC: peripheral blood mononuclear cells
NK cell: natural killer cell
RSV F: RSV fusion protein
RSV G: RSV attachment protein
RSV SH: RSV small hydrophobic protein
PRRs: pattern recognition receptors
PAMPs: pathogen associated molecular patterns
TLR: toll-like receptor
MyD88: myeloid differentiation factor 88
TRIF: TIR-domain-containing adapter-inducing interferon-β
TIR: Toll-IL-1 receptor
VLP: virus-like particle
VLP-H/G: virus-like particle expressing RSV attachment (G) protein
GCH: goblet cell hyperplasia
CTL: cytotoxic T lympocyte
H and E: hematoxylin and eosin
PAS: periodic acid Schiff

Chapter I

Introduction

Pathogen-induced acute respiratory tract disease is the leading cause of mortality among all infectious diseases worldwide. Of these pathogens, human respiratory syncytial virus (hRSV or RSV) is recognized as the most important cause of pediatric respiratory tract disease. In fact, in many areas, it surpasses microbial pathogens as the leading cause of pneumonia and bronchiolitis in infants younger than one year old. Although RSV is primarily considered a pediatric pathogen, RSV can infect individuals of all ages, often multiple times throughout life. Elderly and immunocompromised populations are particularly sensitive to RSV infections, further emphasizing the urgent need to develop vaccines against RSV. RSV is a high priority for vaccine development, but to date attempts to develop a vaccine have been unsuccessful. It is likely that understanding the pathogenesis of RSV disease, including the innate immune response to infection, will help in designing a safe and effective vaccine.

RSV the virus

RSV, a member of the paramyxoviridae family of viruses, consists of a single stranded, negative sense strand of RNA surrounded by a nucleocapsid. RSV RNA encodes for 10 surface and structural proteins important for infection and proliferation of the virus (Figure 1.1a). Five of these proteins are involved in capsid formation and

Figure 1.1 RSV structure and genome

a.

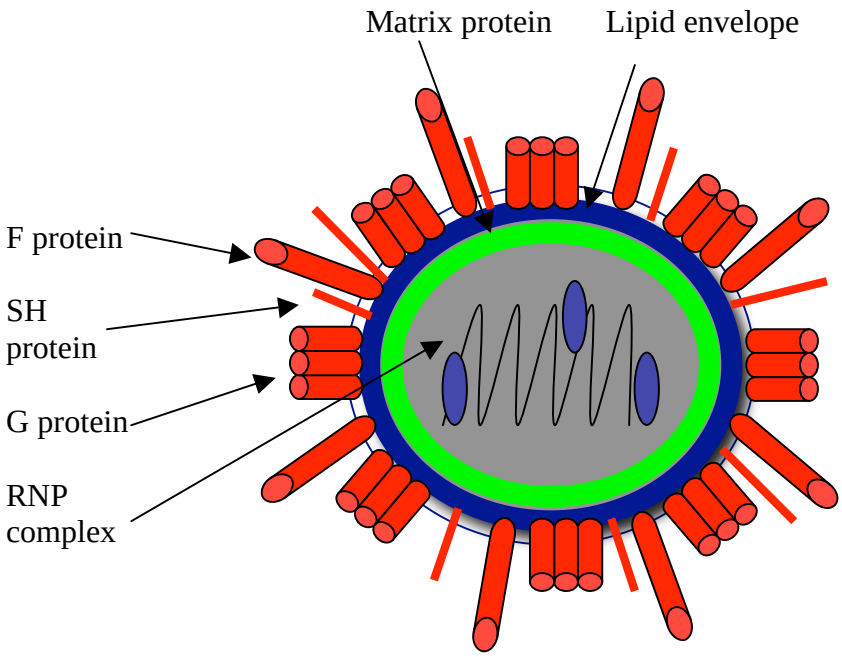

b.

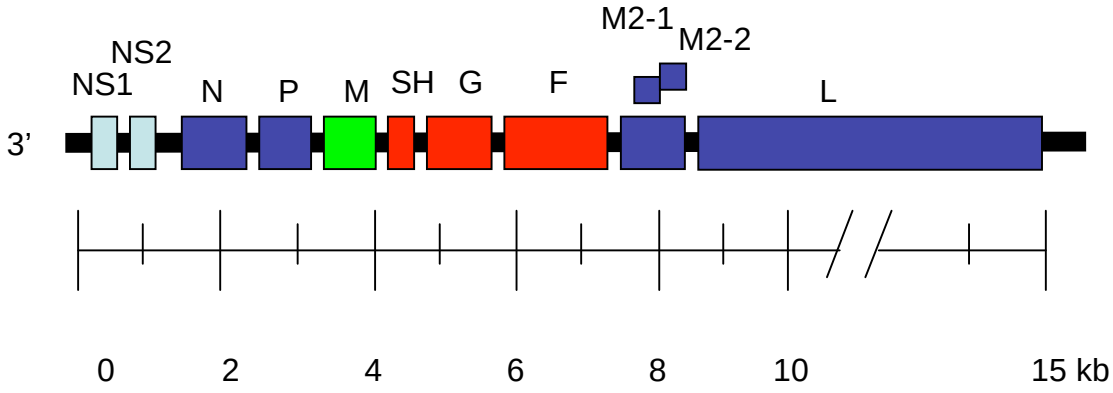

Figure 1.1 RSV structure and genome

The cartoon in figure 1.1a illustrates the individual components that comprise the structure of RSV. The ribonuclear protein complex (RNP complex) contains genetic information important for proliferation of viral progeny. The RNP complex is surrounded by a protein matrix and a lipid envelope that provide protection and structure to the virus. Importantly, glycoproteins including the F and G proteins are shown extending out from the lipid capsule. These proteins are thought to facilitate infection of host cells and are important immunogens. Figure 1.1b depicts the non-segmented linear strand of RNA that encodes for 11 RSV proteins. The relative length in kilobases (kb) of each segment is denoted by the ruler. This single RNA strand is translated from left to right. Protein messages are grouped by color, based on synergy.

virus structure or RNA synthesis: the N protein which associates with genomic RNA, L protein, the major polymerase subunit, P phosphoprotein, an essential cofactor in RNA synthesis, M2-1 and M2-2 proteins, which are involved in transcription and coordinating the tempo of transcription and RNA replication, respectively (reviewed in (28)).

Following successful assembly of the nucleocapsid, the virus is packaged into a lipid bi-layer derived from the host cell membrane during budding. Four RSV proteins associate with the lipid bi-layer to form the viral envelope: M, F, G, and SH (Figure 1.1b). The matrix (M) protein lines the inner envelope surface and is important in viral assembly and budding. The fusion (F), attachment (G), and small hydrophobic (SH) proteins are heavily glycosylated transmembrane proteins (reviewed in (28)). The F and G proteins are considered important for infection of host cells and importantly, are the only known antigenic determinants for RSV. The significance of these antigenic determinants will be discussed in more detail in later sections. The F protein is thought to mediate direct viral fusion of the viral envelope to the host plasma cell membrane (30). F protein remaining on the host plasma membrane facilitates host cell-cell fusion that can form syncytia, or large clumps of cells, *in vitro*. F is a type I transmembrane protein having an N-terminal cleaved signal peptide and a membrane anchor near the C-terminus (reviewed in (28)). Initially, F is synthesized as an inactive F_0 precursor that assembles into a homotrimer and is activated following cleavage in the trans-Golgi complex by cellular endoproteases. This reaction yields two disulfide-linked F_1 subunits and a small p27 fragment. The F_1 subunit contains heptad repeats that associate during viral fusion to bring viral and host membranes into close proximity (55). The role of the F_0 fragments in

directing viral fusion remains largely unexplored, although it has been suggested that the F_0 of bovine RSV (bRSV, a close relative of hRSV) may play a role in mediating mucous secretion in the lungs (179).

Initially, the G protein was suggested to be the major attachment protein because antibodies against G inhibited attachment of virions to host cells while antibodies against F abrogated fusion but not attachment (96). However, unlike other paramyxoviruses that require both the G and F proteins for successful attachment, RSV F seems to act independently from G to facilitate infection under certain conditions. For example, recombinant RSV lacking the G and SH proteins was able to infect cultured cells and induce syncytia formation with wild-type-like efficiency in certain cultured cell lines (163). Additionally, VSV recombinantly engineered to express RSV F protein was able to infect and form syncytia in cultured cells (81). However, RSV lacking G and SH proteins was significantly attenuated *in vivo*, perhaps suggesting a major, but not entirely exclusive, role for G in viral attachment (163).

The G protein is unlike other paramyxovirus glycoproteins. It is a type II transmembrane protein with a single hydrophobic region near the N-terminal end that serves as both the uncleaved signal peptide and a membrane anchor, and it is also expressed as a secreted form. The secreted form lacks the entire 65 amino acid (aa) N-terminus, including the signal/anchor (72, 97, 138). Its ectodomain (aa 65-312) is heavily glycosylated by N-linked and, primarily, O-linked carbohydrates. The estimated 24-25 O-linked carbohydrate side chains and 4 N linked side chains increase the molecular weight of the protein, synthesized in Vero cells, from 32,500 kD to approximately 90,000 kD

(31, 173). Interestingly, recent studies have suggested an immunomodulatory role for both the membrane-bound and secreted forms of the RSV G protein, which will be discussed in later sections. Considerably less is known about the role of the SH protein, although some reports suggest that SH may play a minor role in immune surveillance (51).

The remaining two proteins, NS1 and NS2, are not packaged into the virion. In fact, they appear to be nonessential accessory proteins involved in modulating the host response to infection. Both NS1 and NS2 appear to be involved in dampening IFN α/β production by interfering with IRF-3 and STAT 2 signaling pathways (98, 150, 151). Additional evidence suggests that these proteins can antagonize SOCS proteins and likely play direct roles in limiting dendritic cell maturation, the latter resulting in weak or incomplete activation of protective immune responses (115, 117).

RSV the pathogen

RSV is the most important cause of respiratory tract disease in infants and young children. This association has been recognized for over 40 years. The WHO estimates that annual infection and mortality figures for RSV infection are 64 million and 160,000, respectively, in the United States alone (144, 164). Roughly 65% of all infants have been infected with RSV before 1 year and by 2 years nearly all children have been infected with the virus (28). RSV may also cause repeated infections throughout life. Both primary and repeat infections are associated with a range of illness from common cold-

like symptoms to serious lower respiratory tract disease such as bronchiolitis, pneumonia, ottis media, and persistent wheezing (73). Additionally, immunocompromised patients, particularly those with T and B cell deficiencies, are highly susceptible to RSV infection and exhibit increased risk of developing severe RSV-induced disease. Notably, RSV can cause significant disease in elderly patients and is associated with higher mortality than influenza in non-pandemic years (122). Therefore, RSV is a serious pathogen in infant, elderly, and immunocompromised populations.

RSV inoculation can occur through mucous membranes of the eyes and nose by either aerosol or direct contact modalities. Epithelial cells of both the upper and lower respiratory tract are major targets of RSV infection and serve as temporary reservoirs for the virus during active infection. In particular, ciliated cells of the small bronchioles and type 1 pneumocytes are targeted for infection. However, non-ciliated epithelial cells, intraepithelial dendritic cells, and resident macrophages can, also, likely be infected by the virus (62). RSV is a cytopathic virus that causes necrosis of epithelial cells and proliferation of bronchiolar epithelial cells. Furthermore, some specialized respiratory cell functions like cilial motility are diminished (1, 120). A peribronchiolar mononuclear infiltrate consisting primarily of monocytes, T cells, and neutrophils is observed during the initial stages of infection, along with submucosal edema and mucous secretion. Interestingly, a pronounced eosinophilic infiltrate is observed in some severe RSV disease patients, although the mechanisms for this infiltration are not yet clearly defined (reviewed in (28)). Therefore, the severity and duration of disease, in part, likely depends

on the amount of airway obstruction occurring from virus/host interactions, including sloughing of dead epithelial cells, mucus secretion, and accumulating immune cells.

RSV pathogenesis

The observation that RSV can induce such a diverse range of symptoms suggests that both environmental and genetic factors likely play key roles in disease pathogenesis, although these processes remain poorly defined at best. Certain environmental factors, such as infant age (<6 months), premature birth (<35 weeks of gestation), low birth weight, immunosuppression, congenital heart disease, frequency of RSV infections, and old age have been associated with RSV disease. Increased risk of exposure, such as day cares, hospitalizations, and multiple siblings also may also contribute to disease susceptibility (170). However, it is important to remember that only a small percentage (2-5%) of all children infected with RSV develop severe disease, while the majority of patients develop mild respiratory symptoms that often remain undiagnosed, thereby complicating the search for disease susceptibility markers. Also, the immunosupressed and elderly patients, two populations exhibiting varied defects in important immune regulatory mechanisms that control infection, are at increased risk of developing RSV disease, indicating that environmental factors alone cannot fully account for disease susceptibility.

Although infant health and underlying disease can contribute to RSV susceptibility, more than 60% of all infants hospitalized were previously healthy,

suggesting that a possible genetic predisposition to disease may influence susceptibility (122). This hypothesis is substantiated, in part, because 50% or more of infants hospitalized with RSV infection in the first 6 months of life can exhibit recurrent wheezing up to 11 years or more of age. Also, severe RSV disease during infancy may predispose for asthma or asthma-like symptoms later in life (37% of RSV bronchiolitics vs. 5.4% of controls) (147). Recently, evidence suggesting genetic polymorphisms in important innate immune signaling pathways ranging from viral recognition to inflammatory processes targeted towards elimination of the virus may predispose for severe RSV-induced disease (9, 16, 90, 125, 140, 165). These observations suggest that host responses to RSV, particularly innate immune responses, may be an important component of disease pathogenesis. Therefore, much of the current RSV research is focused on understanding how host immune responses may contribute to RSV disease to better facilitate development of therapies and vaccines.

Role of innate immunity in recognizing RSV

If a virus successfully transverses host membranes and reaches its target cells, a myriad of host innate immune processes are poised to sense the virus and alert the immune system to the presence of the invading pathogen. These innate immune mechanisms exist to sense pathogens, contain the spread of the pathogen from one host cell to another, and to provide the correct immunologic signals needed to ultimately eliminate the pathogen from the infected area. Leukocytes and resident tissues express a

Figure 1.2 TLRs are PRRs that recognize invading pathogens by their PAMP

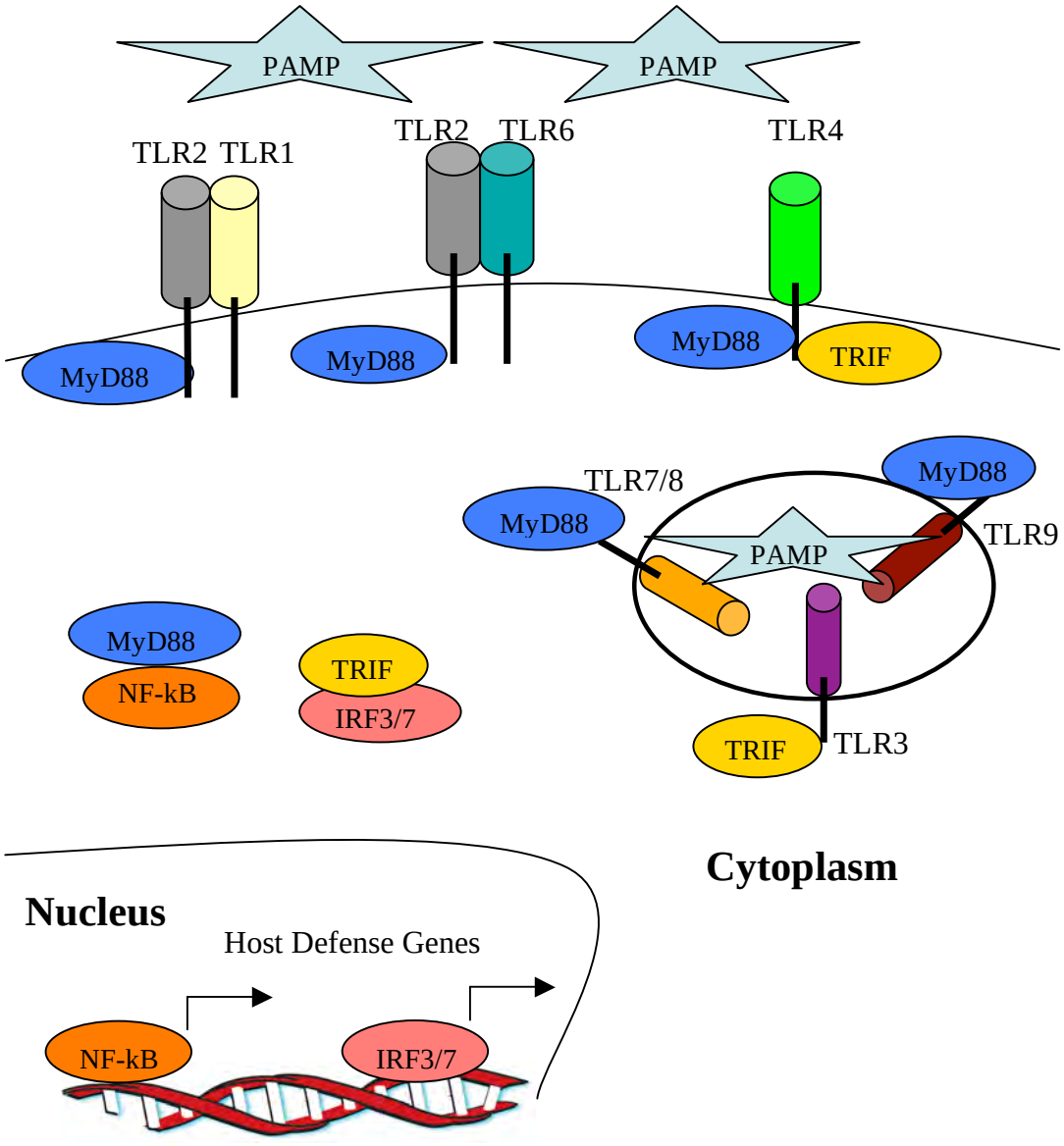

Figure 1.2 TLRs are PRRs that recognize invading pathogens by their PAMP

TLRs are pattern recognition molecules (PRRs) expressed on host cell surfaces and in host cell endosomes that recognize conserved molecular structures (PAMPs) on bacteria, fungi, or viruses. TLR2 and TLR4 can recognize both bacterial and viral motifs while TLR3,7,8,9 can recognize viral motifs. Once TLRs recognize their cognate ligand, they activate distinct signaling pathways (i.e., MyD88 and TRIF) that ultimately initiate transcription of host defense genes.

variety of pattern recognition receptors (PRRs) that sense pathogen-associated molecular patterns (PAMPs), evolutionarily conserved molecules among families of different microbes. Included in this family of PRRs are Toll-like receptors (TLRs). TLRs interact with PAMPs, including RSV, thereby initiating a complex cascade of signals that promote host defense genes (Figure 1.2). TLR signaling occurs through a common Toll-interleukin-1 (IL-1) receptor (TIR) domain. All TLRs recruit MyD88 to the TIR with the exception of TLR3, which recruits TIR domain containing adaptor inducing beta interferon (TRIF). MyD88 signaling activates transcriptional gene regulators including mitogen-activated protein kinase, NF-κB, and IFN regulatory factors (IRF). These transcriptional regulators promote cytokine, chemokine, and interferon (IFN) production that make up the inflammatory mileu at the sites of infection (reviewed in (3, 10, 158))(Figure 1.3).

As indicated, TLRs can recognize a diverse range of microbial signatures. TLRs are divided into two major categories: TLRs expressed on cell surfaces or in endosomes. Thirteen different TLRs have been identified in humans and eleven in mice. TLRs recognize various components of bacteria, fungi, protozoa, and, in particular, viruses. Certain TLRs implicated in recognizing viral components include TLR3 (dsRNA), TLR 7/8 (ssRNA), TLR9 (dsDNA)(83, 148), which are located in endosomes, and TLR2 (HCMV, HCV core)(27, 32), TLR4 (MMTV, RSV F protein)(90, 137), and TLRs 1 and 6, located on cell surfaces. TLRs 1 and 6 are unique amongst all TLR because they dimerize with TLR2 to propagate signaling(3). Endosomal TLR ligation drives IRF-3/7 activity leading to the production of IFN-α/β, a critical pleiotropic activator of anti-viral

Figure 1.3 TLR/pathogen interactions induce innate signaling responses within host cells

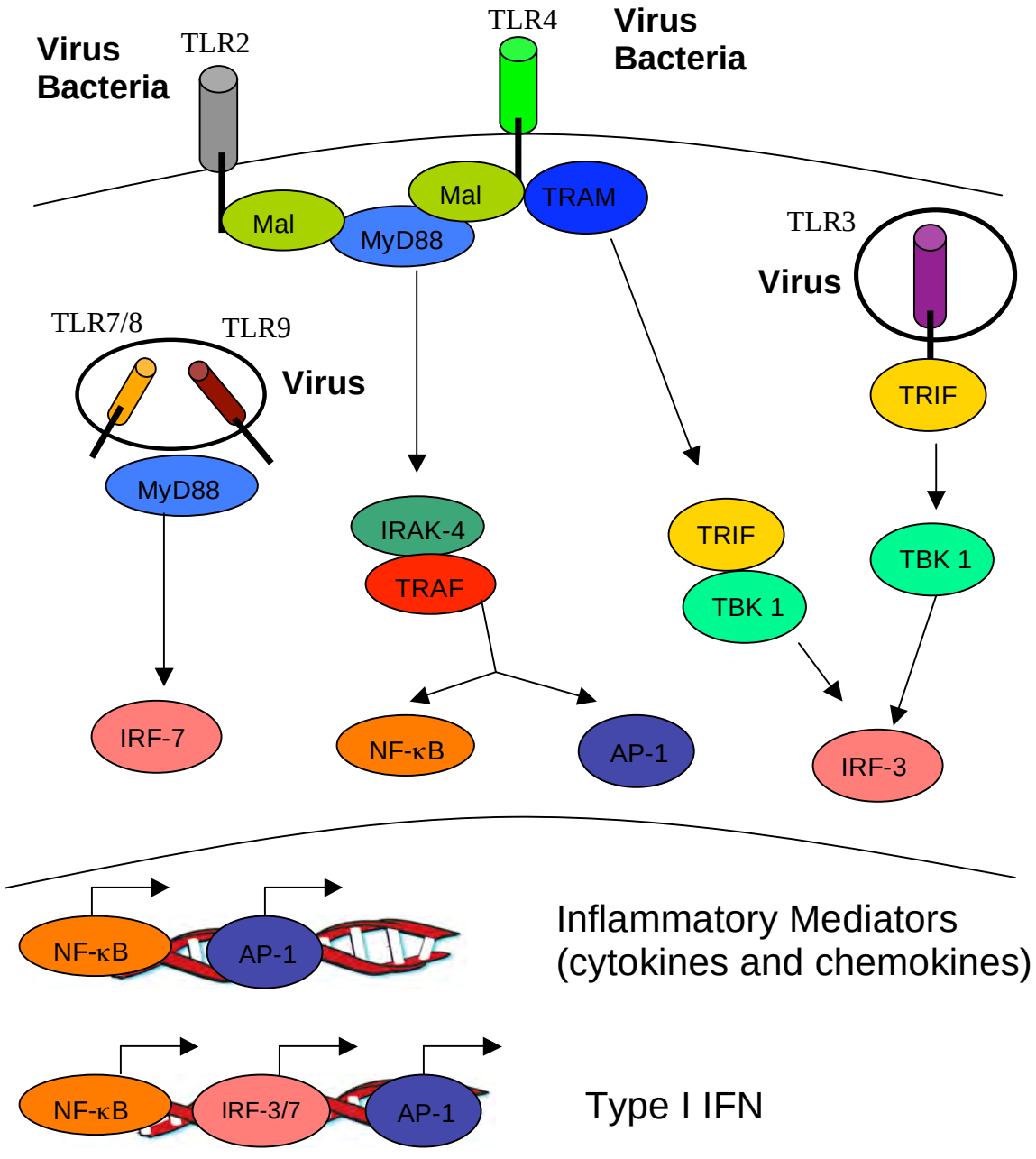

Figure 1.3 TLR/pathogen interactions induce innate signaling responses within host cells

Intracellular TLR stimulation pathways are depicted in this cartoon. Engagement of all TLRs by foreign antigens except TLR3 leads to MyD88 activation. Once activated, MyD88 initiates a signaling cascade of phosphorylation events that promote IRAK-4 and TRAF6 activation. TRAF6 can activate AP-1 and NF-κB. AP-1 and NF-κB are transcription factors that, once activated, translocate to the nucleus and initiate transcription of inflammatory mediators including IL-1β, IL-6, IL-8, IL-12, TNF-α, CCL2, CCL3, and CCL5. Additionally, MyD88 activation following TLR7,8,9 ligation initiates a signaling cascade that activates the transcription factor IRF-7. TLR3 ligation leads to TRIF activation. This event leads to TBK1 activation and to the activation the transcription factor IRF-3. Furthermore, both TLR2 and TLR4 share a common intracellular signaling molecule, Mal, that interacts with MyD88 to propagate downstream signaling events. TLR4 is unique among all TLRs because it can activate both the MyD88 dependent and TRIF dependent signaling cascades. If the TRIF and MyD88 pathways are both engaged either through TLR4 signaling or the combinatory effects of different TLR signaling pathways (i.e. TLR2 and TLR9) the resulting activation of NF-κB, AP-1, and IRF-3/7 promote the transcription of Type I IFN. Thus, TLR activation initiates a series of highly complex and intricate pathways targeted against the invading pathogen.

responses (148).

Surface TLR ligation is important for NF-κB driven responses, including pro-inflammatory cytokines such as IL-1β, IL-6, IL-8, IL-12, TNF-α and chemokines such as CCL2 (MCP-1), CCL3 (MIP-1α), CCL5 (RANTES), important molecules involved in inflammation and chemotaxis of leukocytes to sites of infection (reviewed in (84)). Unlike other TLRs, TLR4 ligation can propagate signaling through both NF-κB and IRF pathways because it contains an intracellular MyD88 and TRIF recruitment site (reviewed in (84)). TLRs 3, 7, and 4 plus CD14 are known to interact with RSV, thereby providing multiple pathways by which the host innate immune response can mediate responses to RSV infection (90, 141, 142).

Linking innate and adaptive immune responses against RSV

Lung epithelial cells and resident antigen presenting cells (APCs), including macrophages and dendritic cells (DCs), the first line of innate immune sentinels, express TLRs that recognize RSV motifs and coordinate the initial inflammatory response against RSV. The inflammatory mileu generated during these interactions has direct effects on virus replication and recruitment of additional leukocytes, including NK cells, neutrophils, monocytes, T cells, and circulating DCs into the lungs, each playing critical roles in the establishment of protective immune responses (140, 149, 177). DCs are unique APCs that can link the innate and adaptive immune responses against pathogens, including RSV, by undergoing functional maturation (Figure 1.4). This process is

defined by heightened cytokine production, including IL-12, IL-1β and TNF-α, that can further augment inflammation, increase expression of MHC I and II molecules, and increase expression of co-stimulatory molecules CD86, CD80, and CD40(88). In this maturation state, DCs promote adaptive immunity through the activation and subsequent clonal expansion of both T and B lymphocytes. Furthermore, the make-up of the inflammatory mileu directly impacts a DCs ability to polarize the type (i.e., Th1-like or Th2-like) of acquired immune response generated following pathogen recognition. Interestingly, research has shown that a weak or incomplete Th1 polarizing inflammatory mileu can lead to Th2-like responses (140). While most individuals who do not develop RSV-induced disease seem to establish protective Th1-like responses, RSV-susceptible individuals seem to exhibit Th2 immune responses, similar to asthmatic responses, that are thought to be involved in disease pathogenesis (reviewed in (12)). Therefore, disease susceptibility may be multi-factorial, encompassing underlying genes that control immune responses to RSV and/or the ability of RSV to influence major components of the innate immune response including the initial inflammatory mileu.

Host adaptive immune responses to RSV

RSV infection, like other respiratory viral infections, is usually completely resolved by innate and adaptive immunity. Host immune responses, both soluble and cell-mediated, have been proposed to be important for protection against RSV infections (5, 25, 26, 29, 58, 99, 145). The RSV F protein, one of the two major antigens expressed

Figure 1.4 Dendritic cells (DCs) link innate and adaptive immune responses

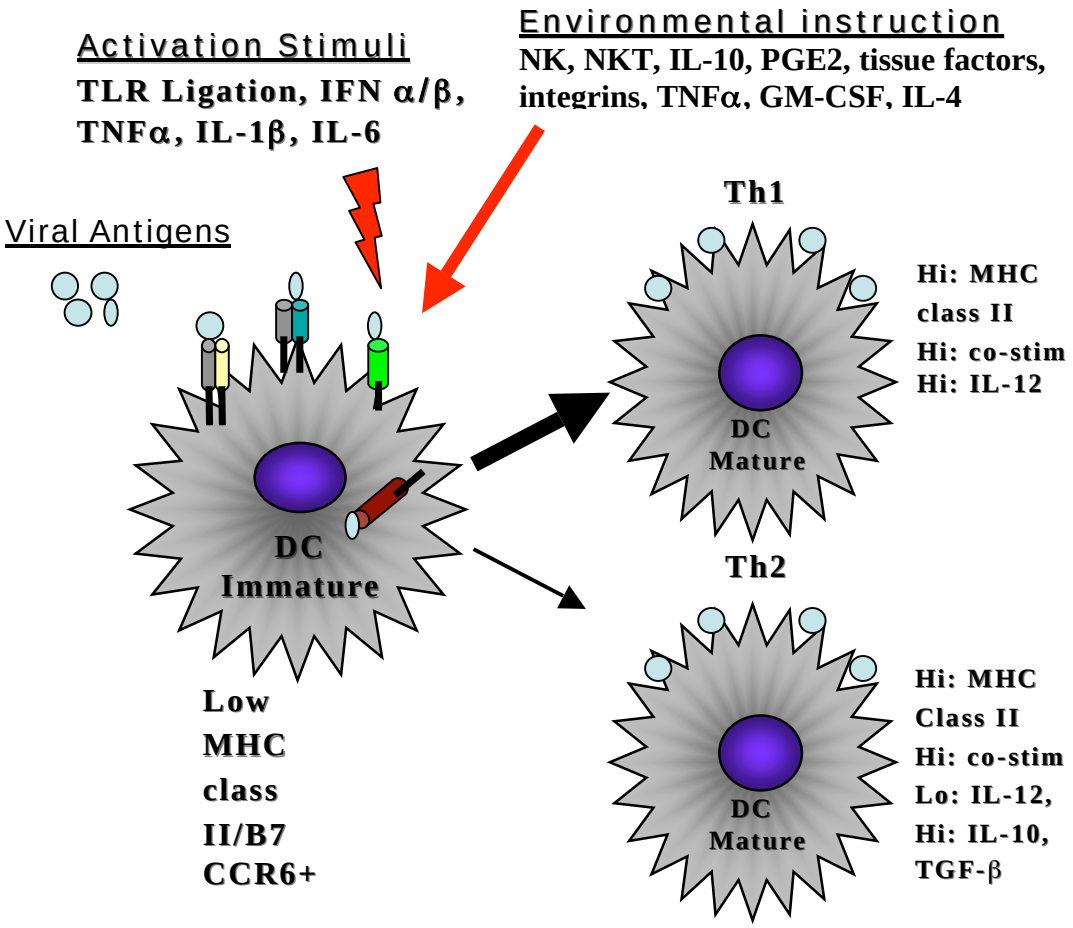

Figure 1.4 Dendritic cells (DCs) link innate and adaptive immune responses

Immature Dendritic cells (DCs) survey host tissues for the presence of foreign pathogens including viruses. Using receptors such as TLRs immature dendritic cells can sense invading virus and alert the immune system to their presence. Both the activation stimulus, including direct TLR/pathogen interactions, and environmental factors within the infected host tissue can greatly influence the type (Th1 or Th2) of acquired response that a DC can generate. It is thought that strong inflammatory signals (illustrated by a heavy arrow) lead to a mature Th1 polarizing DC while weak or blunted signals (illustrated by skinny arrow) lead to a mature Th2 polarizing DC (140).

on virion surfaces (29), is thought to be an important target of neutralizing and protective antibodies (29, 49, 159). Indeed, monoclonal antibodies specific for the RSV F protein are used clinically for RSV disease prophylaxis in high-risk infants. However, the protective effects quickly wane due to the half-life of circulating antibodies (between 21-28 days) (6, 128). The F protein is also a major target of CD8 T cells in mice (24), but the association between cell-mediated immunity and protection from RSV disease in humans has not been well established (132). The role of the G protein, the other major antigen on virion surfaces, in stimulating protective immune responses is less clear, although it is thought that antibodies to this molecule do have a role in protection (70, 111, 113). CD8 T cell epitopes have not been defined for the G protein however recent studies have implicated the G protein in defining CD8 T cell responses (18).

The coordinated efforts of innate and adaptive immunity are sufficient to clear most primary infections. However, the establishment of long-term protection is essential to avoid subsequent infections and likely to prevent RSV induced disease. The fact that the overwhelming majority of individuals infected with RSV can and will be re-infected with the virus, often times during the same infection cycle, suggests that long-term protective immune responses are not effectively established. Furthermore, the observation that certain populations exhibit aberrant responses to RSV infection, including severe RSV-induced disease, suggests that not only ineffective, but also, deleterious, and perhaps misguided (i.e., Th2 responses greater than Th1) immune responses are likely being induced. Possible factors contributing to these observations include age at time of infection, underlying genetic factors that limit innate immune

activation, poor immunogenicity of RSV antigens, and/or viral mechanisms that subvert immune surveillance and/or limit robust immune activation.

Host factors that contribute to disease susceptibility

Perhaps the most compelling evidence that host immune responses can cause severe RSV disease is derived from early RSV vaccine trials in infants using a formalin-inactivated RSV (FI-RSV) preparation (82). The vaccine was poorly protective and, in RSV naïve individuals, it primed for more severe RSV disease upon subsequent natural RSV infection. Surprisingly, approximately 80% of vaccinated individuals were hospitalized with enhanced RSV disease, and two patients died. Retrospective analysis in both humans and animal models revealed that poor neutralizing antibodies were generated against RSV, suggesting that incomplete antibody affinity maturation might contribute to enhanced disease (41), along with other factors as well. For example, further analyses revealed a strong Th2-like biased immune response characterized by Th2-like cytokines (IL-4, IL-5, and IL-13), eosinophilia, goblet cell hyperplasia/metaplasia, mucous overproduction, IgE greater than IgG antibody production, and airway hypersensitivity against subsequent RSV infections after FI-RSV vaccination (12, 14, 169). Therefore, the host immune system can greatly influence disease pathogenesis. While these data are highly suggestive of aberrant immune activation leading to RSV disease, the relevance of vaccine-enhanced disease to natural RSV disease is still somewhat unknown.

Although post-hoc analysis of human samples administered FI-RSV and animal models have provided some answers to vaccine-enhanced disease, the underlying host mechanisms that contribute to natural disease still remain poorly defined. Growing evidence suggests that defects in innate immunity, particularly in TLR signaling, may contribute to RSV disease susceptibility. Our lab previously reported that RSV F protein interacts with TLR4, which can signal through MyD88, to activate an innate immune response (71, 90). These results have been confirmed and extended by others, further supporting the hypothesis that TLR signaling is involved in the innate immune response to RSV (16, 61). Recently Awomoyi et al. suggested that defects in TLR signaling, TLR4 in particular, may be linked to RSV-induced pathology in pre-term high risk infants (9), although the overall effect of TLR4 on RSV pathogenesis remains somewhat unclear. Supporting these findings, Holt et al. demonstrated that PBMCs isolated from children with TLR4 mutations exhibited decreased NF-κB activation and subsequently displayed decreased cytokine production in response to RSV, suggesting that weakened immune responses may contribute to RSV-induced disease (165). Together, these studies provide evidence suggesting that TLR-dependent signaling is important for activating early inflammatory responses to RSV and that aberrant TLR signaling may promote RSV-induced disease.

Adaptive immune responses, in addition to innate responses, may play key roles in determining susceptibility to RSV-induced disease. Studies in mice revealed that CD4 and CD8 T cells can mediate disease severity, and observations from humans with severe combined immunodeficiency further suggest a T cell component to RSV-enhanced

disease (25, 26, 57, 123, 171). Additionally, a genetic polymorphism in the gene that encodes the Th2 cytokine, IL-4, that increased expression, was found to be associated with increased susceptibility to RSV (13, 136, 139). Collectively, these and other studies support the hypothesis that immune-mediated events likely greatly contribute to RSV disease and underscore the need to examine further how RSV/host interactions initiate immune responses that may skew towards or away from RSV disease.

Virus factors that contribute to disease susceptibility

RSV has an extremely high rate of infectivity and is often considered one of the most contagious human pathogens. Surprisingly, RSV can cause repeated infections throughout life, despite having limited strain and antigenic diversity. In fact, RSV has a single serotype with two major antigenic groups (A and B). Between the two serotypes the F protein is highly conserved (90% sequence homology and 50% antigenic identity), while the G protein is more divergent (53% sequence homology and 1-7% antigenic identity) (reviewed in (28)). Unlike other respiratory viruses, such as influenza, that can evade immune recognition by antigenic drift and/or antigenic shift, RSV causes disease with little to no modification, suggesting that RSV possesses compensatory mechanisms that can limit or subvert immune surveillance and/or activation. RSV is thought to cause pathology, both directly and indirectly, through limited cytopathic effects on epithelial cells (176) and modulation of host immune responses, respectively. This hypothesis has been substantiated by studies indicating that the NS1/NS2 and RSV G proteins help the

virus evade innate immune activation. First, the NS1/NS2 proteins can effectively block synthesis of host Type I IFN (102). Mechanistically, NS1/NS2 can block IRF-3 activation and can down-regulate JAK/STAT pathways, specifically STAT2, both of which are critical for Type I IFN production (102). Furthermore, RSV infection of STAT1 knockout mice revealed a role for JAK/STAT responses in modulating Th1/Th2 balance, i.e., STAT1 knock-out mice exhibited heightened Th2 responses following RSV infection, suggesting that manipulation of these host proteins may increase susceptibility to RSV disease in an otherwise normal host (44).

The RSV G protein contains a number of important features that are thought to both limit immune activation and contribute to disease susceptibility. Initial reports suggested immunizations containing the G protein alone (i.e. subunit vaccine) or vaccinia virus-delivered G protein elicited an unbalanced, Th2-dominated immune response (59, 68, 124). However, more recent studies suggest that the unbalanced response observed in these cases may be due to the soluble form of the G protein (sG), not the membrane bound form (mG) or to the method of antigen delivery (78, 79). It has been suggested that sG protein, which represents 80% of G protein released from cells within 24 hours post-infection (42, 79), can subvert host immune detection in part by inhibiting Toll-like receptor 3- and 4- mediated IFN-β production and that the Th balance can be restored using TLR adjuvants (66, 146). Furthermore, infection of human epithelial cells and monocytes with RSV lacking G resulted in increased NF-κB derived cytokine (IL-6, IL-8) and chemokine (RANTES) production, suggesting that RSV proteins can dampen advantageous host pro-inflammatory responses (134). However, other studies have

suggested that disease enhancement is related to two mucin-like domains (GCRR) in the G protein ectodomain (GCRR) (56, 92). This GCRR domain includes a CX3C chemokine motif that has been hypothesized to affect leukocyte trafficking to lungs (69), indirectly promoting Th2 responses by inhibiting important immune pathways that support Th1 responses. Additionally, the GCRR has been hypothesized to limit neutralizing antibody function by acting as an antigen decoy, thereby limiting effective host responses against RSV (19). Therefore, it seems highly possible that proteins synthesized by RSV during active replication may directly contribute to RSV induced disease by manipulating the natural host response to RSV infection.

Research aimed at understanding the mechanisms by which RSV interacts with host immune systems and vice versa has begun to establish a somewhat less murky picture of how these interactions can skew subsequent immune responses either towards or away from disease. Insights from the early FI-RSV vaccine trials, coupled with new information related to host genetic susceptibilities to RSV and an increased understanding of how RSV limits host innate immune responses, is guiding research efforts to develop vaccines against RSV, but these insights also underscore an important cautionary point. Since immune responses are, in part, responsible for exacerbated disease pathology, great care must be taken in designing vaccines that can be both protective and safe in humans.

Animal models used to study RSV

Resulting from the failed RSV vaccine trials of the 1960s, suitable animal models have been sought to elucidate possible mechanisms of enhanced disease as well as basic pathways involved in host responses to RSV infection. Given the potential for heightened morbidity and mortality from an RSV vaccine, animals including mice, cotton rats, calves, and primates can be used as useful surrogates to study RSV pathogenesis (23, 28, 40, 59, 119, 130, 160, 169). While none of the models can definitely predict human responses to RSV, each model has been useful in determining certain aspects of disease susceptibility and pathogenesis. Mice provide a particularly useful model to study RSV for a number of reasons, including availability of immunologic reagents, relative ease of care, wide variety of inbred and congenic strains, and similarity between mouse and human genomes (approximately 99% of 30,000 genes are similar). Furthermore, different inbred mouse strains can display variable degrees of susceptibility to RSV, thereby providing a highly useful tool to study underlying genes that confer susceptibility or resistance to disease. For example, inbred C57BL6/J mice are naturally more resistant to RSV infection than BALB/c mice which display a heightened susceptibility to infection (152). In addition to natural susceptibility differences, certain mice, BALB/c in particular, faithfully reproduce many aspects of FI-RSV vaccine enhanced disease, thereby providing researchers with a useful model to study safety and efficacy of experimental vaccines (131, 169). Interestingly, cotton rats (*Sigmodon hispidus*) reproduce aspects of FI-RSV vaccine-enhanced disease and are approximately 100 times more permissive to RSV infection than mice, but the small number of immunologic reagents limits the usefulness of this model. Furthermore, because mice

and humans can differ in responses to certain vaccines, primates can be used to more accurately predict immunologic responses, but research with primates is generally cost-prohibitive. Therefore, the majority of research examining RSV pathogenesis and vaccine responses is often confined to studies in suitable mouse models.

Developing a novel vaccine strategy for RSV

Previous attempts to develop RSV vaccine

As previously indicated, FI-RSV vaccination not only resulted in poor protection but also, disease enhancement and, in some cases, death upon subsequent RSV infection (82, 85). Many subsequent studies have attempted to define the reasons for this response. These studies consistently showed that enhanced disease is accompanied by unbalanced Th2-biased cytokine responses, weak CD8+ T cell responses, pronounced eosinophilia, and induction of low affinity and non-neutralizing antibodies (39, 41, 133, 135, 169). Less clear are the precise properties of the FI-RSV vaccine that led to these results (reviewed in (99)). Absence of these characteristics of enhanced disease is now one of the benchmarks for development of a successful RSV vaccine. Subunit vaccines designed to exploit the potential immuogenic potential of the G and F proteins alone have had limited success in mice (65, 67, 68). One interesting strategy, incorporation of G and/or F protein along with a known TLR agonist, has yielded protective effects in mice (66), but these adjuvants have not been approved for use in humans in the United States.

Thus far, no vaccine approach reported in animal models has translated into a licensed vaccine for use in humans.

Virus-like particles as vaccine candidates

A virus-like particle (VLP) vaccine strategy has not been reported for RSV. VLPs are large particles, the size of viruses, composed of repeating structural arrays on their surfaces and in their cores, structures that mimic those of infectious viruses ((reviewed in (77, 121)). VLPs are formed by the assembly of the structural proteins and lipids into particles but without the incorporation of the viral genome. Thus, VLPs are incapable of multiple rounds of infection typical of an infectious virus, yet they retain the superb antigenicity of virus particles. Native viral antigens arrayed on VLP surfaces and in their cores likely contribute to potent humoral responses, CD4 T cell proliferation, and expansion of cytotoxic CD8 T cells, unlike less immunogenic subunit vaccines often comprised of individual purified viral proteins (20-22, 53, 94, 101, 143, 156). The potential of VLPs as safe, effective vaccines for viral disease is increasingly recognized. Indeed, two VLP vaccines are now licensed for use in humans, the papilloma virus vaccine and the hepatitis B virus vaccine, and a number of other VLP vaccines are being evaluated in preclinical and clinical trials (reviewed in (77)). Therefore, VLPs expressing one or both RSV glycoproteins may be an attractive strategy for designing an effective RSV vaccine.

VLPs as candidate vaccine for RSV

There is only one report of VLPs formed with RSV proteins (162). These particles have not been well characterized and the efficiency of VLPs released from infected cells is unknown. Furthermore, their detection required incorporation of a minigenome. However, it has previously been reported that the expression of the four major structural proteins of NDV, an avian paramyxovirus, results in the very efficient release of particles that structurally and functionally resemble virus particles ((127) McGinnes et al., in preparation). Further, these particles (ND VLPs) stimulated potent anti-NDV immune responses in mice, including neutralizing antibody responses (McGinnes et al., in preparation). These results suggest that ND VLPs could serve as a platform for the expression of antigens from human viruses, including RSV G and F proteins, and that these particles could serve as an effective RSV vaccine.

Research objectives

In chapters II and III the role of TLRs in activating innate immune responses against RSV has been explored. We examined whether RSV could promote activation of innate immunity through TLR2 signaling. TLR2 is expressed on the surface of immune cells and tissues as a heterodimer complex with either TLR1 or TLR6 (3). TLR2 and TLR1 or TLR2 and TLR6 complexes recognize bacterial peptidoglycan motifs as well as a diverse range of viruses, including HCV, HSV, LCMV, and HCMV and strongly

promote early innate inflammatory responses after viral recognition (27, 32, 89, 177). Genetic analysis and vaccine studies in BALB/c mice indirectly suggest that TLR2 signaling may be involved in RSV recognition. However, these studies did not investigate whether TLR2 directly interacts with RSV (36, 66, 76). We wished to examine further the inferred relationship between RSV and TLR2 because identifying novel pathways by which RSV activates innate immunity could aid the development of safe and effective RSV vaccines. In this study, we demonstrate that RSV interacts with TLR2 and TLR6, but not TLR1, and this interaction activates innate immunity.

Furthermore, in chapter IV, we report that the ectodomain of the RSV G protein, fused to the cytoplasmic tail (CT) and the transmembrane (TM) domain of the NDV hemagglutinin-neuraminidase (HN) protein, can be efficiently incorporated into VLPs containing the NDV NP and M protein, and these particles can be quantitatively prepared and used as an immunogen. We demonstrated that immunization with these particles stimulated robust soluble and cell-mediated immune responses. Additionally, they conferred protection in BALB/c mice, following live RSV challenge, characterized by increased viral clearance in lung tissue. Finally, infectious RSV challenge of mice following VLP-H/G immunization did not result in enhanced lung pathology typified by FI-RSV immunization (33, 34, 119)

Chapter II

Introduction

The role of TLR in activating innate immune responses against RSV has become increasingly clear. Previous studies in mouse models lacking particular TLRs clearly demonstrated an association between RSV and host TLRs in activating intracellular signaling pathways that lead to the induction of pro-inflammatory innate immune responses. These studies have implicated particular TLRs, including TLR3, 4, and 7 in mediating innate immune responses to RSV. In this chapter we describe an additional TLR pathway, TLR 2/6, that is important for activating innate immunity against RSV. The involvement of multiple TLRs in the host innate immune response is likely very important because signals generated by different TLRs after pathogen recognition likely activate different components of the innate immune response, ultimately shaping host acquired immune responses which lead to proper viral clearance, or in certain instances, may lead to a RSV induced disease phenotype.

Results

BALB/c mice exhibit differences in sensitivity to TLR2 ligands and RSV compared to C57BL6/J mice

Kinetic studies were conducted to examine the duration of RSV infection in different inbred strains of mice. Data shown here confirm previous reports suggesting that C57BL6/J mice are resistant to RSV infection, as based on peak virus titer and detection of virus in lung homogenates of infected mice throughout the duration of the time course (Table 2.1) (162). Furthermore, BALB/c mice are more permissive to RSV infection when compared to C57BL6/J mice and to semi-permissive B6.129F2/J mice. At the peak of virus infection (day 4), BALB/c mice had 30-fold more virus in lung homogenates than C57BL6/J mice. Therefore, experiments were conducted to further characterize the early inflammatory response to RSV in BALB/c and C57BL6/J macrophages. Macrophages from BALB/c mice showed decreased responsiveness to live RSV stimulation and the TLR2 agonist Pam_2CSK_4 (Figure 2.1). Furthermore, BALB/c macrophages showed decreased upregulation of surface TLR2 following RSV stimulation, suggesting a possible association between RSV and TLR2 signaling (Figure 2.2). Since mice lacking specific TLRs are only available on the C57BL6/J background, we wished to test the aforementioned association in this model.

TLR2 and TLR6 but not TLR1 recognize RSV

The role of TLRs in response to RSV was examined using TLR deficient mice. Thioglycollate-elicited peritoneal macrophages from C57BL/6, TLR2 KO, and TLR4 KO

Table 2.1 Kinetics of RSV infection in various inbred mouse strain

	C57BL6/J	BALB/c	B6.129F2/J
Day	RSV Titer log10	RSV Titer log10	RSV Titer log10
2	< LLD (n=12)	0.93 +/- 0.11 (n=9)	1.51 +/- 0.19 (n=6)
3	< LLD (n=3)	ND	ND
4	0.82 +/- 0.07 (n=22)	2.54 +/- 0.16 (n=9)	2.32 +/- 0.07 (n=9)
5	< LLD (n=3)	ND	ND
7	< LLD (n=3)	1.98 +/- 0.23 (n=9)	1.8 +/- 0.28 (n=3)
8	< LLD (n=3)	ND	ND
10	ND	< LLD (n=6)	ND
13	< LLD (n=3)	ND	ND
14	< LLD (n=3)	< LLD (n=3)	ND

Table 2.1 Kinetics of RSV infection in various inbred mouse strains

Wild-type C57BL/6, BALB/c, and B6.129F2/J mice were infected i.n. with RSV A2 (2.4×10^6 PFU/mouse). Lung samples were collected post-infection at the time-point indicated and enumerated for PFU using an immunoplaque assay described in the methods section. Mean titer is represented as $\log_{10}$ PFU/gram of lung tissue +/- SEM. LLD indicates below lower limit of detection. ND indicates not determined.

Figure 2.1 C57BL6/J PECs are more responsive to TLR ligands and RSV than BALB/c PEC

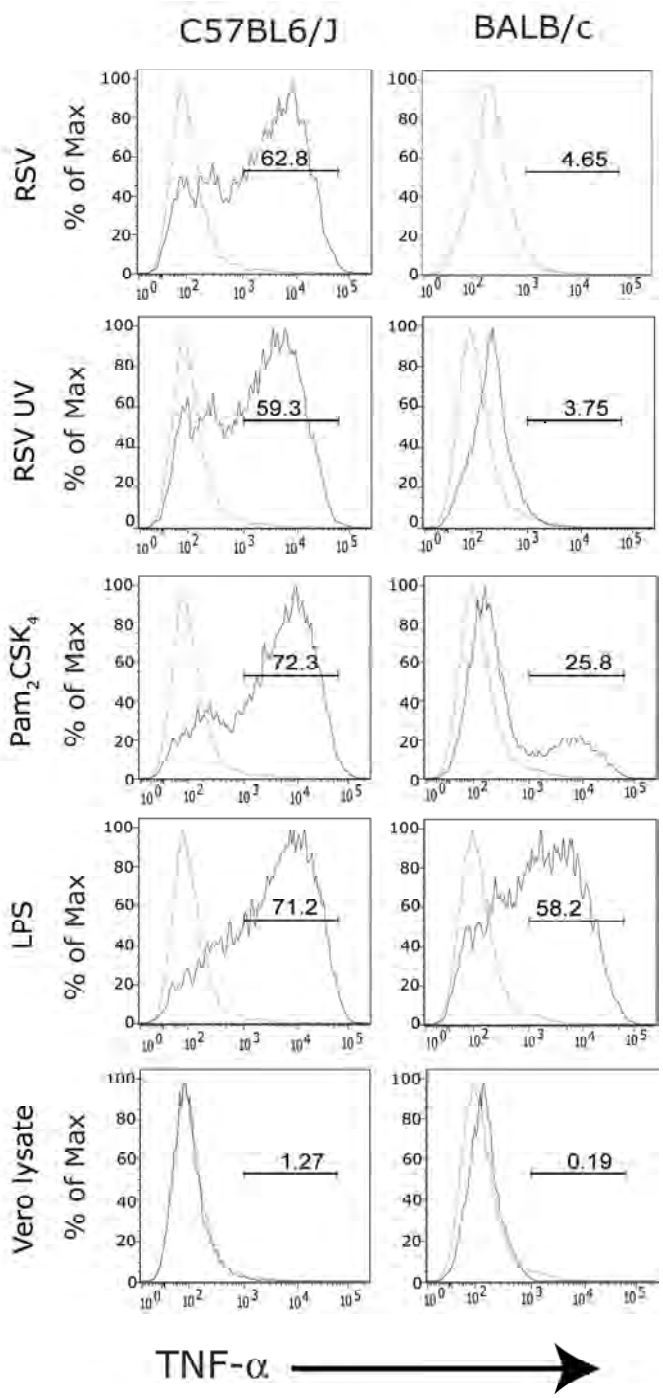

Figure 2.1

C57BL6/J PECs are more responsive to TLR ligands and RSV than BALB/c PECs

Macrophages were harvested four days after thioglycollate treatment from C57BL6/J and BALB/c mice. Macrophages were stimulated with RSV (0.3 MOI), UV-inactivated RSV (0.3 MOI equivalent), LPS (TLR4 ligand, 100 ng/ml), Pam_2CSK_4 (TLR2 ligand, 100ng/ml), or Vero cell lysate (50 ul) in the presence of Brefeldin A as indicated. Cells were stained for CDllb, permeabilized, and stained for intracellular TNF-α. Values indicate % of $CDllb^+$ macrophages producing TNF-α. TNF-α production (black line) was compared to isotype control (grey line).

Figure 2.2 C57BL6/J PECs express more surface TLR2 than BALB/c PECs after RSV stimulation

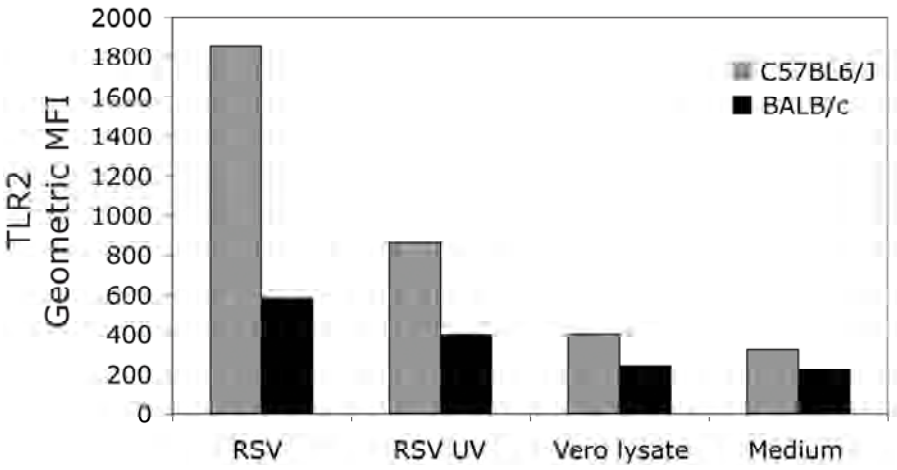

Figure 2.2 C57BL6/J PECs express more surface TLR2 than BALB/c PECs after RSV stimulation

Macrophages were harvested four days after thioglycollate treatment from C57BL6/J and BALB/c mice. Macrophages were stimulated with RSV (0.3 MOI), UV-inactivated RSV (0.3 MOI equivalent), Vero cell lysate (50 ul), or medium alone (50 ul) for 24 hours. Cells were harvested and stained for CDllb and TLR2 expression. Values indicate mean fluorescence intensity (MFI) of TLR2 expression on $CDllb^{+}$ macrophages.

mice were stimulated with RSV in the presence of Brefeldin A, and intracellular cytokine levels were measured by flow cytometry. Macrophages from both TLR2 KO and TLR4 KO mice produced lower levels of intracellular TNF-α compared to wild-type cells following RSV infection (Figure 2.3). Interestingly, macrophages from TLR2 KO mice produced the lowest levels of TNF-α, i.e., less TNF-α compared to TLR4 KO mice and wild-type mice (4% vs. 33% and 51% respectively), suggesting a major role for TLR2 in the induction of pro-inflammatory cytokines following RSV stimulation. Controls indicated that TLR2 KO mice responded normally to LPS (TLR4 ligand) stimulation and that TLR4 KO mice responded normally to Pam_2CSK_4 (TLR2 ligand).

To examine whether RSV replication was required to elicit TNF-α production, wild-type macrophages were stimulated with live RSV or UV-inactivated RSV (confirmed by immunoplaque assay, data not shown) and intracellular TNF-α was measured. The response to RSV and RSV-UV was equivalent, indicating that RSV replication was not required to stimulate intracellular TNF-α production (Figure 2.4). To limit the possibility that contaminating products in the Vero cell-propagated RSV might activate TLR2 signaling, sucrose-purified RSV and UV-inactivated purified RSV (a generous gift from Dr. Trudy Morrison) were used to stimulate wild type macrophages. RSV was purified using methods previously described (54, 87). Purified RSV stimulated wild-type macrophages equivalently to Vero cell-propagated RSV, indicating that RSV itself, and not contaminating products in the medium, activated TLR2 signaling (Figure 2.5).

Figure 2.3 TLR2 associates with RSV

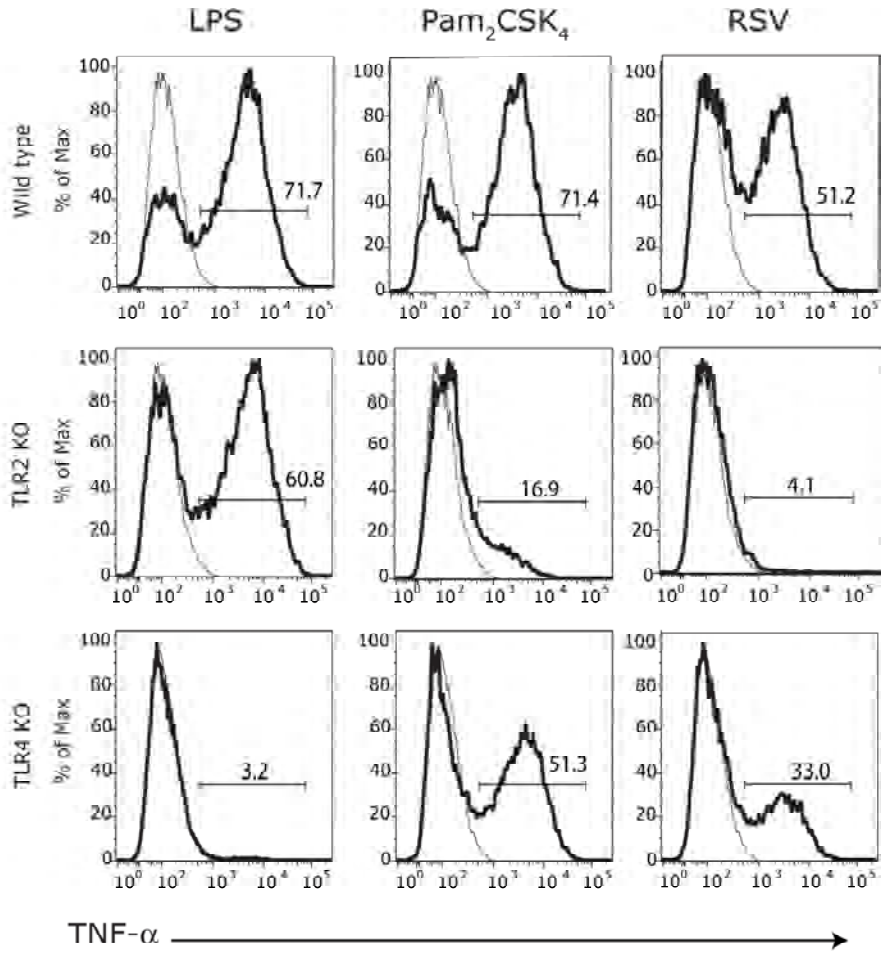

Figure 2.3 TLR2 associates with RSV

Macrophages were harvested four days after thioglycollate treatment from wild type, TLR2 KO, and TLR4 KO mice. Macrophages were stimulated with RSV (0.3 MOI), LPS (TLR4 ligand, 100 ng/ml), or Pam_2CSK_4 (TLR2 ligand, 100 ng/ml) for 24 hours in the presence of Brefeldin A as indicated. Cells were stained for CDllb, permeabilized, and stained for intracellular TNF-α. Values indicate % of $CDllb^+$ macrophages producing TNF-α. TNF-α production (black line) was compared to isotype control (grey line).

Figure 2.4 RSV replication is not required to elicit TLR2 responses

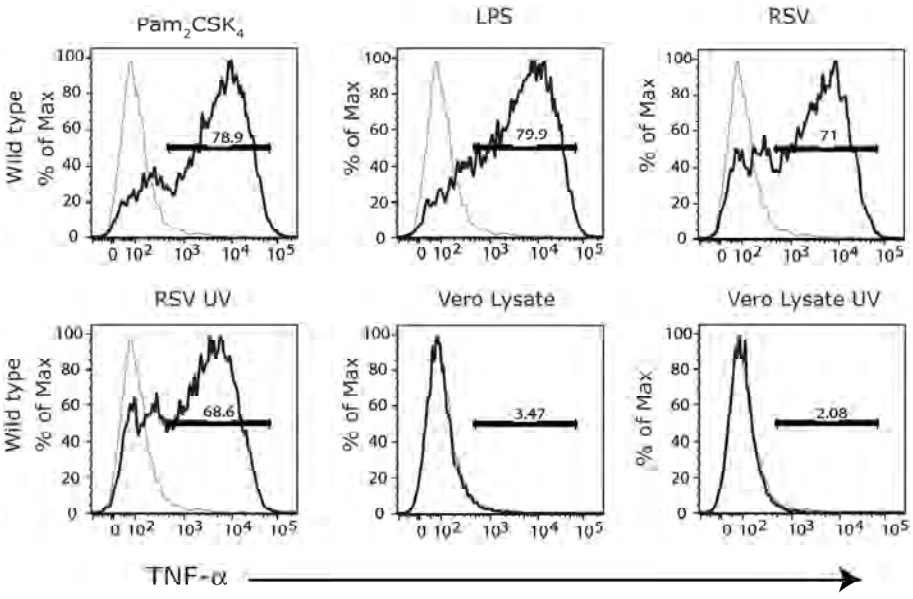

Figure 2.4 RSV replication is not required to elicit TLR2 responses

Macrophages were harvested four days after thioglycollate treatment from wild-type mice. Macrophages were stimulated with Pam_2CSK_4 (TLR2 ligand, 100 ng/ml), LPS (TLR4 ligand, 100 ng/ml), RSV (0.3 MOI), UV-RSV (0.3 MOI equivalent), Vero cell lysate (50 ul),or UV-Vero cell lysate (50 ul), for 24 hours in the presence of Brefeldin A. Cells were stained for CDllb, permeabilized, and stained for intracellular TNF-α. Values indicate % of $CDllb^+$ macrophages producing TNF-α. TNF-α production (black line) was compared to isotype control (grey line).

Figure 2.5 Sucrose-purified RSV stimulates PECs similar to Vero cell-propagated RSV

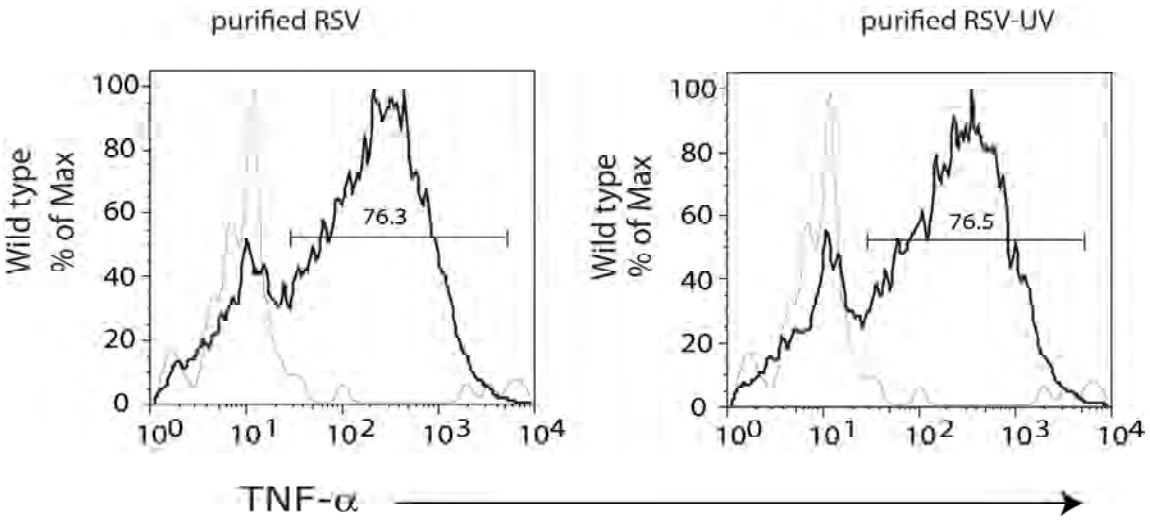

Figure 2.5 Sucrose-purified RSV stimulates PECs similar to Vero cell-propagated RSV

Macrophages were harvested from wild-type mice four days after thioglycollate treatment. Wild-type macrophages were stimulated with sucrose purified RSV (0.02 MOI) or UV-inactivated sucrose purified RSV (0.02 MOI equivalent) (**d**). Cells were stained for CDllb, permeabilized, and stained for intracellular TNF-α. Values indicate % of $CDllb^+$ macrophages producing TNF-α. TNF-α production (black line) was compared to isotype control (grey line).

Figure 2.6 TLR2 dimer partner TLR6, but not dimer partner TLR1, recognizes RSV

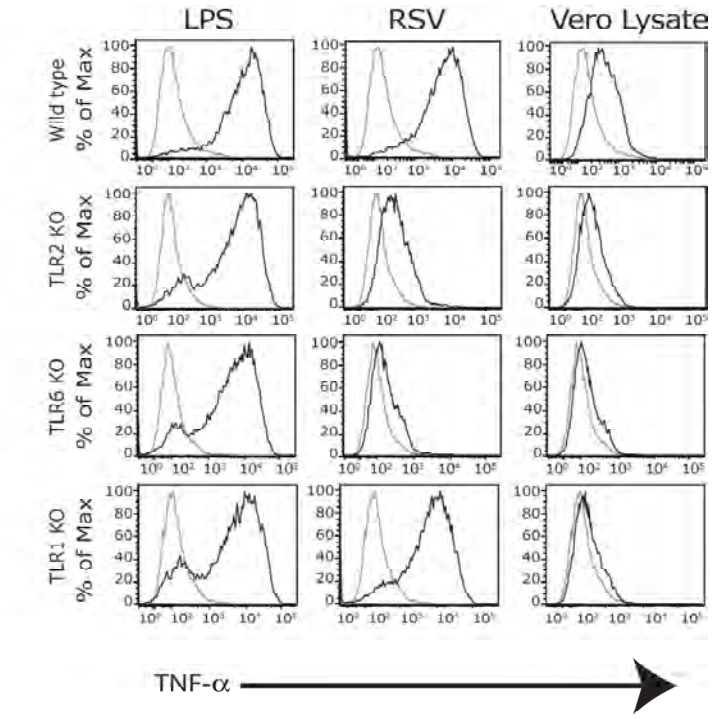

Figure 2.6 TLR2 dimer partner TLR6, but not dimer partner TLR1, recognizes RSV

Macrophages were harvested four days after thioglycollate treatment from wild type, TLR1 KO, TLR2 KO, and TLR6 KO mice. Macrophages were stimulated with RSV (0.3 MOI), LPS (TLR4 ligand, 100 ng/ml), or Vero cell lysate (50 ul) for 24 hours in the presence of Brefeldin A. Cells were stained for CDllb, permeabilized, and stained for intracellular TNF-α. TNF-α production (black line) was compared to isotype control (grey line).

TLR 2 and TLR 6 but not TLR1 initiate inflammatory responses following ligation with RSV

Since TLR2 can partner with either TLR1 or TLR6 on the cell surface to propagate downstream signaling, we examined whether TLR1 or TLR6 in conjunction with TLR2 was involved in RSV signaling. Wild type, TLR2 KO, TLR1 KO, and TLR6 KO macrophages were stimulated with RSV, and TNF-α levels were measured. A role for TLR6, but not TLR1, was observed in RSV-induced, TLR-mediated cytokine production (Figure 2.6). As expected, MyD88 KO mice, lacking signaling via TLR2, TLR1, and TLR6, did not produce TNF-α in response to RSV (data not shown).

We further examined the role of TLRs in cytokine and chemokine secretion following RSV challenge by measuring cytokine protein levels from *in vitro* cultured macrophages using ELISA. Macrophages from TLR2 KO and TLR6 KO mice produced significantly less IL-6 (Figure 2.7), and CCL2 (MCP-1) (Figure 2.8) compared to wild-type cells following RSV infection.

Additionally, a role for TLR4 in the production of inflammatory cytokines IL-6 and CCL2 was observed in the TLR4 KO mice. CCL5 (RANTES) production was also decreased in both TLR2 KO and TLR6 KO mice compared to wild-type macrophages after RSV challenge (Figure 2.8). CCL5 production in TLR4 KO was lower compared to wild-type cells but was higher compared to TLR2 KO or TLR6 KO macrophages (WT>TLR4 KO>TLR2 KO and TLR6 KO).

Figure 2.7 TLR2 and TLR6 mediate inflammatory cytokine production in response to RSV

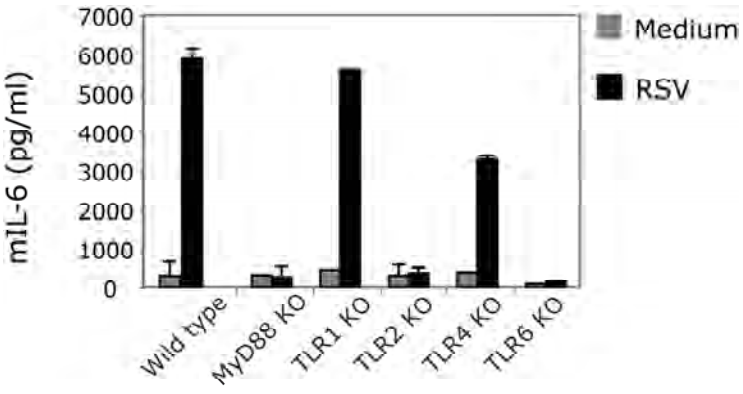

Figure 2.7 legend

Macrophages were harvested from wild type, MyD88 KO, and TLR KO mice and were stimulated with RSV (0.3 MOI) or medium control for 24 hours. Culture supernatants were harvested and tested for IL-6 production using ELISA. Error bars are +/- SD.

Figure 2.8 TLR2 and TLR6 mediate chemokine production in response to RSV

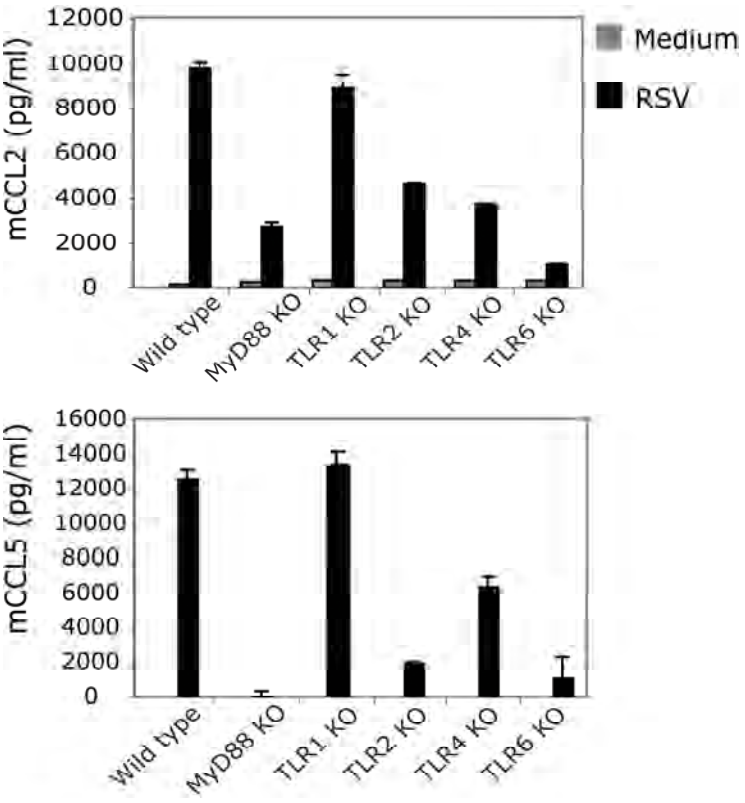

Figure 2.8 TLR2 and TLR6 mediate chemokine production in response to RSV

Macrophages were harvested from wild type, MyD88, and TLR KO mice and were stimulated with RSV (0.3 MOI) or medium control for 24 hours. Culture supernatants were harvested and tested for CCL2 and CCL5 production using ELISA. Error bars are +/- SD.

Furthermore, MyD88 KO mice exhibited decreased production of each cytokine and chemokine assayed in response to RSV. Since MyD88 is essential for TLR2, TLR6, and partially for TLR4 signaling, these data supports the hypothesis that TLR-driven MyD88-dependent signaling was important for early cytokine and chemokine production in response to RSV.

Next, type I IFN responses to RSV in TLR KO mice were examined. RSV induced similar levels of type I IFN in the wild type-mice compared to each TLR KO group (Figure 2.9). Poly I:C (TLR3 ligand) has been shown to stimulate type I IFN production independent of TLR1,2,4,6 (175). RSV-induced type I IFN production was similar to Poly I:C-induced type one interferon production in wild type and TLR KO mice. LPS has also been shown to induce type I IFN production albeit to a lesser extent than Poly I:C. As expected wild type and TLR 1,2,6 KO mice produced equivalent amounts of type I IFN to LPS, while TLR4 KO did not respond to LPS. This data suggests that RSV induces type I IFN production independent of TLR2 and TLR6 signaling.

Figure 2.9 TLR2 and TLR6 are not involved in type I interferon production following RSV recognition

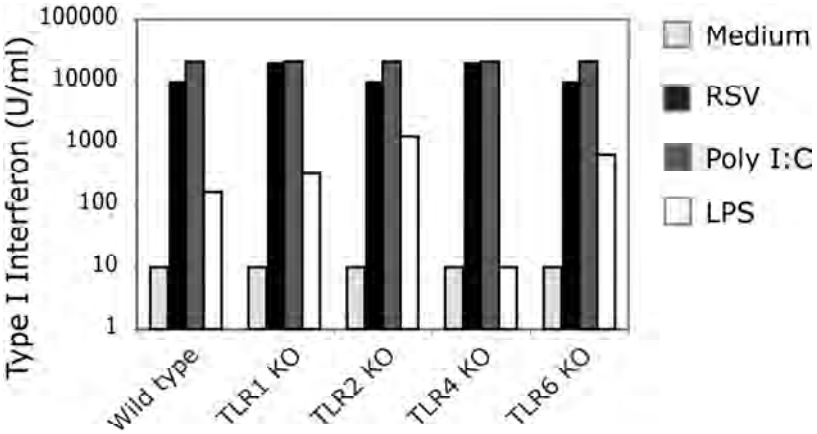

Figure 2.9 TLR2 and TLR6 are not involved in type I interferon production following RSV recognition

Macrophages were harvested from wild-type, TLR1, TLR2, TLR4 and TLR6 KO mice. Macrophages were stimulated with RSV (2 MOI), Poly I:C (TLR 3 ligand, 50 ug/ml), LPS (TLR 4 ligand,100 ng/ml), or medium alone for 24 hours. Harvested supernatants were tested for type I interferon production.

Discussion

Activating host immune responses during RSV infection is dependent on complex signaling events initiated in part by TLRs. These coordinated signaling events promote the production of cytokines, chemokines, and IFN α, β, and γ that ultimately dictate the type of inflammatory environment (Th1 or Th2) in the lung. Interestingly, the type of inflammatory environment generated during these early signaling events likely alters subsequent Th responses because susceptible infants exhibit skewed Th2 responses (12). Since recent findings have implicated TLR-mediated inflammation as potentially involved in the immunopathogenesis of RSV disease, emphasis has been placed on understanding how TLRs can influence immune responses against RSV (9, 16, 90, 125, 140, 165).

Initial studies conducted by Kurt-Jones et al. used C57BL/10ScNCr strain (TLR4 mutant due to a deletion mutation) to examine the interactions between RSV and TLR4. However, during the final publication review, the strain designation was changed to C57BL/10ScCr (TLR4-deficient and IL-12 deficient), an error that was not caught by Kurt-Jones et al. during revision (unpublished). Nevertheless, the authors demonstrated that intranasal (i.n.) infection of RSV in the TLR4 mutant mice resulted in delayed viral clearance at 10 days post infection compared to wild-type mice. In a follow-up study published by the same group, Haynes et al. again used the C57BL/10ScN mice (TLR4-deficient) to confirm their original findings (71). Importantly, Haynes et al. indicated in the text that “C57BL/10ScNCr strain is homozygous for a null mutation of the TLR4

gene…a related mouse strain, C57BL/10ScCr (not used in these studies), has a reported defected in interleukin 12 (IL-12)-induced production of gamma interferon (IFN-γ)…The C57BL/10ScN mice used in the present study were IL-12 responsive and expressed IFN-γ at levels similar to those of the wild-type." In contrast to these studies other investigators examined the perceived interaction between TLR4 and paramyxoviruses, including RSV, PMV, and Sendai virus, and found no association. Briefly, Ehl et al. investigated whether deficiencies in TLR4, or deficiencies in IL-12R, could contribute to RSV susceptibility in the C57BL/10ScCr mouse (45). The authors concluded that increased susceptibility to RSV in this mouse model was due to defects in IL-12R rather than defects in TLR4. Second, studies by Van der Sluijs et al. explored the possible interaction between Sendai virus and TLR4 using C3H/HeJ (TLR4 mutant) mice (166). In summary, the authors were unable to find evidence of an interaction between Sendai virus and TLR4. Furthermore, studies by Faisca et al. examined the interaction between pneumonia virus of mice (PVM), a member of the pneumovirus genus, and TLR4 using TLR4 mutant mice (46). Since RSV and PVM share many similarities the authors suggested that the responses to both pathogens in the mouse should be similar. Additionally, the authors indicated that PVM is a natural mouse pathogen while RSV is not suggesting that PVM would be a more suitable model for examining TLR4 and pneumovirus interactions in the mouse. In summary, the authors concluded that there was no evidence of an interaction between TLR4 and PVM. Collectively, these studies seemed to suggest that some members of the paramyxoviridae family, including Sendai, PVM, and RSV, do not interact with TLR4 to activate innate immune responses.

However, data briefly summarized below suggest that RSV does indeed interact with TLR4 to promote innate immune activation.

Following the Kurt-Jones et al. and Haynes et al. observations, Haeberle et al. used C3H/HeJ mice (TLR4 point mutation leading to LPS unresponsiveness) and demonstrated that NF-κB activation by RSV *in vivo* involves TLR4 (61). Additionally, studies by Boukhvalova et al. in cotton rats establish that the formalin-inactivated vaccine strain of RSV stimulates a Th2-like response and this effect can by blocked using TLR4 antagonists (16). Furthermore, studies by Vogel and colleagues demonstrate a clear linkage between RSV disease in high- risk infants and particular TLR4 polymorphic alleles suggesting that TLR4 plays a significant role in RSV pathogenesis in humans (9). Interestingly, Rassa et al. demonstrated that MMTV, a murine retrovirus, also activated innate immunity via TLR4 (137). Therefore, literature published by several different groups seems to indicate an important role for TLR4 in the activation of innate immunity in response to RSV infection. Herein we have outlined some important factors that could highly affect study outcomes. First, different inbred mouse strains do express different levels of baseline and induced TLR, including TLR4 that could likely contribute to differences in innate and acquired immune activation. Importantly, C57BL/10ScN, C57B10/ScCr and C57BL/6 are distinct mouse strains that possibly differ in TLR expression. Once TLR4 is activated, Macrophages and DCs start producing a variety of soluble factors that direct T helper cell differentiation and activation of innate and adaptive immune pathways in a fashion that is not completely understood. Second, the dose of RSV administered can influence disease outcome because high inocula of RSV

are required to elicit immune activation in mice. Third, frozen RSV stocks have been shown to lose a substantial amount of activity over time (> 6 months). Therefore, it is critical to use recently propagated stocks for *in vivo* experiments to ensure optimum immune activation in mice. Fourth, the cell lines in which RSV is propagated can greatly affect infectivity. For example, studies by Taylor et al. have shown that genetically similar mice infected i.n with equivalent titers of RSV isolated from different cell lines show significant differences in the amount of virus recovered from the lungs (160). Collectively, differences in these parameters could influence experimental results between investigators.

The present study used C57BL6/J mice that lacked the TLR4 gene (TLR4 KO), and data presented here supports our original observations, further suggesting a role for TLR4 mediated innate immune activation in response to RSV, e.g., TLR4 deficiency blunted the cytokine response to RSV infection. Additionally, we extended our initial observations by demonstrating that TLR2 signaling can also activate innate immunity in response to RSV.

Studies presented here also provide evidence for direct interactions between RSV and TLR2 and TLR6, but not TLR1. These findings are important because the lung cytokine and chemokine milieu is thought to directly shape cellular processes within the lung that prevent or promote RSV-induced disease (12). Macrophages from TLR2 and TLR6 KO mice exhibited decreased production of TNF-α *in vitro*. TNF-α has been linked to both viral clearance and exacerbated airway disease, suggesting one mechanism by which the characteristics of the immune response might dictate disease outcome. In

fact, previous work indicates that RSV does indeed modulate TNF-α secretion, i.e. the small hydrophobic (SH) protein inhibits TNF-α secretion (51). RSV likely inhibits a major inflammatory component of TLR2 signaling by limiting TNF-α signaling. Additionally, recent findings suggest that TNF-α can modulate TLR2 expression. Therefore, it is possible that RSV could further alter immune activation by limiting TLR2 expression (157). Signaling through TLR2 and TLR6 controlled expression IL-6, an important inflammatory mediator that is linked to RSV pathology (104). In a model of airway allergic inflammation, TLR2 engagement can induce IL-6 production in response to mycoplasma and the lack of IL-6 production was associated with impaired bacterial clearance (174). Therefore, TLR2-dependent IL-6 production, in conjunction with TNF-α, may play a key role in mediating viral clearance.

TLR2 and TLR6 signaling promoted production of chemokines CCL5 and CCL2. Both chemokines are linked to RSV pathogenesis (35, 122, 161). CCL5 is produced primarily by Th1 polarized cells and can influence both innate and acquired leukocyte migration (95). CCL2 functions as a potent chemotaxic molecule for monocytes, including neutrophils, and can influence Th polarization towards Th2 by stimulating IL-4 production in T cells (60). In fact, recent studies associate increased CCL2 production with skewed Th2 responses in RSV G primed BALB/c mice. However, this study did not address whether CCL2 causes or results from a Th2 polarized inflammatory environment (35). It is likely that CCL2 can influence Th2 polarization, as mice deficient in CCL2 cannot mount strong Th2 responses (60). Interestingly, studies by Liu et al. demonstrate a role for TLR3 and RIG-I in mediating IFN-β production and NF-κB/RelA transcription

by lung epithelial cells in response to RSV (100). Furthermore, our studies indicated that TLR2 and TLR 6 signaling was important for NF-κB dependent cytokine and chemokine production but not type I IFN production, suggesting that activation of innate immunity occurs via multiple TLRs in response to RSV to provide optimum protection against RSV-induced disease. In light of the finding presented here it is possible that defects in TLR2 signaling could bias responses towards Th2 cytokine and chemokine responses in genetically susceptible individuals. Our *in vitro* studies examined the early inflammatory response initiated by peritoneal macrophages in response to RSV. Additionally, Suzuki et al. demonstrated that murine alveolar macrophages and peritoneal macrophages express similar levels of TLR2 and respond equally to TLR2 ligands, suggesting that alveolar macrophages and peritoneal macrophages likely exhibit similar responses to RSV(155). Lung epithelial cells express TLR2 and may produce additional inflammatory components that further contribute to the early inflammatory environment (8, 154). Collectively, these findings suggested that control of cytokine and chemokine production by TLR2 is likely critical for supporting viral clearance while limiting RSV-induced disease.

Chapter III

Introduction

In the previous chapter we described a role for TLR2 and 6, but not TLR1 in propagating innate immune signals following RSV recognition. In this chapter we extended these findings by examining the role of TLR2 and TLR6 in controlling RSV replication. Furthermore, we examined the role of these TLR in activating DCs and the consequences of abrogated TLR2 and TLR6 signaling on the recruitment of innate leukocytes, including neutrophils, into the lungs of RSV-infected mice. Herein, these findings confirmed a physiological role for TLR2 and 6 signaling in the clearance of RSV from the lungs. Furthermore, TLR2 and 6 signals were also involved in DC maturation and the early recruitment of neutrophils into the lungs. Thus these data suggest TLR2/6 signals are important for modulating pro-inflammatory responses against RSV. This also suggests that TLR2/6 signaling may play a critical role in determining disease susceptibility following natural RSV infection.

Results

RSV replication in TLR KO mice

To examine the role of TLRs in RSV replication after *in vivo* infection, C57BL/6, TLR2 KO, TLR4 KO, and TLR6 KO mice were infected by intranasal (i.n.) instillation of 2.4×10^6 PFU/mouse of RSV. Lungs were harvested four days after infection and virus levels were determined by immunoplaque assay. Kinetic studies examining the day of peak virus titer in RSV resistant C57BL/6 as well as RSV permissive BALB/c and semi-permissive B6.129F2/J mice indicated virus titer peaked at day 4 in all strains tested (Table 2.1). These findings were in agreement with previous studies that demonstrated peak viral titer in mouse models occurs approximately 4 days after infection (152). Importantly, data summarized in Table 2.1 and previous studies have shown that wild-type C57BL/6 mice readily cleared RSV, resulting in significantly diminished virus recovery compared to more susceptible mouse strains such as BALB/c even at the day of peak viral load, day 4 post-infection (152).

Although the TLR KO mice were back-crossed onto the resistant C57BL/6 background, RSV was readily recovered from the lungs of TLR2, TLR4, and TLR6 KO mice. A significantly higher peak viral load was observed in TLR2 KO and TLR6 KO mice compared to wild type mice on the C57BL/6 background (Figure 3.1). These data also indicated a significant difference in peak viral titer between TLR4 KO mice and C57BL/6 wild-type mice with higher viral loads in TLR4 KO mice. These findings confirm our original observations using mice with deficiencies in TLR4 on the C3H and

Figure 3.1 RSV replication in TLR KO mice

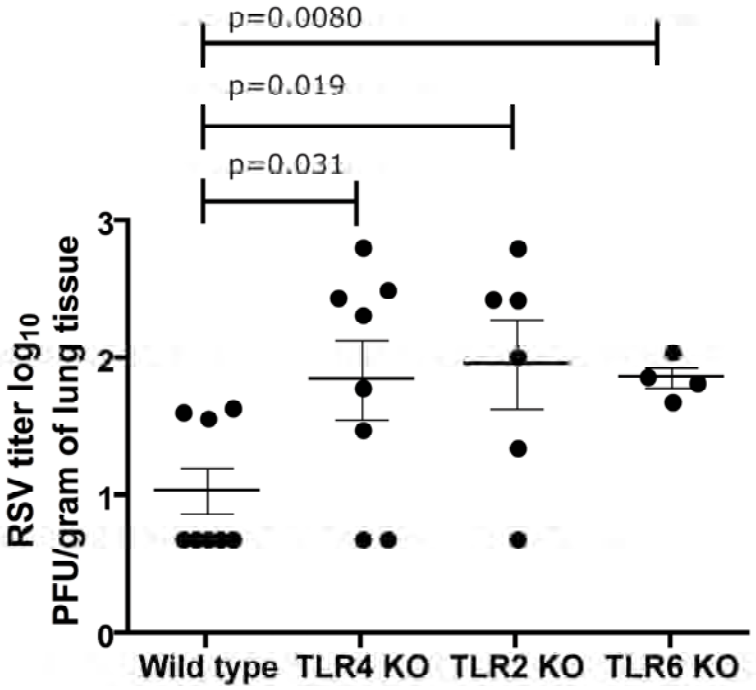

Figure 3.1 RSV replication in TLR KO mice

Wild type (n=8), TLR4 KO (n=8), TLR2 KO (n=6), and TLR6 KO (n=4) mice were infected by intranasal inoculation with RSV A2 strain (2.4×10^6 PFU/mouse). Lungs were harvested 4 days after infection and plaques were enumerated using a Vero cell immunoplaque assay described in materials and methods. Titer is represented as $\log_{10}$ PFU/gram of lung tissue. Solid lines represent the mean $1\log_{10}$ for each group. Error bars are +/- SEM. Note: Mice that were negative for RSV by plaque assay were scored at 0.5 times the lower limit of detection.

the C57BL/10 genetic backgrounds, which indicated that TLR4 was involved in RSV clearance (90). Significantly higher virus titers in TLR2 KO and TLR6 KO lungs suggest an important role for TLR2 and TLR6 in controlling RSV replication *in vivo*.

TLR2 signals promote neutrophil recruitment and DC activation in response to RSV

To examine a possible role for TLR2 in the production of early inflammatory mediators in wild-type vs. TLR2 KO mice in response to RSV, wild-type C57BL/6, TLR2 KO, and MyD88 KO mice were infected, i.n., with 2.4 x 10^6 PFU/mouse of RSV. Uninfected groups of each were used to control for lung cytokine production and leukocyte infiltrate. Whole lungs and bronchoalveolar lavage (BAL) were collected at 24, 48, and 96 hours post-infection. Total cellular CCL2 levels were measured from lung homogenates, since CCL2 is produced following TLR2 activation. A significant decrease in CCL2 was observed in TLR2 KO compared to wild-type lungs at 24 hours post-infection (Figure 3.2). CCL2 was undetectable at 48 and 96 hours post-infection in all groups (data not shown). MyD88 KO mice did not produce detectable levels of CCL2 compared to wild-type. Although uninfected mice produced detectable basal levels of TNF-α, IL-6, and CCL5, we were unable to observe differences in cytokine and chemokine production in lung homogenates between groups (data not shown). This data suggested TLR2 signaling is involved in early CCL2 production within the lungs of RSV infected mice. Since CCL2 is a potent leukocyte chemoattractant, the early recruitment of leukocytes to the lung following RSV infection

Figure 3.2 TLR2 signaling promotes CCL2 production *in vivo*

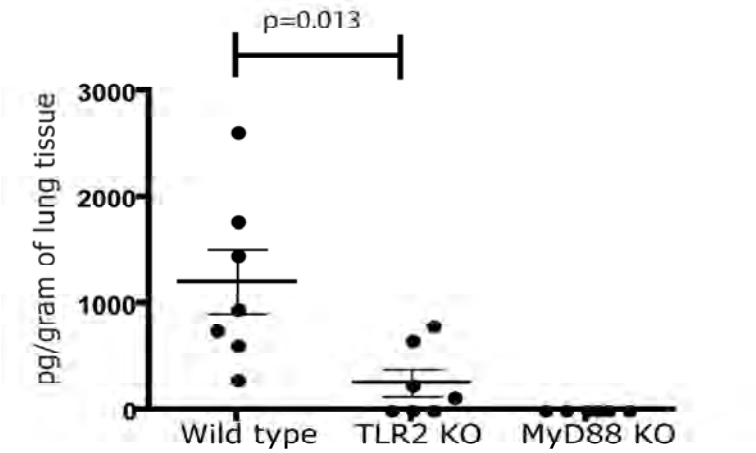

Figure 3.2 TLR2 signaling promotes CCL2 production *in vivo*

Wild-type, TLR2 KO, and MyD88 KO mice were infected by intranasal instillation with RSV A2 strain (2.4 x 10^6 PFU/mouse). Uninfected mice (n=3) were used to control for lung cytokine production. Lung tissue was harvested 24 hours post-infection. Tissues were homogenized and tested for CCL2 production by ELISA (Wild type and TLR2 KO, n=7) (MyD88 KO, n=6). Data are represented as pg/gram of lung tissue. Solid lines represent the mean for each group. Error bars are +/- SEM.

was studied. A large neutrophil (7.4^{+}-$F4/80^{-}$) influx was observed in the BAL of wild-type mice at 24 hours post-infection. In contrast to wild-type mice, fewer neutrophils were observed in TLR2 KO mice BAL at 24 hours post-infection suggesting that TLR2 signaling induced neutrophil migration into RSV infected lungs (Figure 3.3). Furthermore, low levels of neutrophils were detected in the BAL of wild type and TLR2 KO mice at 48 hours post-infection and were undetected in BAL at 96 hours post-infection suggesting neutophil migration occurs very early during the innate immune response to RSV. Neutrophils were undetected in uninfected mice indicating RSV infection was necessary to induce neutrophil migration into the lung.

Additionally, a reduced number of activated DCs ($CD11^{hi}$ $CD11b^{hi}$ $CD86^{+}$) was observed in the BAL of TLR2 KO mice compared to wild type DCs at 24 and 48 hours post-infection (Figure 3.4). MyD88 KO mice exhibited a reduced number of neutrophils and activated DCs in response to RSV infection, further indicating a role for TLR2 dependent signaling in activating innate immunity against RSV. Additionally, T cell, NK cell, and eosinophil migration into the BAL of wild-type vs. TLR2 KO mice was examined. These cell populations were detected in the BAL at very low frequencies, and no differences were observed between the groups (data not shown).

Figure 3.3 TLR2 signals promote neutrophil influx following RSV infection

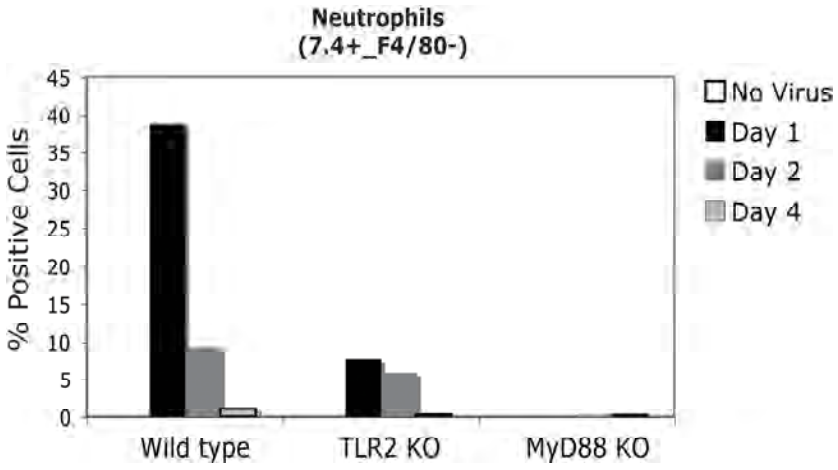

Figure 3.3 TLR2 signals promote neutrophil influx following RSV infection

Wild-type, TLR2 KO, and MyD88 KO mice were infected by intranasal inoculation with RSV A2 strain (2.4 x 10^6 PFU/mouse). Uninfected mice (n=3) were used to control for BAL infiltration. 24, 48, and 96 hours after infection, BAL were harvested from mice. BAL from each group (n=3 per group) was pooled and neutrophils were enumerated by flow cytometry. Neutrophil (7.4+-F4/80-) populations are indicated as % positive cells of total gated cells.

Figure 3.4 TLR2 signals promote DC maturation in response to RSV

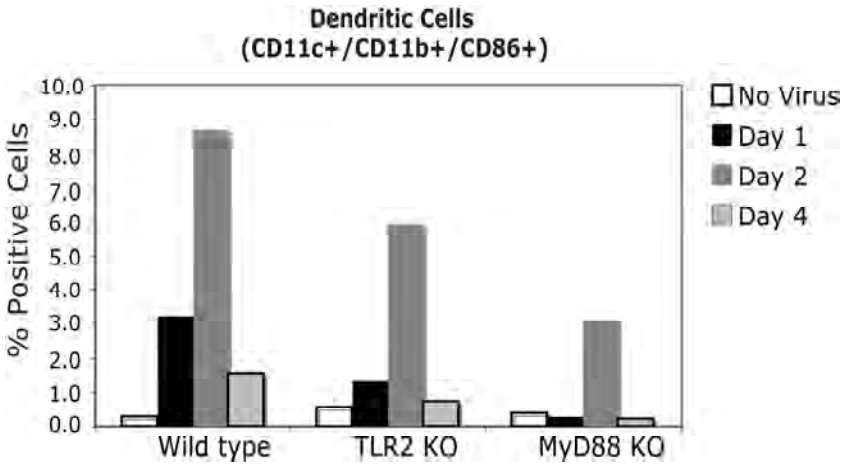

Figure 3.4 TLR2 signals promote DC maturation in response to RSV

Wild-type, TLR2 KO, and MyD88 KO mice were infected by intranasal inoculation with RSV A2 strain (2.4 x 10^6 PFU/mouse). Uninfected mice (n=3) were used to control for BAL infiltration. 24, 48, and 96 hours after infection, BAL were harvested from mice. BAL from each group (n=3 per group) was pooled and activated DCs were enumerated by flow cytometry. DC (CD11b+-CD11c+-CD86+) populations are indicated as % positive cells of total gated cells.

Discussion

Data presented in this chapter confirmed a role for TLR2/6 mediated innate signaling in controlling virus replication because TLR2 KO and TLR6 KO mice were less effective in controlling viral replication than wild type controls. Interestingly, data presented in chapter II, indicating equivalent type I IFN responses between TLR KO strains compared to control mice, suggests early NF-κB-derived inflammatory mediators may be more critical in controlling virus replication in mouse lungs than type I IFN. Data suggesting TLR3 KO mice can control RSV replication similar to wild-type mice further supports this hypothesis. One possible explanation is that lowered secretion of macrophage derived TNF-α in these mice decreased the host response and subsequently affected viral clearance. TLR2 signaling was examined *in vivo* by infecting TLR2 KO mice with RSV. We were unable to detect differences in TNF-α, IL-6, and CCL5 production *in vivo* at 24 hours post infection suggesting peak production of these factors may have occurred at an earlier time point during the response. However, this does not exclude the possibility that these mediators could play an important role in limiting virus replication at earlier time points (i.e. <24 hours) during infection since each has been shown to plays an important role in inflammation.

TLR2 signaling did mediate CCL2 production *in vivo*. Interestingly, studies examining acute sepsis peritonitis using mouse models showed that CCL2 production was indirectly involved in neutrophil influx through the production of leukotriene B_4, suggesting that CCL2 production can influence neutrophil migration (105). Moreover, we observed a decrease in lung neutrophils in the bronchoalveolar lavage of TLR2 KO mice at 24 hours post-infection. These findings indicated that TLR2 mediated CCL2

production might be important for early neutrophil migration to the lung in response to RSV infection.

Neutrophils are innate leukocytes that traffic to sites of infection via chemokine gradients and greatly aid clearance of virally infected cells. The presence of neutrophils correlates with RSV-disease severity and, further, these cells secrete inflammatory mediators including reactive oxygen species and cytokines (i.e. IL-8) that further drive inflammation and indiscriminately kill both infected and uninfected tissues (11, 80, 167, 168). Therefore, heightened TLR2 signaling may mediate neutrophil associated airway inflammation through CCL2 production.

Early inflammatory components can profoundly influence DCs ability to shape innate and acquired immune responses. Therefore, we examined the affect of TLR2 signaling on DCs activation. Within the lung, immature DCs sense viruses including RSV in part through TLR and can promote either Th1 or Th2 T and B cell responses after receiving activation signals from components that make up the inflammatory environment (42, 75). We observed a decrease in activated lung DCs ($CD11b^{hi}$ $CD11c^{hi}$ $CD86^{+}$) in TLR2 KO mice at 24 and 48 hours post-infection, suggesting TLR2-mediated signals generated during RSV infection could influence DC activation. Interestingly, Rudd et al. showed that a lack MyD88 dependent signaling in DCs can promote Th2 responses after RSV infection (140). Since DCs can express TLR2, it is tempting to speculate that TLR2 signaling may contribute to Th2 polarizing DCs in response to RSV. Additionally, TLR2 signaling may further contribute to RSV responses by facilitating

interactions between DCs and neutrophils that can further shape T and B cell polarization (110).

Collectively, these studies indicated TLR2 in addition to previously discovered TLRs including TLR3, TLR7, and TLR4 plus CD14 activate innate immune responses upon RSV recognition (90, 141, 142). TLR2 and TLR6 but not TLR1 signaling activated inflammatory components that are thought to promote clearance of RSV and prevent RSV-induced disease. Since the early inflammatory environment greatly shapes subsequent immune responses, these findings provide new insight into how TLR signaling could contribute to a beneficial anti-RSV immune response. Interestingly, TLR4 signaling can influence TLR2 expression following certain stimuli, suggesting the optimal induction of multiple signaling pathways may be required to elicit protective rather than deleterious innate immune responses following RSV infection, consistent with a role for both TLR4 and TLR2 in the response to RSV (48).

Finally, data presented in Chapters II and III suggested that TLR2 signaling was involved in activating Th1-like responses. Therefore, RSV vaccines incorporating TLR2 adjuvant may help elicit strong Th1 responses. This strategy was evaluated in mouse models of RSV disease using the TLR2 ligand peptidoglycan as an adjuvant and showed effectiveness in limiting RSV-induced disease (66). Alternatively, TLR2 antagonist therapies may provide some benefit to susceptible children during active infection by dampening inflammation and limiting neutrophil associated airway inflammation. In light of the findings presented here, therapies targeting TLR2 signaling may prove beneficial in limiting RSV infection and preventing RSV-induced disease.

Chapter IV

Preface

This chapter contains information relating to the construction, expression, of quantification of VLP-H/G and the use of VLP-H/G as a vaccine against RSV in mice. Dr. Trudy Morrison and her lab generated the data pertaining to construction, expression, and quantification of VLPs. Dr. Morrison's laboratory also conducted antibody titration assays. I contributed to the execution of the vaccine study by growing RSV, infecting mice, harvesting tissues and blood, running virus plaque assays, performing CTL assays, preparing tissues for histology, scoring tissue sections, running statistics, and preparing manuscript for publication.

Introduction

RSV remains a high priority for vaccine development. However, no licensed vaccines are available for use. Monoclonal antibody therapy can be beneficial in high-risk infants, but this treatment is cost-prohibitive for the general population. While the overall goal for any vaccine is to induce protective immune responses in the recipient, any potential RSV vaccine must not only elicit strong, protective immune responses but also must protect against enhanced disease seen with early vaccine trials that demonstrated disastrous results following immunization with formalin-inactivated RSV. Despite numerous strategies aimed at combining efficacy and safety into a potential RSV vaccine, this successful combination has remained elusive. In this chapter we describe a novel approach to create a potential RSV vaccine using virus-like particle (VLP) technology (Figure 4.1). This platform has been used to successfully generate vaccines against HPV and HBV, and both vaccinations have proven to be safe and efficacious in humans. Taking advantage of the antigenic nature of the RSV G protein, we have incorporated a G protein chimera into a VLP comprised only of the NDV M and NP proteins. The data described here demonstrates that VLPs expressing RSV G (VLP-H/G) can elicit safe and protective responses in BALB/c mice and may be a promising candidate for a human vaccine.

Figure 4.1 Producing VLPs *in vitro*

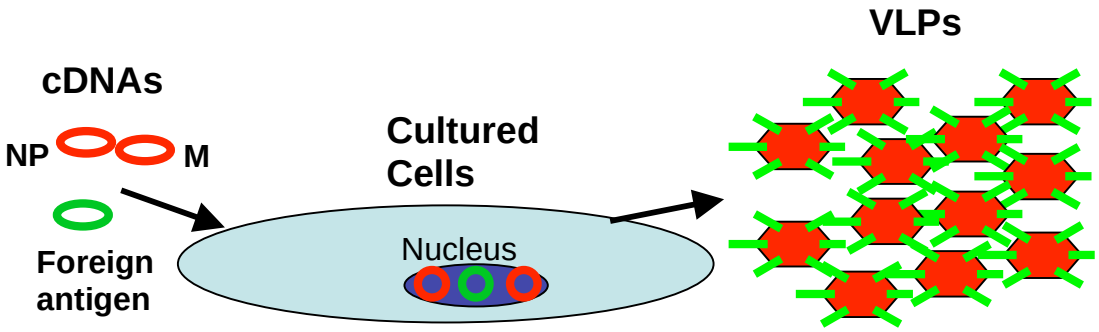

Figure 4.1 Producing VLPs *in vitro*

This cartoon illustrates the formation of VLPs using cDNAs that encode viral proteins necessary for virus assembly. The cDNAs encoding NDV NP and M along with a cDNA for a foreign antigen are transfected into cultured cells, and the nucleus transcribes the foreign DNA. Cellular machinery assembles the VLPs that then bud from the cell surface forming infections particles that lack a genome. The VLPs are quantified as described in the Materials and Methods and injected into hosts as a potential vaccine.

Results

Construction and Expression of a NDV HN/RSV G protein chimera gene

To incorporate significant levels of RSV G protein into ND VLPs, the ectodomain of the RSV G protein was fused to the NDV HN protein cytoplasmic and transmembrane domains (Figure 4.2) to create a chimera H/G protein. The sequences at the junction between the HN and G protein domains are shown in Figure 4.2 .

The chimera protein was expressed in COS-7 cells and in avian cells and compared to the expression of the wild-type RSV G protein in transfected cells as well as the RSV G protein in RSV-infected Vero cell extracts (Figure 4.3). The chimeric protein (lanes 1, 2, 5, and 6) was made in amounts similar to wild-type protein (lanes 3 and 7) and co-migrated with the wild-type protein made in transfected cells. Both the wild-type and chimeric proteins were heterogeneous in size, indicated by the vertical lines on the left sides of each panel, a phenomenon likely due to inefficient glycosylation. The heterogeneity also varied somewhat between monolayers, as illustrated in Figure 4.3, lanes 1, 2, 5, and 6. Interestingly, the maximal sizes of both the wild type and chimera proteins varied with the cell type, as previously reported (52, 112). The G protein made in infected (or transfected, not shown) Vero cells (Figure 4.3, lane 9) as well as HEK 293T cells (not shown) migrated the slowest while the G protein or H/G chimera protein made in transfected COS-7 cells (Figure 4.3, lanes 1-3) (or HEp-2 cells, not shown) were slightly smaller. The proteins expressed in avian cells (figure 4.3, lanes 5-7) were the smallest.

Figure 4.2 Constructing H/G chimera protein

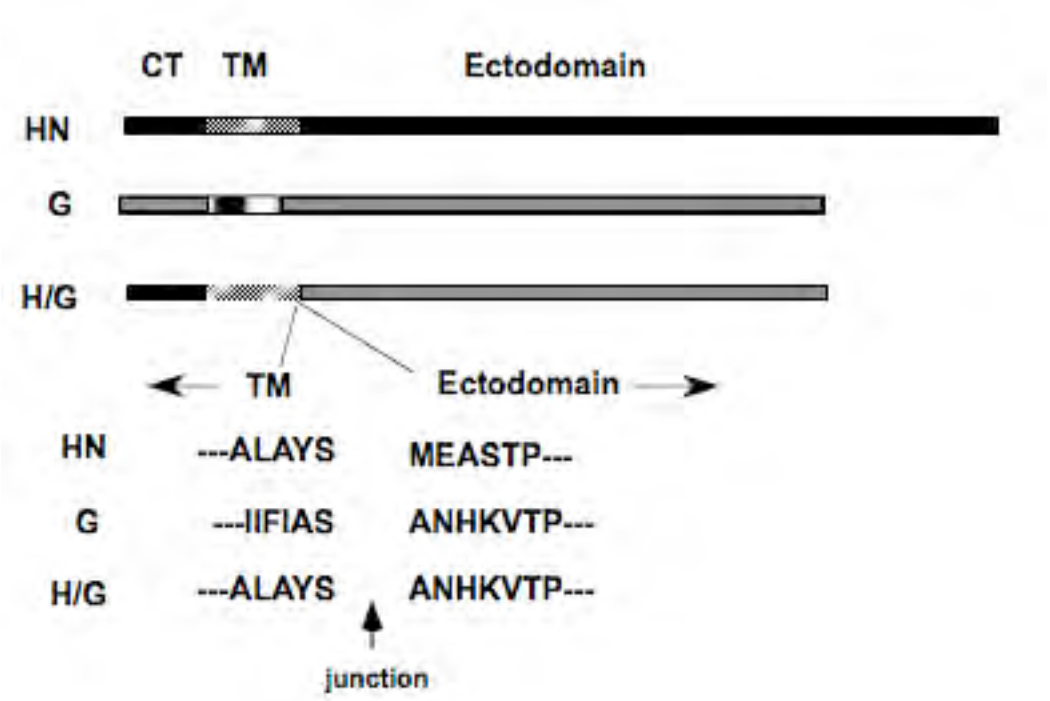

Figure 4.2 Constructing H/G chimera protein

The diagram shows the locations of the cytoplasmic domain (CT), transmembrane domain (TM), and ectodomains domain of the NDV HN protein and the RSV G protein and the domains present in the NDV HN-RSV G chimeric protein (H/G). Below the bars, the sequences at the junctions of the TM and ectodomains of the three proteins are shown.

Figure 4.3 Expressing H/G chimera protein *in vitro*

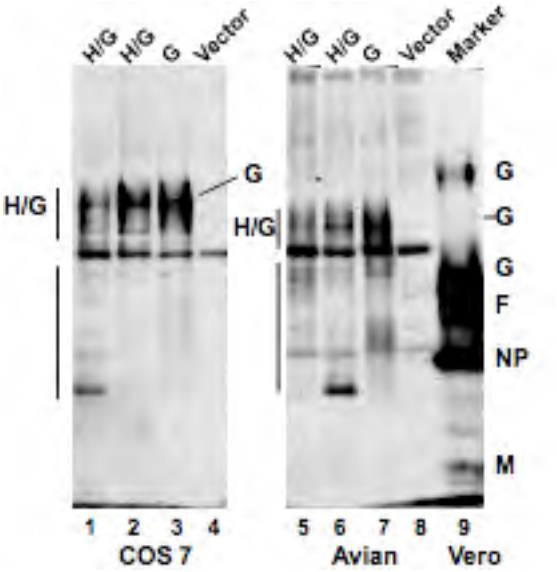

Figure 4.3 Expressing H/G chimera protein *in vitro*

Avian cells and COS7 cells were transfected with cDNAs encoding the proteins shown at the top of the figure. Proteins present in extracts of cells at 48 hours post transfection or extracts from RSV infected cells (Marker) prepared after 4 days of infection were detected by Western analysis using a polyclonal anti-RSV antibody. Lanes 1-4, transfected COS 7 cell extracts, Lanes 5-8, avian cell extracts, Lane 9, RSV infected Vero cell extracts.

Incorporation of H/G chimera protein into ND VLPs

To determine the optimal combination of NDV proteins for the incorporation of the H/G protein into ND VLPs, avian cells were transfected with the H/G chimera protein cDNA and the NDV NP and M protein cDNAs and various combinations of the NDV F and HN protein cDNAs. VLPs were purified from cell supernatants, and their protein content was determined by Western blots (Figure 4.4). The NDV NP present in the VLPs is shown in the top panel while the bottom panel shows the H/G protein content. Clearly, maximal incorporation of the chimera was achieved in the presence of only the NDV NP and M proteins. Inclusion of the NDV F protein had little effect but, inclusion of HN protein inhibited incorporation of the chimera protein.

Preparation of these VLPs for their use as an immunogen was accomplished by transient transfection of avian cells with the NDV NP, M protein and the H/G chimera protein cDNAs. Particles released from these cells were purified as described in Materials and Methods. The total protein content of the purified VLPs is shown by silver stains of polyacrylamide gels containing VLP proteins (Figure 4.5, left panel). The silver stain indicated inclusion of the heterogeneous H/G protein, indicated by vertical bars alongside the panel. The presence of the H/G protein was confirmed by Western analysis of the proteins in the purified VLPs (Figure 4.5, right panel). We found that release of these particles from transfected cells was significantly enhanced by inclusion of heparin in the culture supernatant. Since it is known that the RSV G protein binds to glycosaminoglycans (GAGs) (63, 64), we hypothesized that released VLPs with the RSV G protein ectodomain might rebind to GAGs on surfaces of cells, decreasing the

Figure 4.4 Incorporating H/G chimera protein into ND-VLP

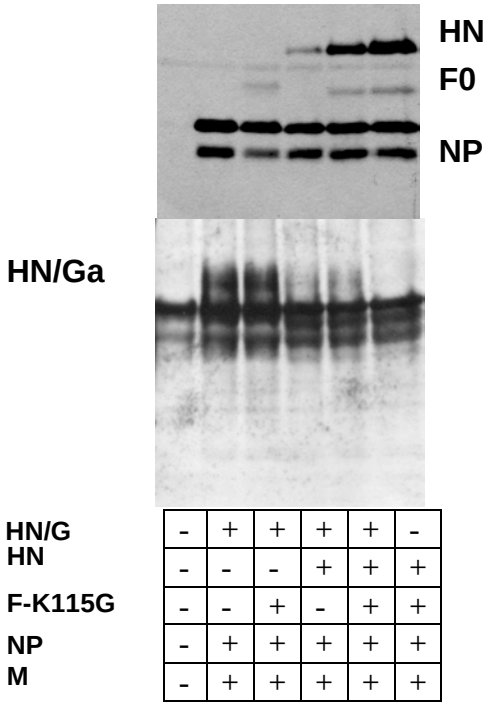

Figure 4.4 legend

Avian cells were transfected with cDNAs shown at the bottom of the panel (0.5 µg/35mm plate). VLPs in the supernatant were collected and purified as described in Materials and Methods. Proteins in the particles were detected by Western analysis (WB) using anti-NDV (top panel) or anti-RSV (bottom panel). The antibodies used do not detect NDV M protein. HN, hemagglutinin-neuraminidase protein; F0, uncleaved NDV fusion protein; NP, NDV nucleocapsid protein; H/G, HN-G protein chimera.

Figure 4.5 Quantifying ND-VLPs expressing H/G protein chimera

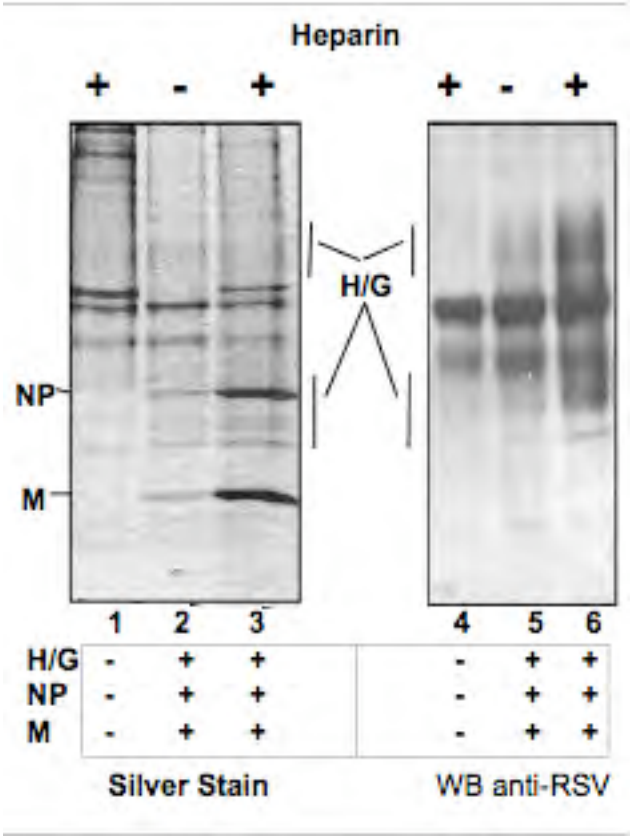

Figure 4.5 Quantifying ND-VLPs expressing H/G protein chimera

Avian cells were transfected with cDNAs encoding the NDV M protein, NDV NP, and the H/G chimera protein, lanes 2, 3, 5, and 6, or with vector DNA only, lanes 1 and 4.Heparin (10 μg/ml) was added to the supernatants of transfected cells as indicated at the top of the panel at 40 hours post transfection. Particles in the supernatant were collected and purified as described in the Materials and Methods. Proteins present in the particles were electrophoresed on polyacrylamide gels. Lanes 1-3 show a silver stain of the proteins in the gel while lanes 4-6 show a Western blot (WB) of the gel using anti-RSV to detect G protein sequences. NP, NDV nucleocapsid protein; M, NDV membrane protein; H/G, HN-G protein chimera.

release of particles into the cell supernatant. Peeples and colleagues have reported that heparin blocks infection with RSV (63). Thus, we attempted to block the rebinding of released VLPs to cell surfaces by adding heparin. Indeed, heparin significantly improved the recovery of VLPs containing the H/G protein (Figure 4.5, compare lanes 2 and 3 and lanes 5 and 6).

Densitometer analysis of silver-stained gels containing several preparations of VLP-H/G similar to that shown in Figure 4.5 and showed that the H/G protein represented from 15-20 percent of the total viral protein in these particles. The amount of HN protein in ND VLPs is approximately 30 percent of the total viral protein. Thus the efficiency of incorporation of the H/G chimera protein is slightly less than that of HN protein incorporation into VLPs.

Murine Immune Responses to VLP-H/G

Antibody responses to the G protein delivered in VLPs were compared with those to the G protein in purified virus. For this comparison, gradient-purified UV-inactivated RSV delivered by intraperitoneal inoculation, as well as infectious RSV delivered intranasally (I.N.) were utilized. For comparisons with UV-inactivated RSV (UV-RSV), amounts of virus and VLPs that had comparable amounts of the G protein were utilized as immunogen. The concentrations of the G protein in VLP-H/G and UV-RSV were determined as described in Materials and Methods and the volumes of VLP-H/G preparation were adjusted so that the concentration of H/G protein was the same as the

concentration of G protein in virus. The normalized preparations of UV-RSV and VLPs contained similar amounts of RSV G protein (Figure 4.6, compare lanes 5 and 6).

Mice (groups of 5) were immunized by intraperitoneal inoculation with 1, 3, 10, or 30 μg total VLP-H/G protein or comparable amounts of UV-irradiated, purified RSV or a single intranasal dose of infectious RSV. Figure 4.7 indicates that antibody responses to G protein delivered by VLPs were somewhat better than G protein responses after UV RSV or infectious RSV immunization, when assayed using G protein made in COS7 cells as target antigen. To explore this conclusion, the antibody titers in serum of mice immunized with the highest concentrations of antigen were determined by serial dilution of the serum using as target antigen G protein made in the human cell line HEK 293T (Figure 4.8). Figure 4.8 also shows antibody titers at day 42 after a boost of antigen at day 28. For comparisons, the titers of serum after immunization with VLP-H/G, using as capture antigen G protein in purified RSV, are also shown. The antibody titers to VLP-H/G increased with time and were similar to titers obtained after UV-RSV immunization. Furthermore, titers in both sets of sera increased slightly with an antigen boost. Thus, using different sources of target G protein with various amounts of glycosylation, the antibody levels obtained after intraperitoneal immunization with VLP-H/G were as good as or better than levels obtained after immunization with inactivated RSV or infectious RSV.

Figure 4.6 VLP-H/G quantification for vaccine dosing

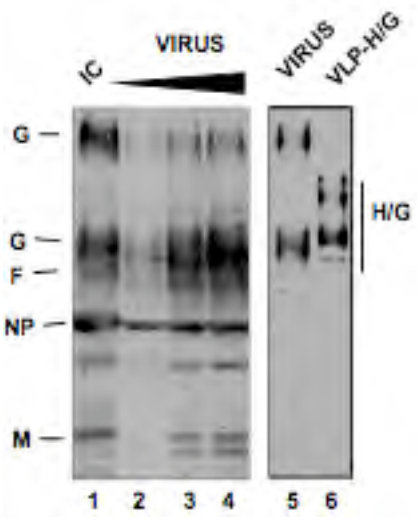

Figure 4.6 legend

Vero cells were infected with RSV (MOI=1) and incubated for 4 days. Virus was harvested and purified as described in Materials and Methods. Increasing amounts of purified virus proteins were electrophoresed on polyacrylamide gels and resolved using Western blotting with an anti-RSV antibody as the probe (lanes 2-4). Proteins in extracts from infected Vero cell extracts (IC) were included as marker proteins (lane 1). Based on these results as well as silver stains (Figure 4.5), the concentration of VLP-H/G stock was adjusted such that the amount of G protein present was equivalent to the G protein in virus stocks. Equivalent volumes of the VLP-H/G and virus stocks were electrophoresed on polyacrylamide gels and the G protein sequences detected using a monoclonal antibody specific to the G protein (lanes 5 and 6). NP, RSV nucleocapsid protein; M, RSV membrane protein; F, RSV fusion protein, G, RSV G protein; H/G, HN-G protein chimera.

Figure 4.7 Antibody responses to RSV G protein in vaccinated mice (COS7 G target antigen)

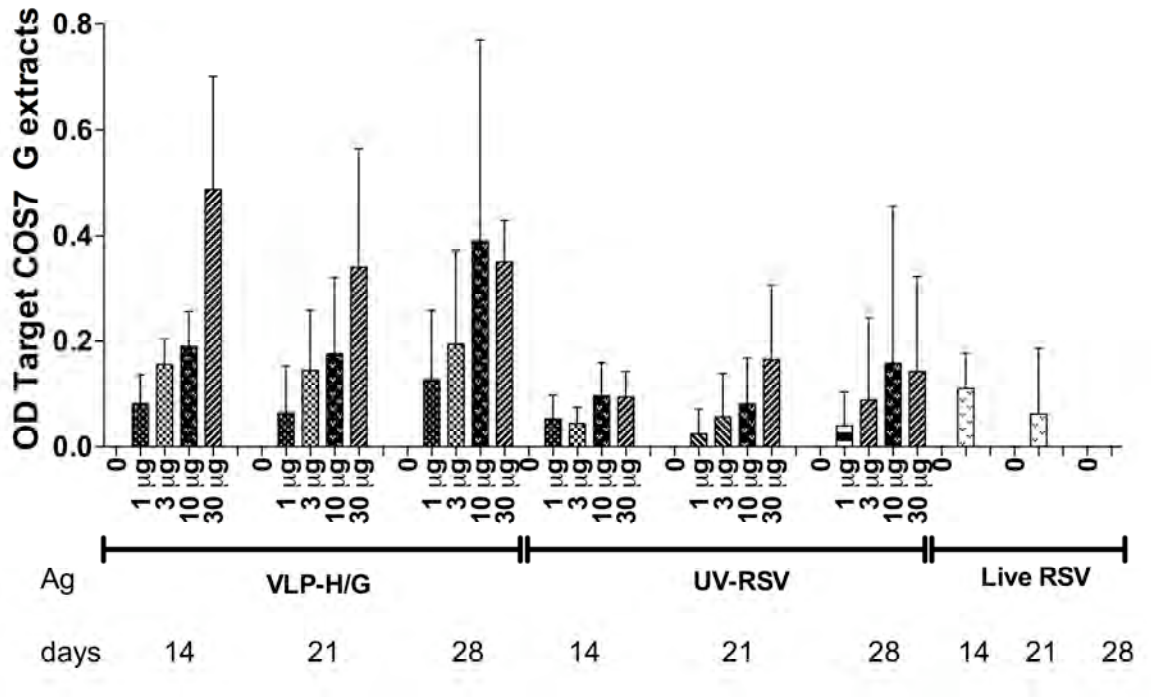

Figure 4.7 Antibody responses to RSV G protein in vaccinated mice (COS7 G target antigen)

Mice (groups of 5) were immunized by intraperitoneal inoculation of 0, 1, 3, 10, or 30 ug of total VLP-H/G protein or comparable amounts of purified UV inactivated RSV (UV-RSV). Another group of mice was immunized by intranasal inoculation with 3 X 10^6 pfu of infectious virus/mouse. Serum was collected at 14, 21, and 28 days post immunization. Antibody present in a 1:100 dilution of each serum sample was detected by ELISA assay as described in Materials and Methods using as target antigen proteins present in COS 7 cells transfected with cDNA encoding the RSV G protein. The panel shows the average OD for each group of mice. The standard deviation within each group is indicated by the vertical line.

Figure 4.8 Antibody responses to RSV G following vaccination (I.P.) (HEK 293T G protein and purified RSV G protein target antigen)

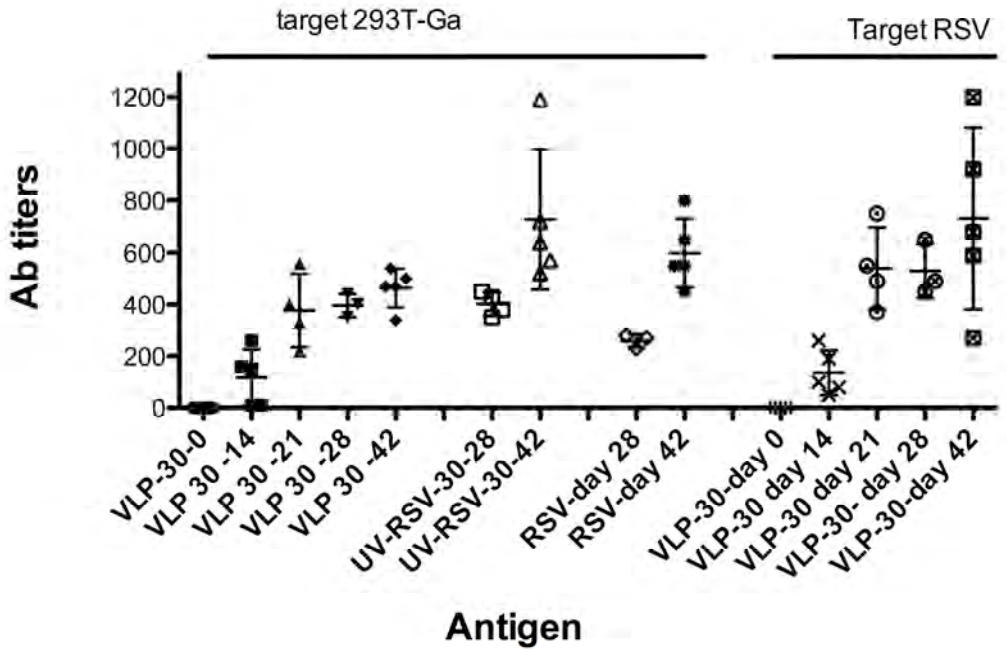

Figure 4.8 Antibody responses to RSV G following vaccination (I.P.) (HEK 293T G protein and purified RSV G protein target antigen)

Antibody titers in mouse serum samples collected 14, 21,or 28 days after immunization with 30 μg of total VLP-H/G protein (i.p.), UV-RSV protein (i.p.), or infectious RSV (3 x 10^6) (i.n) were determined by ELISA using serial dilutions of mouse serum. The titer was defined as the reciprocal of the dilution of sera that gave an OD of 3 fold over background. Titers for individual mice are shown. The mean is shown by a horizontal line and the standard deviation by the vertical line. At 28 days post immunization, VLP-H/G immunized mice were boosted with 10 μg VLP-H/G protein (i.p.), UV-RSV mice were boosted with 10 μg of UV-RSV protein (i.p.), and RSV mice were boosted with infectious virus (3 x 10^6) (IN). Antibody titers in serum samples obtained at 42 days after the initial immunization were also determined as described above.

Protection of Mice from RSV Replication after Intraperitoneal Immunization

To determine if the immune responses to VLP-H/G could protect mice from RSV challenge, BALB/c mice, which had been immunized with 30 μg of total VLP-H/G protein and then boosted with 10 μg of total VLP-H/G protein, were challenged i.n. with infectious RSV. As controls, mice previously infected with infectious RSV were challenged with a second dose of virus. Another set of mice that had not received any immunogen, were also infected. At 4 days post infection, the time previously determined to yield maximal virus titers (118), the virus titer in the lungs was determined. Figure 4.9 showed that virus was detected in the lungs of unimmunized mice, but no virus was detected in the lungs of mice previously immunized with VLP-H/G or, as expected, mice previously infected with live RSV. Thus immunization with VLP-H/G protected mice from RSV replication in lungs.

Intramuscular Immunization with VLP-H/G

Because immunization in humans is most often via inoculation intramuscularly (I.M.), the immune responses of mice to this route of VLP-H/G delivery were also determined. Also included in these studies was formaldehyde-treated RSV (FI-RSV), which served as a positive control for abnormal immune responses to vaccine preparations previously described. A group of mice immunized I.N. with infectious RSV was also included. I.M. immunization of 10 μg and particularly 40 μg of VLP-H/G protein resulted in detectable antibodies specific to the RSV G protein, levels that continued to increase up to 38 days (Figure 4.10). In contrast to the results shown in

Figure 4.9 VLP-H/G vaccination (I.P.) protects mice from RSV replication in lungs

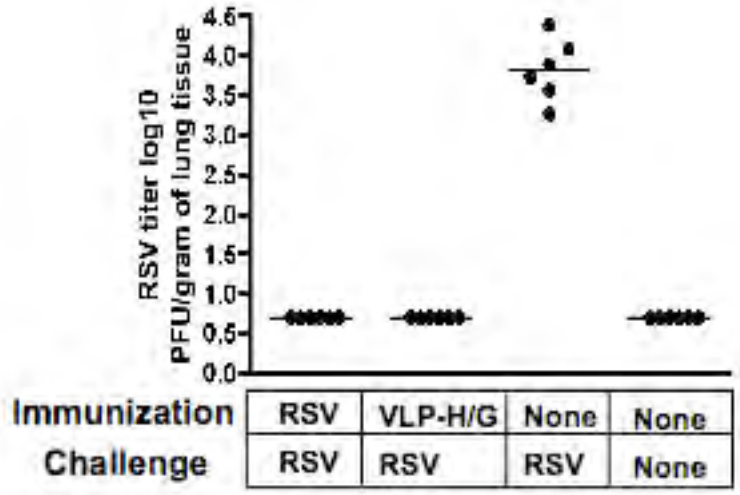

Figure 4.9 VLP-H/G vaccination (I.P.) protects mice from RSV replication in lungs

Groups of 5 BALB/c mice were immunized with infectious RSV (IN 3 x 10^6 pfu/mouse), VLP-H/G (IP with 30 μg/mouse). At 48 days post immunization, mice were boosted with RSV (IN with 3 x 10^6 pfu/mouse) or VLP-H/G (IP with 10 mg/mouse). After 12 days, mice were infected by intranasal inoculation of infectious RSV (3 x 10^6 pfu/mouse). Unimmunized control mice (5 animals) were infected with RSV (IN 3 x 10^6 pfu/mouse). Another group of unimmunized mice was left unchallenged. After 4 days of infection, lungs were removed and virus in lung tissue was titered by plaque assay as described in Materials and Methods. Titers shown for unchallenged mice are the limit of detection of virus.

Figure 4.10 Antibody responses to RSV G following vaccination (I.M.) (293T G protein target antigen)

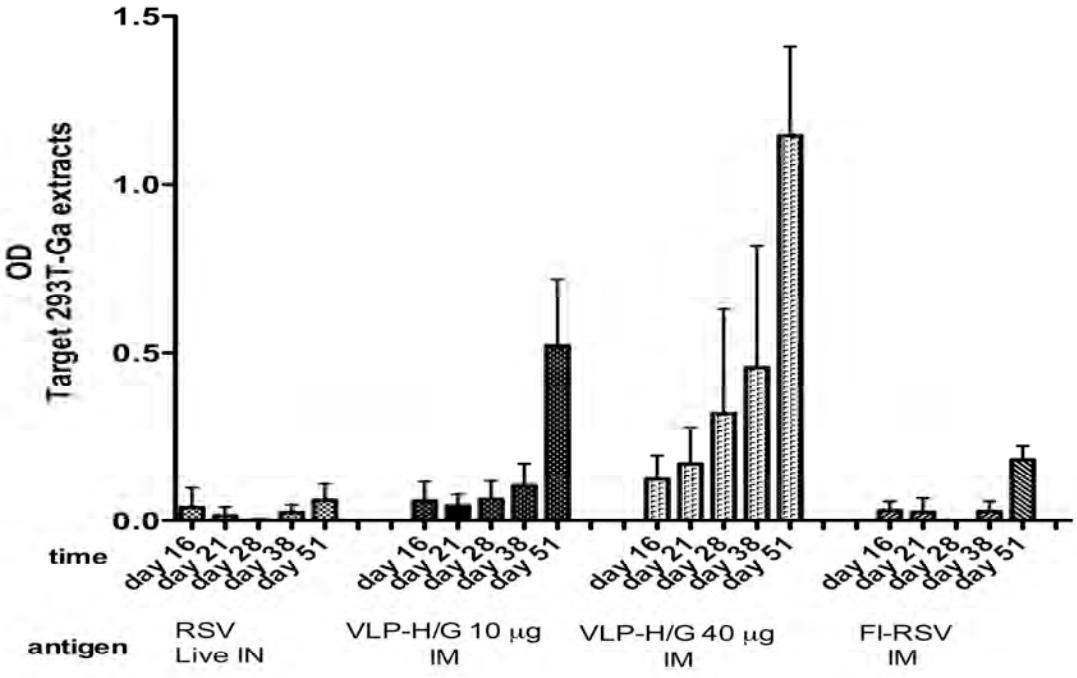

Figure 4.10 legend

BALB/c mice (groups of 5) were immunized by intramuscular (I.M.) instillation of 10 or 40 μg of total VLP-H/G protein. Another group of mice received FI-RSV by I.M. inoculation (equivalent of 5×10^6 pfu/mouse). Control groups of mice received infectious RSV (1×10^6 pfu/mouse by IN inoculation) or no immunogen. Serum was collected at 16, 21, 28, 38, and 51 days post immunization. A boost (10 μg VLP-H/G, 1×10^6 pfu infectious RSV, or 5×10^6 pfu equivalent of FI-RSV) was delivered at day 38. Antibody present in a 1:50 dilution of each serum sample was detected by ELISA assay as described in Materials and Methods using as target antigen proteins from HEK 293T cells transfected with cDNA encoding the RSV G protein. Panel shows the optical density (OD) for each sample. The mean and the standard deviation within each group are indicated by the horizontal line and the vertical line, respectively.

Figure 4.7, immunization by I.N. inoculation of infectious RSV resulted in barely detectable levels of serum antibodies. However, these mice received nearly three times lower amounts of virus than mice in the groups described in Figure 4.7. Sera from mice immunized with FI-RSV also contained barely detectable levels of RSV G protein specific antibodies (Figure 4.10). All antibody levels increased significantly following antigen boost and RSV challenge (Figure 4.10).

To determine if immunization with VLP-H/G could stimulate RSV G protein-specific CTL responses, groups of mice were immunized with a single dose of 10 or 40 μg total VLP protein intramuscularly. Control mice received a single dose of infectious dose of RSV (I.N.). A third group of mice received no immunogen. After 35 days, spleens were harvested, stimulated *in vitro* with irradiated RSV-infected Vero cells, and CTL activity in these cultures was measured. Spleen cells from both groups of VLP-H/G immunized mice exhibited significant CTL activity, activities comparable to that observed in spleen cells from RSV immunized mice (Figure 4.11). Thus, VLP-H/G immunization stimulated robust CTL activity.

To determine the protective effects of IM immunization, mice that had received only one dose of immunogen were challenged with infectious RSV 38 days after immunization. The titers of virus in lungs of these mice after 4 days of infection are shown in Figure 4.12. Remarkably, mice immunized with a single dose of either 10 μg and 40 μg of total VLP-H/G protein were protected from virus replication, as were mice that had been previously infected with live RSV. However, mice immunized with FI-RSV were not protected from virus replication.

Figure 4.11 CTL responses following VLP-H/G vaccination (I.M.)

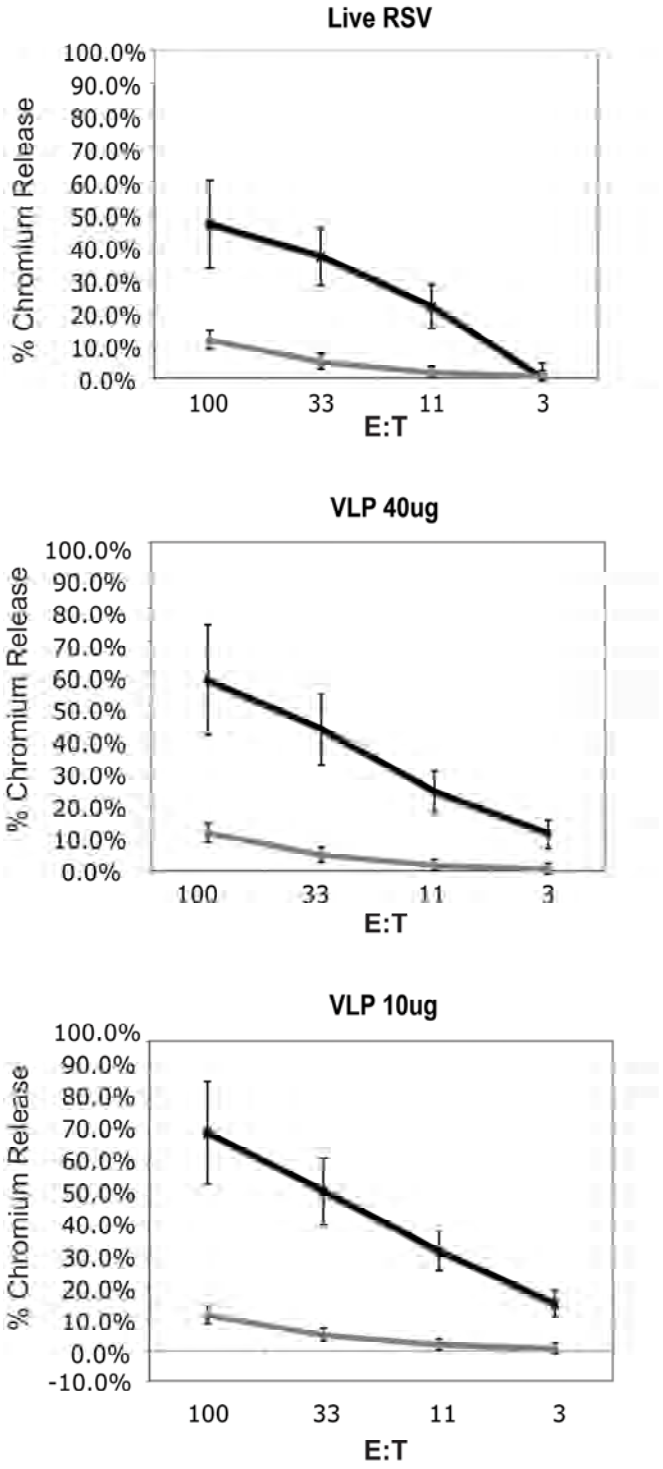

Figure 4.11 CTL responses following VLP-H/G vaccination (I.M.)

CTL activities of mice immunized, I.N., with a single dose of infectious RSV, a single dose, I.M., of 40 μg of VLP-H/G protein, or 10 μg of VLP-H/G were determined as described in Materials and Methods. Spleens were harvested from mice 5 weeks post-immunization. Percent of chromium release is indicated on the y-axis with different effector to target ratios (E:T) indicated on the x-axis. Each panel compares CTL activity after immunization with CTL activity of non-immunized mice.

Figure 4.12 I.M. VLP-H/G vaccination protects from RSV replication in mouse lungs

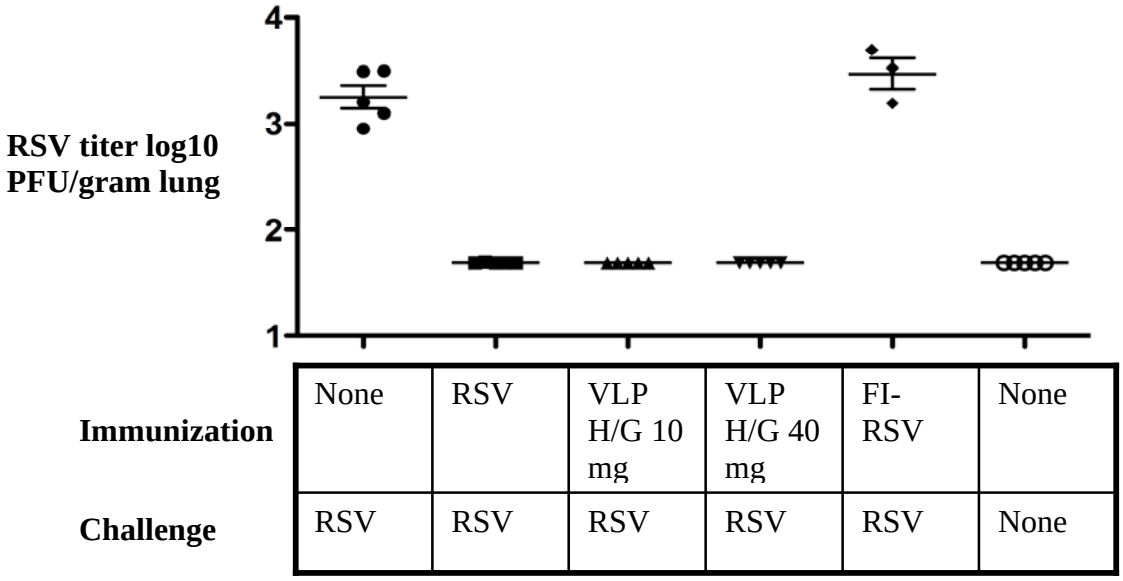

Figure 4.12 I.M. VLP-H/G vaccination protects from RSV replication in mouse lungs

BALB/c mice (groups of 5) were immunized by intramuscular (IM) inoculation of 10 or 40 μg of total VLP-H/G protein. Another group of mice received FI-RSV by IM inoculation (equivalent of 5×10^6 pfu/mouse). Control groups of mice received infectious RSV (1×10^6 pfu/mouse by IN inoculation). After 38 days, all mice were challenged with infectious RSV (1.6×10^6 pfu/mouse). One group of mice received no immunization and no RSV challenge. Four days after infection, lungs were harvested and the virus titers were determined by plaque assay as described in Materials and Methods. Titers shown for uninfected mice are the limit of detection of virus.

Lung Pathology after RSV Challenge

A key property required of an effective RSV vaccine is the absence of abnormal immune responses upon challenge with infectious RSV (Figures 13-14). In experiments utilizing intraperitoneal inoculation, lungs from each group of mice were examined for inflammation at 4 days post infection with RSV. No excess inflammation was observed in mice immunized with VLP-H/G (not shown) when compared to mice immunized with infectious RSV based on hematoxylin and eosin (H&E) analysis of lung tissue. To maximize any potential abnormal responses due to VLP immunization, mice immunized I.M. with 10 or 40 μg of VLP-H/G protein were boosted with 10 μg of VLP-H/G protein 38 days after immunization, infected with RSV 7 days later, and then, lungs were harvested 6 days after infection. Three control groups of mice, that is; mice that were unimmunized and unchallenged, mice subjected to a primary RSV infection, and mice immunized and then challenged with infectious RSV, were included. Positive controls for abnormal responses were mice immunized with FI-RSV and then challenged with infectious RSV. Figure 4.15 shows representative fields of lung sections from each group of mice stained with H&E. Lungs from mice previously immunized with infectious RSV, mice with a primary RSV infection, and VLP-H/G immunized mice showed some influx of lymphocytes. However, the FI-RSV mice showed massive influx of lymphocytes around both blood vessels and airways and in the interstitial spaces with formation of circumferential or near circumferential cuffs around blood vessels and small airways. Lung sections from all mice were scored for inflammation around airways, blood vessels, and in interstitial spaces, and the results are shown in Figures 4.16-18,

Figure 4.13 Normal Mouse lung anatomy

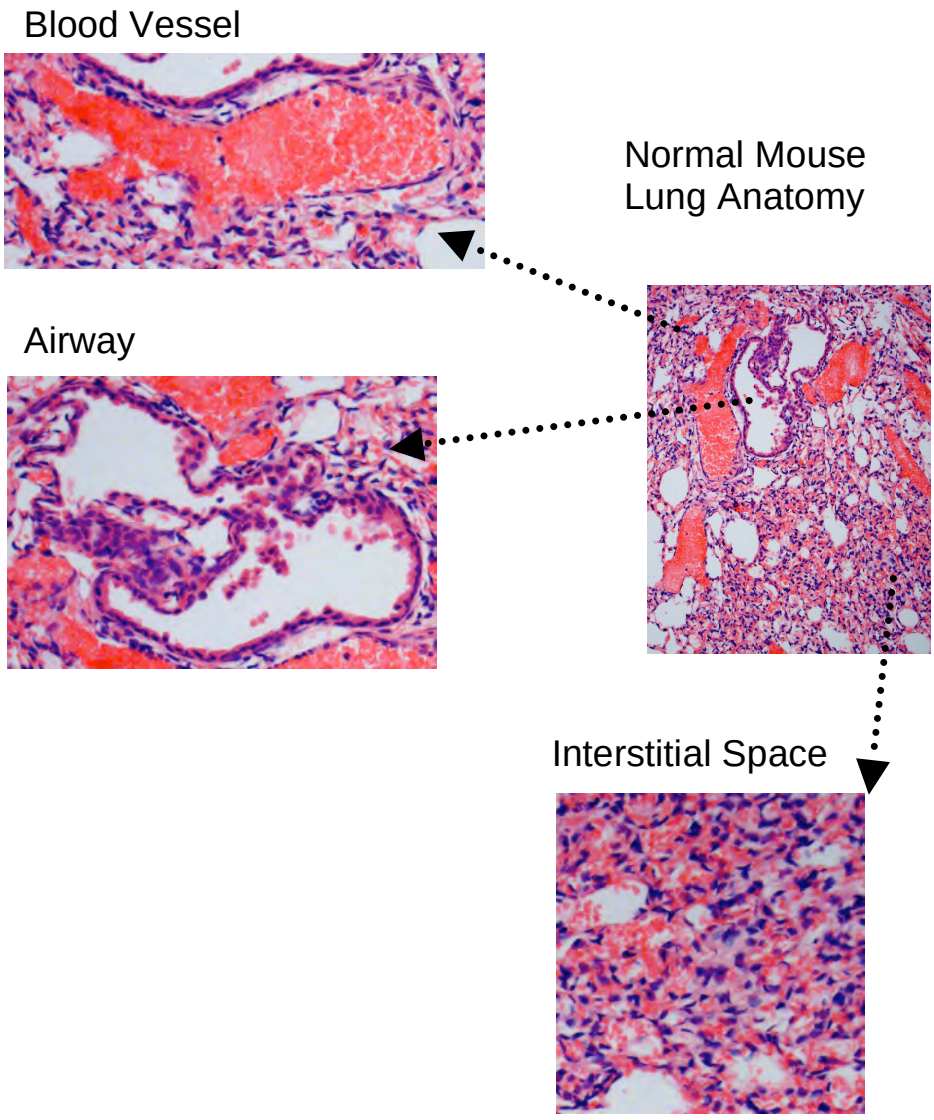

Figure 4.13 Normal Mouse lung anatomy

A representative H&E section of a naïve mouse lung is shown. Lungs were harvested from mice as indicated in materials and methods and fixed for tissue embedding and immunohistochemistry. A gross section of lung is depicted with highlighted areas expanded to show greater detail of indicated anatomical locations.

Fig 4.14 FI-RSV vaccination enhanced pathology in mouse lung

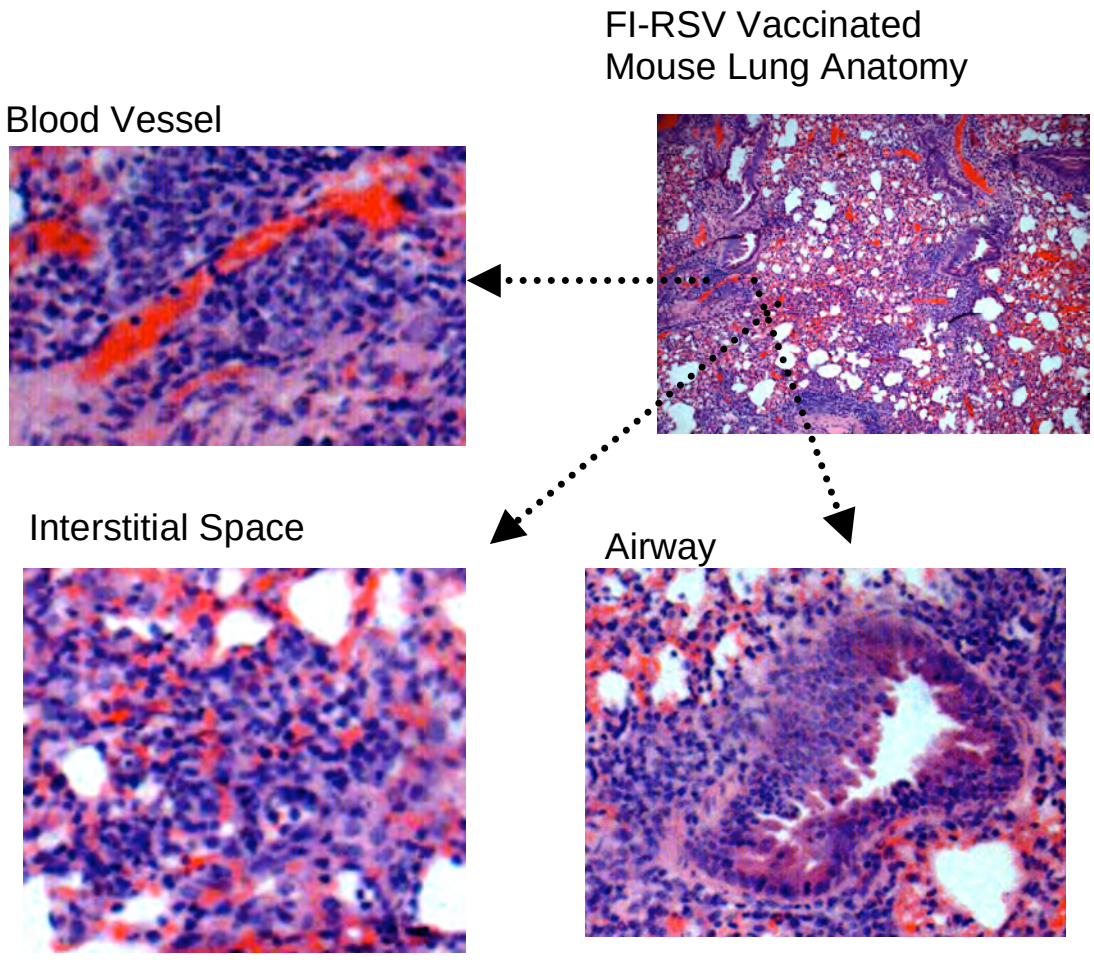

Figure 4.14 FI-RSV vaccination enhanced pathology in mouse lung

A representative H&E section of a FI-RSV immunized mouse lung following RSV A2 infection as described in materials and methods is shown. Lungs were harvested from mice as indicated in materials and methods and fixed for tissue embedding and immunohistochemistry. A gross section of lung is depicted with highlighted areas expanded to show greater detail of indicated anatomical locations. Note the heavy cellular infiltrate invading and surrounding tissues.

respectively. While immunization with FI-RSV recapitulated previously documented abnormal histology of lungs after infectious virus challenge, the lungs from mice immunized with VLP-H/G did not show this abnormal pathology. Rather, the inflammation scores for the VLP-H/G immunized mice showed no statistical differences from scores for mice immunized and then challenged with infectious RSV or mice subjected to a primary RSV infection. In contrast, the differences between the scores of lungs from FI-RSV- and VLP-H/G-immunized mice were statistically significant.

The lung sections of FI-RSV immunized mice also showed abnormal cells lining airways consistent with increased intracellular mucous production (Figure 4.15, panel H) while cells lining airways of VLP-H/G immunized mice did not show this type of morphology (Figure 4.15, panel G). To explore this observation, lung sections were stained with PAS to visualize material consistent with increased mucous production. Representative sections of VLP-H/G immunized mice and FI-RSV mice as well as control mice are shown in Figure 4.19. These sections were scored for the percent of airway linings showing PAS positive staining and the results are shown in Figure 4.20. VLP-H/G immunized mice showed significantly less PAS staining than the FI-RSV immunized mouse lungs ($p= 0.0014$). Thus, comparisons of the lungs of RSV-challenged mice indicate that VLP-H/G-immunized mice do not show the abnormal pathology associated with the FI-RSV vaccine.

Figure 4.15 Mouse lung morphology after VLP-H/G vaccination

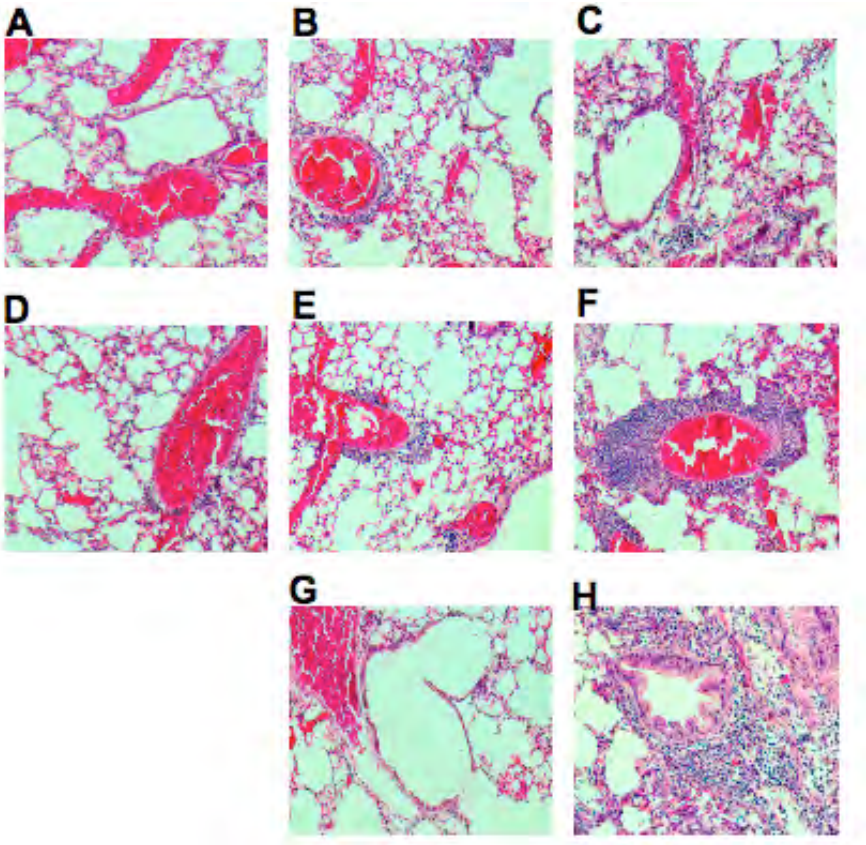

Figure 4.15 Mouse lung morphology after VLP-H/G vaccination

Groups of BALB/c mice were immunized with infectious RSV (1 x 10^6 pfu/mouse IN), 10 μg VLP-H/G (IM) or 40 μg VLP-H/G (IM), boosted with the homologous antigen (1 x 10^6 pfu RSV/mouse or 10 μg of VLP-H/G/mouse) and challenged with RSV (2.88 x 10^6 pfu /mouse). After euthanasia at day 51, lungs were prepared for tissue sections, as described in Materials and Methods, and stained with hematoxylin and eosin (H&E) (Panels A-H). Panel A: no immunogen, no challenge; Panel B: primary RSV infection; Panel C: RSV immunized mice challenged with RSV; Panel D: VLP-H/G 10 μg immunization and RSV challenge; Panels E, G: VLP-H/G 40 μg immunization and RSV challenge; Panels F, H: FI-RSV immunization and RSV challenge. All images were acquired using the same camera settings. Images were adjusted for size and contrast using Adobe Photoshop, using the same settings for all images.

Fig 4.16 Statistical analysis of inflammation around mouse airways after VLP-H/G vaccination

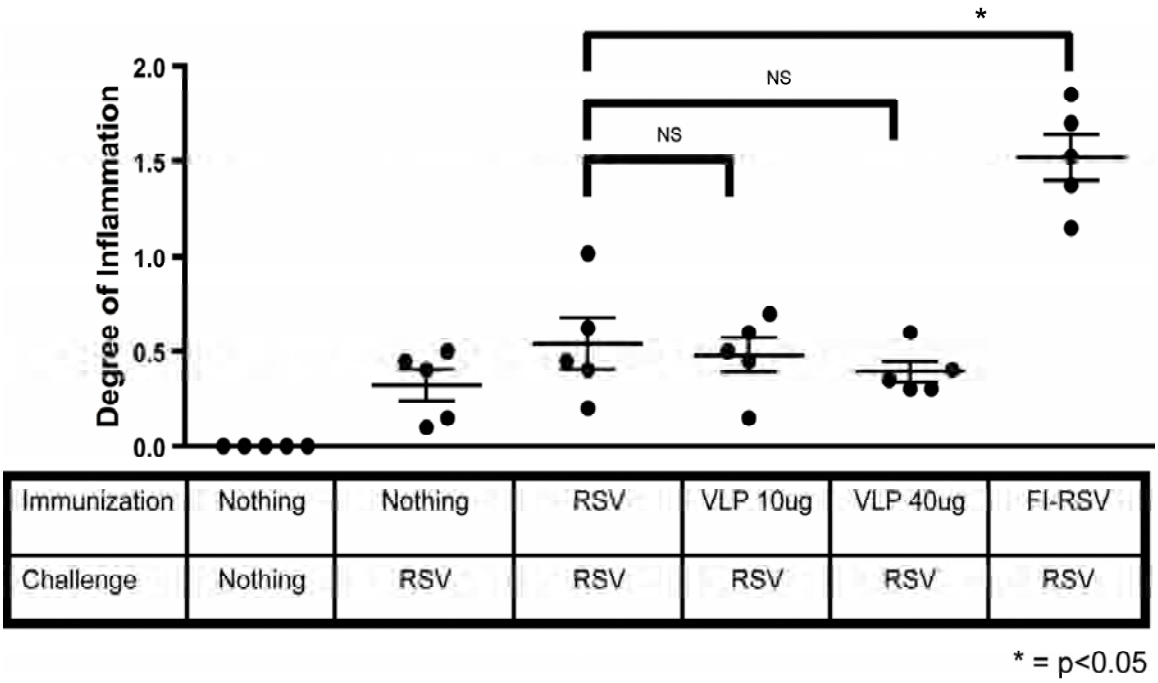

Figure 4.16 Statistical analysis of inflammation around mouse airways after VLP-H/G vaccination

Lung tissue sections were harvested 6 days post-challenge as described in Materials and Methods. Tissues from each mouse were stained with H&E and 10 random blood vessels per mouse were scored blindly by a pathologist for inflammation on a scale of 0-3, as described in Materials and Methods. Each data point represents the average of 10 blood vessels per mouse. Groups of mice are indicated at the bottom of the panels (ns, differences not statistically significant).

Figure 4.17 Statistical analysis of inflammation around mouse blood vessels after VLP-H/G vaccination

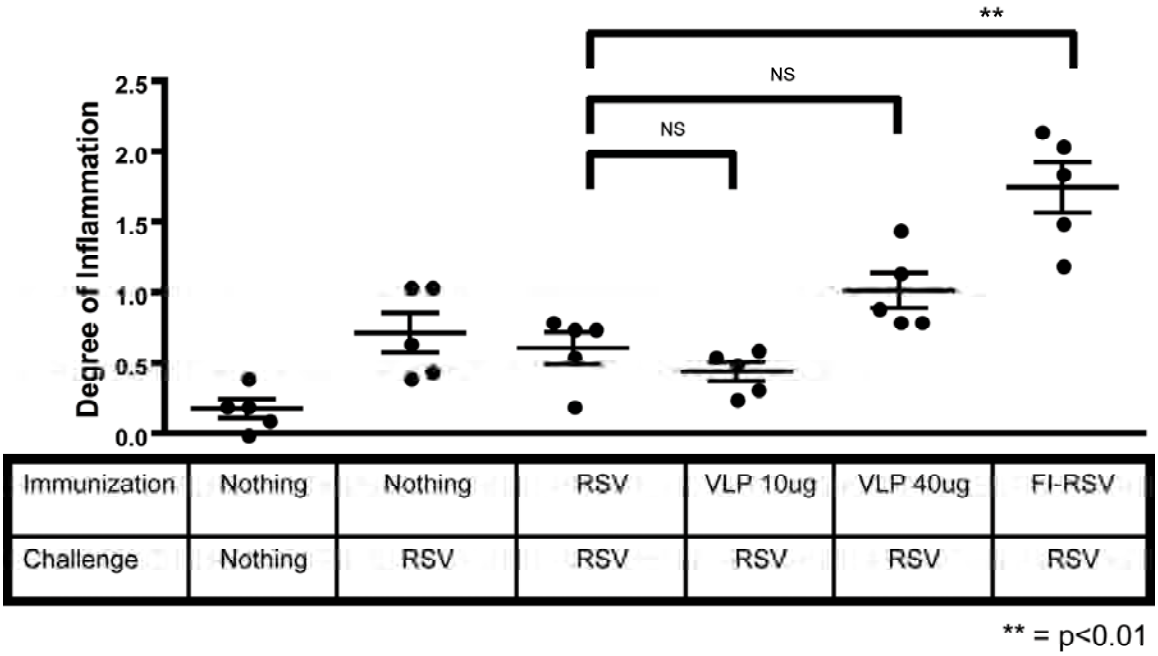

Figure 4.17 Statistical analysis of inflammation around mouse blood vessels after VLP-H/G vaccination

Lung tissue sections were harvested 6 days post-challenge as described in Materials and Methods. Tissues from each mouse were stained with H&E and 10 random airways per mouse were scored blindly by a pathologist for inflammation on a scale of 0-3, as described in Materials and Methods. Each data point represents the average of 10 blood vessels per mouse. Groups of mice are indicated at the bottom of the panels (ns, differences not statistically significant).

Figure 4.18 Statistical analysis of inflammation around mouse interstitial spaces after VLP-H/G vaccination

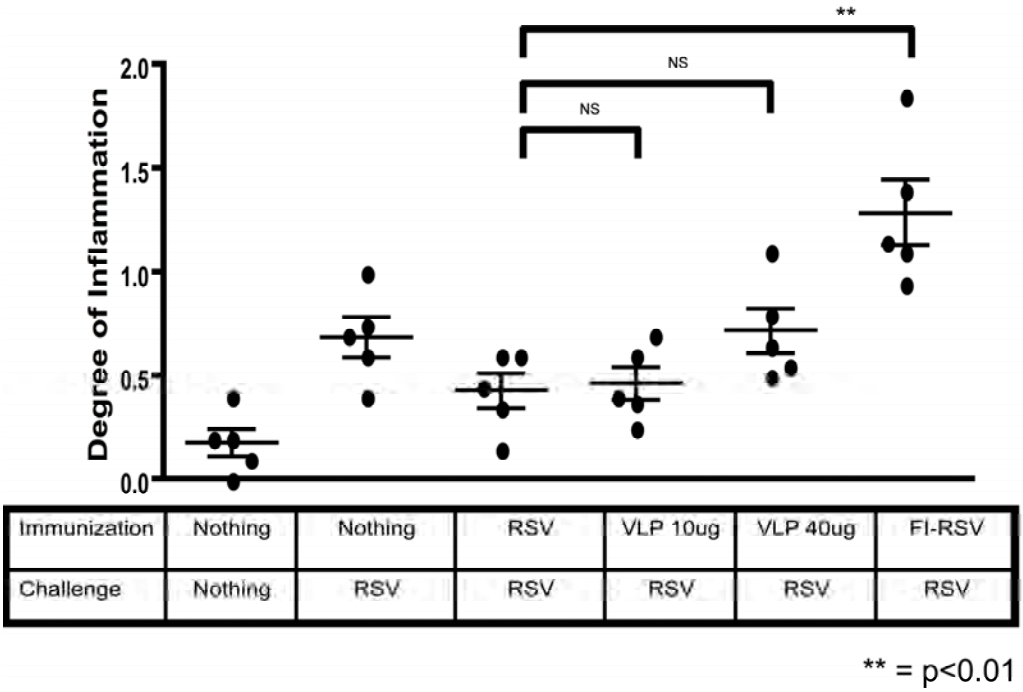

Figure 4.18 Statistical analysis of inflammation around mouse interstitial spaces after VLP-H/G vaccination

Lung tissue sections were harvested 6 days post-challenge as described in Materials and Methods. Tissues from each mouse were stained with H&E and 10 random interstitial spaces per mouse were scored blindly by a pathologist for inflammation on a scale of 0-3, as described in Materials and Methods. Each data point represents the average of 10 blood vessels per mouse. Groups of mice are indicated at the bottom of the panels (ns, differences not statistically significant).

Fig 4.19 PAS staining of goblet cells in mouse airways

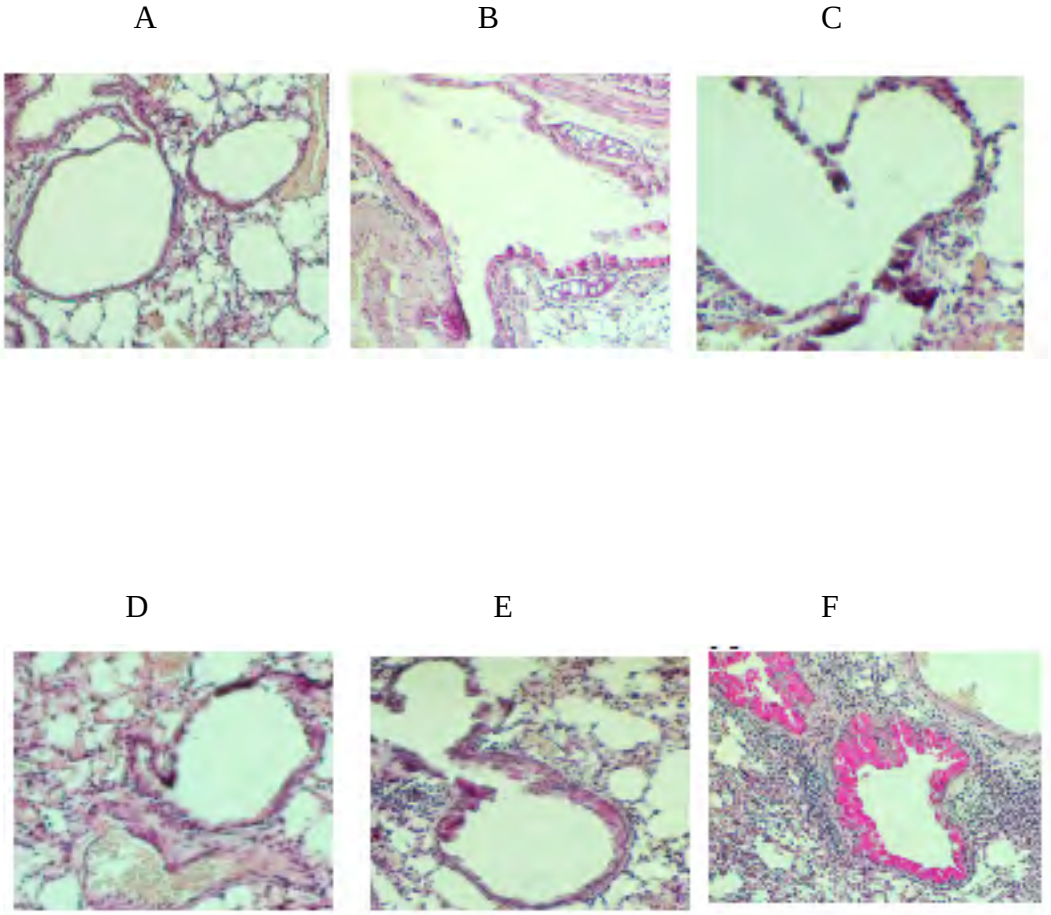

Figure 4.19 PAS staining of goblet cells in mouse airways

Groups of BALB/c mice were immunized with infectious RSV (1 x 10^6 pfu/mouse IN), 10 μg VLP-H/G (IM) or 40 μg VLP-H/G (IM), boosted with the homologous antigen (1 x 10^6 pfu RSV/mouse or 10 μg of VLP-H/G/mouse) and challenged with RSV (2.88 x 10^6 pfu /mouse). After euthanasia at day 51, lungs were prepared for tissue sections, as described in Materials and Methods, and stained with periodic acid-Schiff (PAS) which detects mucous produced by resident goblet cells. Panel A: no immunogen, no challenge; Panel B: primary RSV infection; Panels C: RSV immunized mice challenged with RSV; Panel D: VLP-H/G 10 μg immunization and RSV challenge; Panels E: VLP-H/G 40 μg immunization and RSV challenge; Panels F: FI-RSV immunization and RSV challenge. All images were acquired using the same camera settings. Images were adjusted for size and contrast using Adobe Photoshop, using the same settings for all images.

Fig 4.20 Statistical analysis of goblet cells in VLP-H/G immunized mice

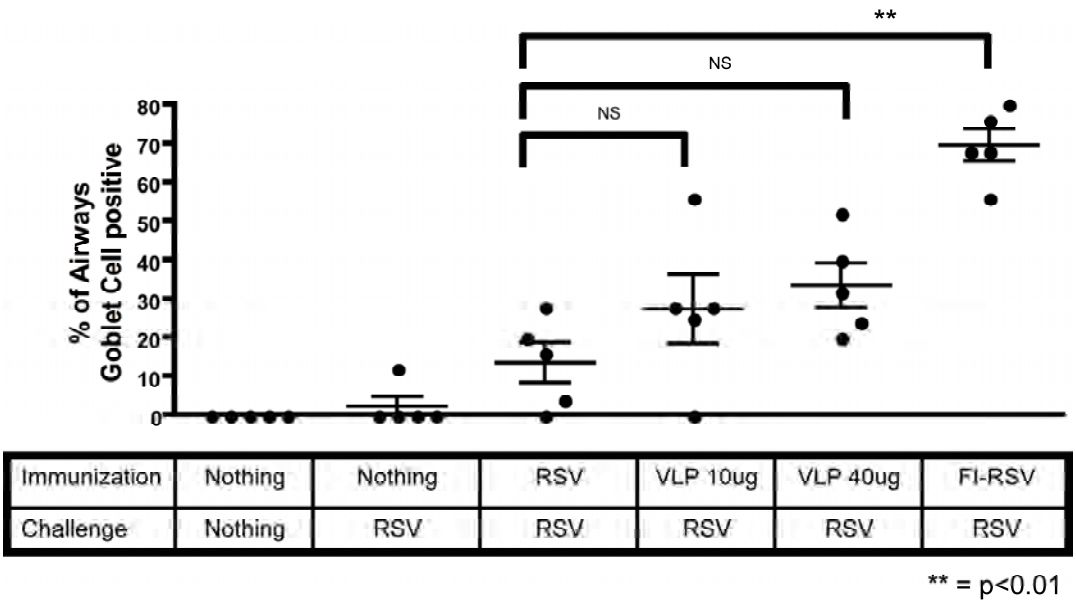

Figure 4.20 Statistical analysis of goblet cells in VLP-H/G immunized mice

Lung tissue sections were harvested 6 days post-challenge as described in Materials and Methods. Tissue sections stained with PAS were scored as the percent of 25 random airways positive for PAS stain. Groups of mice are indicated at the bottom of the panels (ns, differences not statistically significant).

Discussion

Results presented here describe a novel vaccine candidate for respiratory syncytial virus, a virus-like particle that contains an RSV surface protein. The approach takes advantage of the very efficient production of VLPs by the structural proteins of NDV (127). The results presented here demonstrated, first, that the ectodomain of the RSV G protein could be incorporated into particles formed with the NDV NP and M protein and that these particles could be quantitatively produced. Second, these VLPs, VLP-H/G, stimulated soluble immune responses specific to the RSV G protein and primed cytotoxic T lymphocyte responses. Third, immunization of mice with two, or even a single dose of these particles, resulted in the protection of mice from RSV replication in lung tissue. Lastly, upon RSV challenge of VLP-H/G-immunized mice, there was no increased pathology in the lungs compared to lungs of mice immunized by natural infection.

Generation of ND VLPs containing the RSV G Protein

While VLPs are increasingly being considered as vaccines, two have been licensed for use in humans (77), VLPs have not been explored as a potential RSV vaccine**.** We chose to utilize ND VLPs as a platform for the presentation of RSV proteins in a VLP for several reasons. First, only one study of the assembly of VLPs with RSV proteins has been published (162) and the requirements for their formation are relatively undefined. Our preliminary studies showed that the release of RSV VLPs is significantly less efficient than release of ND VLPs (unpublished observations). Second, ND VLPs

stimulate robust soluble and cellular immune responses and the antibody responses are neutralizing (Morrison et al., manuscript in preparation), indicating that these VLPs are potent immunogens. In addition, since NDV is an avian pathogen (4), there is no preexisting immunity to NDV proteins in human populations. Third, that RSV antigens could be incorporated into ND VLPs was suggested by results of our previous studies (Morrison et al, manuscript in preparation) of the requirements for assembly of ND VLPs. Wild-type foreign glycoproteins can be incorporated into ND VLPs due to the phenomenon of phenotypic mixing (17), but at very low frequency (Morrison et al., unpublished observations). However, specific, quantitative assembly of a glycoprotein requires only the cytoplasmic tail and transmembrane domains of an NDV glycoprotein, likely due to specific interactions with the core proteins (Morrison et al., manuscript in preparation). Since both the NDV HN protein (106) and the RSV G protein (29, 172) are type 2 glycoproteins, we chose to make a chimera protein with the NDV HN protein CT and TM domains fused to the RSV G protein ectodomain.

We have also reported that release of ND VLPs requires the M protein, and the efficient assembly of the NDV HN protein into ND VLPs requires both the NP and M proteins (127). Thus, our VLP-H/G particles were built using these two NDV proteins. Wild-type F protein has no negative or positive effect on incorporation of the chimera protein into VLPs. Thus, we were able to eliminate it from these particles. Furthermore, we found that inclusion of the wild-type HN protein interferes with incorporation of the H/G chimeric protein, perhaps due to competition with the chimera protein for binding sites with either NP or M proteins or both. Thus this protein was also omitted.

Importantly, we demonstrated that yields of VLP-H/G particles were significantly enhanced in the presence of heparin in the media. Since the RSV G protein binds to glycosaminoglycans (63, 64), binding that can be inhibited by exogenous heparin, we sought to block rebinding of the released H/G protein containing VLPs to cell surfaces by inclusion of heparin. Indeed, heparin significantly increased the efficiency of recovery of particles in the cell supernatants. This finding also strongly suggests that the H/G chimera protein retains the binding activity of the wild-type G protein.

Immune responses to the RSV G protein upon immunization with VLP-H/G

As has been previously noted by others (112), we found that the maximal sizes of the RSV G as well as the H/G chimera protein varied with the type of cell in which they were expressed, a result likely due to cell type variation in the glycosylation. Importantly, the least glycosylated protein was produced in avian cells, and it was this cell type that was utilized to produce the VLPs. However, the under-glycosylated protein stimulated antibodies that would bind to more heavily glycosylated protein present in transfected COS7 cells (Figure 4.7) or transfected HEK 293T cells (Figure 4.8). The levels of these antibodies raised against the H/G protein were similar to or higher than levels of antibodies raised against comparable amounts of the more fully glycosylated G protein in UV-inactivated RSV using, as target antigen in ELISA, two different sources of target G protein (Figure 4.7-8). Thus, the lower levels of glycosylation in the VLP-associated H/G protein did not adversely affect the levels of anti-G protein antibodies

after immunization. Indeed, the under-glycosylated protein may be a better antigen, as the protein sequence may be more accessible.

Our results also showed that, while the VLP-H/G delivered by either intraperitoneal inoculation or intramuscular immunization resulted in antibody responses to the G protein, antibody levels increased faster and peaked sooner after intraperitoneal immunization than after intramuscular immunization. The titers of antibodies after intramuscular immunization were also lower prior to a boost. Maximal titers after a single dose delivered IM were, on average, 100, in contrast to titers of, on average, 400 after IP immunization. However, after an IM boost and RSV challenge, the IgG antibody levels after IM immunization increased significantly and to levels higher than that seen after boosts delivered by IP (compare Figure 4.8, and Figure 4.10). Both routes of immunization were effective, however, since both routes of immunization resulted in inhibition of RSV replication upon challenge.

Data presented here demonstrated that VLP-H/G particles were also capable of eliciting strong CD8 T cell responses in immunized mice, levels similar to CD8+ T cell responses after virus infection. This observation is in agreement with previous observations that other types of VLPs can stimulate CTL responses (20, 37, 126). VLPs can likely promote CTL responses because viral antigens are displayed in highly repetitive, ordered arrays on particle surfaces, a presentation ideally suited for phagocytosis by resident leukocytes such as macrophages and DCs (38, 116, 126). However, as there is no clear-cut T cell epitope defined for the G protein, the specificity of the CTLs detected here is unclear. Since it was only the G protein ectodomain that

was in common between the immunogen and the antigens used to stimulate spleen cells in culture, it seems most likely that VLP-H/G stimulated G protein specific T cells. Perhaps under glycosylation of the avian cell derived G protein unmasked a T cell epitope. Alternatively, it is perhaps possible that the CTLs detected in these experiments may be due to some type of cross-reaction between the NP or M core proteins of RSV and NDV. However, there are no common short sequences in the RSV NP and M proteins and the NDV NP and M proteins.

Protection provided by VLP-H/G immunization to RSV challenge

The role of the RSV G protein in stimulating protective immune responses is not entirely clear. Some G protein subunit vaccines with a sequence of the G protein induced protection in animals although some have resulted in enhanced lung pathology or short-lived responses. Viral vectored vaccines containing the G protein gene have been shown to be protective in some systems but not others (reviewed in (99)). DNA vaccines containing the G protein gene have demonstrated some protection (reviewed in (99)). However, in many cases, the mechanisms involved in protection observed are unclear.

VLP-H/G immunization protected mice from RSV replication in murine lungs after intranasal challenge with infectious RSV. Protection was observed after intraperitoneal immunization of 30 μg total VLP protein, followed by a boost of 10 μg. Protection was also observed after a single intramuscular injection of VLP-H/G. In addition, protection was obtained after a single dose of 10 μg of total VLP-H/G protein,

an amount that corresponded to approximately 1.5 to 2 μg of G protein per animal. Thus the VLP-H/G was a very potent protective immunogen.

The mechanisms responsible for this protection are not yet clear. Soluble antibody may be involved. However, the anti-G antibodies in the murine sera were not neutralizing in an *in vitro* plaque reduction assay (not shown). These findings were in agreement with previously published literature suggesting that antibodies raised against RSV G can confer protection without being neutralizing (7, 153). For example, BALB/c mice that prophylactically received anti-RSV G immunoglobulin were protected against live RSV challenge (70). While the mechanisms underlying this phenomenon are not yet fully understood, some research has suggested FcγR-dependent and independent mechanisms may explain the protective effects of the anti-RSV G antibody. Fc-dependence was shown by studies in which portions of the IgG heavy chain region were removed to create anti-RSV G light chain fragments (Fab'_2). Upon administration to mice, those receiving the IgG light-chain fragments were more susceptible to live RSV infection than mice receiving the wild-type IgG (111, 113). Therefore, these studies suggest that the Fc portion of the anti-RSV G antibody can confer protection in naïve mice.

Furthermore, it has been suggested that antibodies specific to the F protein are more important for protection than antibody to G protein (128). While antibodies to G are not neutralizing in *in vitro* systems, it is possible that anti-G protein antibodies have an undefined role in preventing the spread of infection in the lung, a role unrelated to virus neutralization as measured by virus neutralization *in vitro*. It is also possible that

cell-mediated immune responses have a role in protection. While no CD8 T cell epitopes have been described for the G protein, data presented here and in other studies suggest a role for G in establishing a cytotoxic CD8 T cell response (18, 47), although a potential mechanism for these responses has not yet been described. In addition, recent results indicate that induction of innate immune responses are important for the development of potent B cell responses (50, 74, 93, 129) and for affinity maturation of antibodies, including anti-RSV antibodies (41).

Enhanced disease after RSV challenge

Major complications to RSV vaccine development are the results of early vaccine trials using formalin-inactivated RSV as an immunogen. This preparation, called lot 100 (86), resulted in enhanced disease upon RSV infection, and the enhanced disease was characterized by heightened pulmonary cellular infiltrates and increased airway hyper-reactivity indicative of Th-2 allergy-like responses (82, 125). Enhanced disease has been mimicked in animal models, including BALB/c mice used here, and is characterized by an increased inflammation of respiratory tissue due to influx of lymphocytes and eosinophils, enhanced mucous secretion, and an unbalanced immune response (39, 119, 125). Increased inflammation associated with FI-RSV immunization was reproduced here as indicated by increased numbers of immune cells around blood vessels, airways, and in interstitial spaces in FI-RSV immunized mice (Fig 4.15-4.17). Airway hyperreactivity is often associated with a strong Th2-biased response and the presence of goblet cells. Goblet cells are implicated in disease pathogenesis because they can produce large

quantities of mucin, which contribute to airway obstruction, further worsening disease (2, 43). Previous studies have shown that RSV can induce goblet cells, a condition referred to as goblet cell hyperplasia (GCH), in the lungs of BALB/c mice and that Th2-sensitized mice exhibit extensive GCH following RSV infection (14, 15, 103). Indeed, results presented here indicated that FI-RSV immunized mice, following RSV challenge, exhibited significant GCH, a metaplastic process resulting in near total replacement of epithelial cells by goblet cells, in most airways.

Many studies over decades have sought to clarify the mechanisms for this enhanced disease. Early reports suggested immunization with the purified G protein alone or vaccinia virus delivered G protein elicited an unbalanced, Th2-dominated immune response (59, 68, 124). More recent studies suggest that the unbalanced response observed in these cases may be due to the soluble form of the G protein (sG), not the membrane bound form (mG) or to the method of antigen delivery (78, 79). It has been suggested that sG protein, which represents 80% of G protein released from cells (42, 79), can subvert host immune detection in part by inhibiting Toll-like receptor 3 and 4 mediated IFN-β production and that the Th balance can be restored using TLR adjuvants (66, 146). It has also been suggested that disease enhancement is related to two mucin-like domains (GCRR) in the G protein ectodomain (GCRR) (56, 92). This GCRR domain includes a CX3C chemokine motif that has been hypothesized to affect leukocyte trafficking to lungs (69), indirectly promoting Th2 responses by inhibiting important immune pathways that support Th1 responses. In contrast, it has been suggested recently that enhanced disease caused, at least by formalin-inactivated RSV vaccines or any

nonreplicating vaccine, is not due directly to the G protein. Rather, it was suggested that these immunogens are poor activators of innate immunity and, as a result, fail to stimulate a strong acquired immune response (41).

To determine if VLP-H/G immunization stimulated symptoms of enhanced disease in mice, inflammation of the lungs of immunized and challenged mice were scored as previously described (114), and airways were scored for goblet cell hyperplasia. There were no statistically significant differences between VLP-H/G and infectious RSV immunized mice. Thus, the VLP-H/G did not induce increased pulmonary inflammation and GCH compared to natural infection. In contrast, the FI-RSV immunized mice showed dramatic inflammation that was statistically very significantly different from that observed for VLP-H/G immunized mice. FI-RSV-immunized mice also displayed dramatically increased GHC that was significantly enhanced over that observed in the VLP-H/G or RSV immunized mice. These results suggest that a VLP vaccine strategy may not predispose animals to enhanced RSV induced disease upon challenge and that the ectodomain of a particle associated G protein does not directly result in enhanced disease.

In sum, many of our results demonstrated that the RSV G protein ectodomain was efficiently incorporated into virus-like particles based on NDV proteins and that these particles stimulated very effective immune responses in mice, immune responses that prevented replication of RSV in lung tissue. Furthermore, these particles did not result in enhanced pulmonary inflammation typified by FI-RSV or UV-RSV.

Chapter V

Conclusions and Future directions

RSV continues to pose a serious global health threat, but efforts to limit this pathogen are handicapped by the limited understanding of the virus itself and the mechanisms by which it induces disease in humans. While the cytopathic effects of RSV infection in lung tissue can play a role in the etiology of RSV-induced disease, a growing body of evidence suggests that host immune responses, induced following infection, are major contributors to disease susceptibility. While research aimed at understanding how both innate and acquired immune responses could contribute to disease susceptibility have provided some important insights into this phenomenon, a complete understanding of the host/virus interactions that predispose for disease still remains somewhat elusive.

This body of research endeavors to provide additional insights into how innate and acquired immune mechanisms can shape host responses to RSV infection. Data presented in chapter II and III further support the hypothesis that innate immune mechanisms, including TLRs, are important for recognizing RSV and shaping immune responses in the lung. Multiple TLRs including TLR2,3,4,6,and 7, as well as RIG-I, are now known to associate with RSV. These observations underscore the diverse repertoire and complexity of signaling utilized by the host innate immune system to control RSV. Since multiple innate immune signaling pathways are likely required to promote viral clearance and prevent disease, a breakdown in any one pathway may predispose for disease. In fact, evidence supporting this hypothesis has been shown in RSV susceptible

infants with TLR4 polymorphisms that blunt innate immune responses (10,174). Perhaps defects in TLR2 signaling may also predispose for disease. This would be an interesting hypothesis to examine.

Furthermore, TLR2 signaling influenced DC maturation, suggesting that TLR2 can directly modulate acquired immune responses. In fact, studies examining vaccinia virus (VV) and TLR2 interactions demonstrated that TLR2/VV interactions could influence DC-dependent expansion of T and B cells (178). This study showed that TLR2 signals were important for generating anti-VV CD8 T cells and for the functional maturation of DCs. Based on these findings and studies by Rudd et al. showing a role for MyD88 responses in RSV disease susceptibility (140), it is tempting to speculate that defects in TLR2 signaling could predispose for RSV disease by modulating the DCs ability to prime Th1 or Th2 anti-RSV immune responses.

Alternatively, RSV itself has been shown to interfere directly with innate immune signaling (i.e., TLR3/4-mediated type I IFN production) (144). Since TLR2 signals are important for controlling viral replication, RSV may possess the ability to interfere with TLR2-mediated signaling thereby dampening innate immunity. While evidence supporting this hypothesis has not been demonstrated, it has been suggested that the RSV SH protein can neutralize TNF-α function (51). These studies showed rPIV5 expressing the RSV SH protein could inhibit TNF-α induced NF-κB expression in an *in vitro* system. Since data presented here demonstrated TLR2 signals induced strong TNF-α responses following RSV interactions, it is likely that RSV has developed mechanisms to

counteract at least some of the positive effects of TLR2 signaling. However, questions regarding how RSV might interfere with TLR2 remain unexplored.

Furthermore, data presented here clearly demonstrate some type of association between TLR2 and RSV, but the ligand for TLR2 on RSV remains undetermined. Previous research has demonstrated that RSV surface proteins can interact with TLRs (i.e., RSV F and TLR4) (99), suggesting, perhaps, that the RSV G protein, or the RSV SH protein, could be potential candidates for this interaction. The RSV G protein is an intriguing candidate, but the protein is difficult to isolate, exists in two different forms, and is highly glycosylated, which could mask the antigenic portion of the molecule. Therefore, more extensive analysis is needed to determine the ligand for TLR2 on RSV.

Of interest, VLPs expressing RSV G protein introduced in chapters IV could potentially provide insight into these questions because the G protein is presented on the surface of VLPs in its native context and is underglycosylated when grown in avian cells, perhaps rendering the G protein more immunogenic than the fully glycosylated form. Additionally, the RSV G protein expressed in this vector system could help uncover a potential role for the G protein in stimulating innate immunity, through either TLR2 or some other innate immune receptor. Moreover, this expression system could help answer some important questions regarding the role of RSV G in stimulating acquired immune responses as well.

Early studies suggested that RSV G protein did not play a major role in generating strong acquired immune responses since neutralizing antibodies are targeted against F and not G. More recent studies have questioned the validity of this hypothesis because

the G protein, the soluble form of G in particular, has been shown to down-regulate and, perhaps, even directly inhibit some acquired immune responses. Some studies even suggest that soluble G can antagonize the function of anti-RSV neutralizing antibodies by serving as an antigen decoy (21). Furthermore, data presented in Chapter IV argue that the G protein can affect the generation of RSV specific CTLs. However, a defined CD8 epitope for this protein has not been characterized. Collectively, these observations suggest a more complex role for the RSV G protein than previously recognized. Perhaps a clearer understanding of how the G protein could manipulate both innate and acquired immune responses would reveal more clues to the pathogenesis of RSV induced disease.

In summary, data presented in chapters II-IV have provided some novel insights into the questions surrounding host/RSV interactions that can lead to innate and acquired immune responses. Indeed, RSV pathogenesis is a multi-factorial process likely resulting from both host immune responses and cytopathic effects of RSV on lung epithelium. It appears that RSV has successfully managed either to subvert some immune pathways through virally encoded proteins or to misdirect immune responses by exploiting multiple TLR signaling pathways, perhaps even both. Therefore, understanding how RSV manipulates both innate and acquired responses may be the key determinant in understanding the underlying mechanisms of RSV induced pathogenesis.

Chapter VI

Materials and Methods

Chapters II and III

Animals:

Knockout mice were extensively back-bred onto the C57BL/6 background. Backcrossing was confirmed by satellite marker analysis (Charles River Laboratories) and mice were genotyped by PCR of tail DNA. Eight to 10 week female TLR1 KO (F9), TLR2 KO (F11), TLR4 KO (F11), TLR6 KO (F10), and MyD88 KO (F12) mice (back-bred from knockout mice originally provided as a gift from Dr. Shizuo Akira) were housed under specific pathogen-free conditions at the University of Massachusetts, Worcester campus. Age- and sex-matched C57BL/6, BALB/c, and B6.129F2/J wild-type mice were purchased from The Jackson Laboratories.

Growing RSV virus:

Human RSV A2 strain was grown in Vero cells. Briefly, 85-90% confluent T175 flasks of Vero cells were infected with RSV at 1 MOI in 5 ml of DMEM. Cells were infected for two hours at 37^0C and 5% CO_2. After infection, 7 ml of DMEM with 10% FBS (Gibco), 0.1% Pen/Strep (Cellgro), and 0.001% Cipro (Bayer) was added to the flask. Flasks were incubated for approximately 4 days or until extensive syncytia formation was observed. On the day of harvest, all except 3 ml of supernatant was removed and placed on ice in 50 ml conical tubes, approximately 3 ml per tube. Cells

were scraped from the flask, added in equal distribution to conical tubes, and sonicated three times, 5 seconds per time, at 25W on ice. Cell debris was removed by centrifugation at 600 g for 7 minutes at 4^0C. Virus supernatant was stored in 30% sucrose at -80^0C. Uninfected flasks were treated identically to generate Vero cell lysate control.

Harvesting peritoneal macrophages:

Mice were i.p. injected with 4% thioglycollate (Sigma). Four days after injection mice were euthanized and the peritoneum was flushed with normal saline. Contaminating red cells were lysed with red blood cell lysing buffer (Sigma) according to manufacturer specifications. The resulting peritoneal exudate cell suspension was analyzed by flow cytometry and consisted of > 90% macrophages based on $CD11b^+$ expression (data not shown). Cells were resuspended in DMEM containing 10% FBS (HyClone) and 0.1% Pen/Strep, quantified using a hemocytometer, and added to tissue culture plates (Costar) for further analysis.

Macrophage stimulation assays:

Peritoneal macrophages were seeded in 96 well round bottom tissue culture treated plates (Costar) at 1.0×10^6 cells/ml. Cells were stimulated with live RSV A2 strain (0.3 MOI), UV-inactivated RSV A2 strain (0.3 MOI equivalent), TLR4 ligand pLPS (100ng/ml)(Sigma), TLR2 ligand Pam_2CSK_4 (100ng/ml)(Sigma), and Vero cell lysate control (50ul/well), as indicated in the text. UV inactivation of RSV was

performed using a UV stratalinker 2400 (Stratagene) at a voltage of 1 x 10^6 microjoules/cm^2. Inactivation was confirmed by immunoplaque assay.

Macrophages were stimulated for 24 hours at 37^0C and 5% CO_2. After stimulation cell supernatants were removed and stored at -20^0C for ELISA analysis. Intracellular TNF-α production was determined using FITC conjugated anti-TNF-α antibody (BD Pharmingen) and macrophages were gated using PE conjugated anti-CD11b antibody (BD Pharmingen).

***In vivo* infection:**

Mice were lightly anesthetized with isoflurane and intranasally (i.n.) challenged with 2.4 x 10^6 PFU of RSV A2 strain or equal volume of Vero cell lysate control.

Collection and analysis of BAL cells and lung tissue:

Mice were anesthetized with isoflurane and exsanguinated by severing the right caudal artery. Bronchoalveolar lavage (BAL) cells were harvested by lavaging the lung four consecutive times with 1 ml PBS containing 0.1% BSA. BAL cells were pooled and pelleted by centrifugation at 2000 rpm for 5 minutes. Cells were surface stained with FITC conjugated anti-mouse CD11b (clone M1/70, BD Pharmingen), PE conjugated anti-mouse CD86 (clone GL-1, BD Pharmingen), PE conjugated anti-mouse F4/80 (clone BM8, eBioscience) APC conjugated anti-mouse CD11c (clone HL3, BD Pharmingen), and/or Alexa-647 conjugated anti-mouse neutrophils (clone 7/4, Serotec).

Lung tissue was removed following BAL harvest. One half of total lung tissue was stored in 30% sucrose for plaque assay. The remaining half of lung tissue was stored in protease inhibitor (Roche) for ELISA analysis. Tissues were stored at -80^{0}C until analysis. For analysis, lungs were thawed on ice and weighed. Lungs were homogenized using a pellet pestle and centrifuged at 2600 g for 10 minutes at 4^{0}C to clarify supernatant.

RSV immunoplaque assay:

Twenty-four well tissue culture plates (Costar) were seeded with 1.5 x 10^5 Vero cells/well in DMEM containing 10% FBS (Gibco), 0.1% Pen/Strep (Cellgro), and 0.001% ciprofloxacin (Bayer). Cells were incubated overnight at 37^{0}C and 5%CO_2. Media were removed from confluent monolayers and serial dilutions of RSV stock or lung tissue clarified supernatants were absorbed to monolayers. All samples were run in duplicate wells. Plates were incubated at 37^{0}C and 5% CO_2 for 2 hours for optimum infection. After incubation, supernatant was removed and 1 ml of M199 media (Gibco) containing 0.01% Pen/Strep mixed 1:1 with 2% methylcellulose (Sigma) was overlayed on monolayers. After 6 days of incubation at 37^{0}C and 5% CO_2, or when extensive syncytia developed, overlay was removed and monolayers were fixed with 1 ml of ice-cold Acetone:Methanol (60:40). Fixative was removed after 10 minutes and plates were air-dried. Plates were blocked in 5% nonfat dry milk (Biorad) for 10 minutes at room temperature. Primary RSV anti-F and anti-G antibodies (Clone 131-2A, 131-2G, Chemicon) were added to wells for two hours followed by secondary HRP anti-mouse Ig

antibody (Clone 187.1, BD Pharmingen) for one hour. Antibodies were diluted in 5% milk and plates were incubated at 37^0C and 5% CO_2. Plates were hand washed twice with PBS containing 0.5% Tween 20 (Sigma) after each antibody incubation step. Individual plaques were developed using DAB substrate kit (Vector) per manufactures specifications. Limit of detection for our immunoplaque assay is approximately 1.4 $\log_{10}$ PFU/gram.

ELISA analysis:

Clarified lung homogenates and cell supernatants were analyzed for IL-6 (BD Pharmingen), TNF-α (BD Pharmingen), CCL2 (MCP-1) (BD Pharmingen), and CCL5 (RANTES) (R&D Systems) using a sandwich ELISA assay as indicated in the text. ELISAs were performed per manufacturer specifications. IFN-β was measured from cell supernatants by ELISA according to the following protocol: monoclonal rat anti-mouse IFN-β (Yamasa Corp., Japan, clone 7F-D3) was used as the capture antibody and polyclonal rabbit anti-mouse IFN-β (PBL Biomedical Laboratories, #32400-1) for detection together with HRP-conjugated goat anti-rabbit IgG as the secondary reagent (Cell Signaling Technology, Inc. #7074). Mouse IFN-β (PBL Biomedical Laboratories, #12400-1) was used as the standard.

Type I Interferon bioassay:

Macrophages were stimulated with RSV A2 (MOI 2), TLR 3 ligand Poly I:C (Amersham) (50ug/ml), and TLR4 ligand LPS (100ug/ml) or medium alone for 24 hours.

Supernatants were removed and UV-treated to inactivate the infectivity of the virus. Serial 2-fold dilutions of UV-inactivated supernatant were added to fresh NTCT929 cells at 1 x 10^5cells/ml in 96 well flat-bottom tissue culture plates (Costar). Cells were incubated for 24 hours at 37^0C and 5%CO_2. After 24 hours supernatants were removed and infected with VSV at 2.5 x 10^3PFU/ml. The highest dilution that resulted in a 50% reduction of VSV-induced cytopathic effect is defined as 1 U/ml of type one interferon.

Flow cytometric analysis:

Harvested cells were washed twice with cold PBS containing 2.0% BSA, enumerated using a hemocytometer, and transferred to 96 well round bottom tissue culture plates (Costar). Cells were incubated in anti-mouse CD16/CD32 Fc block (BD Pharmingen) for 15 minutes at room temperature. Cells were washed twice with wash buffer and surface stained with indicated antibodies and appropriate isotype controls per manufacturers specifications. Cells were washed twice with wash buffer and resuspended in wash buffer for analysis. For intracellular cytokine staining, cells were cultured overnight in the presence of GolgiStop^{TM} (BD Pharmingen). Following surface staining cells were treated with BD Cytofix/Cytoperm^{tm} Plus Kit (BD Pharmingen) per manufacturers specifications. Cells were stained with indicated intracellular antibodies and appropriate isotype controls for 30 minutes at 4^0C in the presence of Perm/Wash buffer. After incubation cells were washed twice with perm/wash buffer and resuspended in wash buffer for analysis. Cells were analyzed using a BD LSR II Flow Cytometer and FlowJo 8.4.2 software (TreeStar).

Statistical analysis:

Statistical significance was determined using an unpaired, two-tailed Student's t test. Values of $p<0.05$ were considered significant. Error bars are +/- SD or +/- SEM as indicated in the figure legend. Statistics were generated using Graph Pad software v4.0c (Prism).

Chapters IV

Cells, Virus, Plasmids

ELL-0 (avian fibroblasts) were obtained form the American Type Culture Collection as were Vero cells, COS-7 cells, and Hep2. ELL-0 cells and Hep2 cells were maintained in Eagle's minimal essential medium (EMEM) (Gibco) supplemented with 10% fetal calf serum (FCS) and 2 mM glutamine. COS-7 cells were grown in DMEM supplemented with nonessential amino acids, vitamins, penicillin, and streptomycin, and 10% fetal calf serum. Vero cells were grown in DMEM supplemented with penicillin, streptomycin, and 5% fetal calf serum. RSV, A2 strain, was obtained from Dr. Ralph Tripp.

The RSV G protein cDNA was a codon optimized synthetic gene obtained from Novavax, Inc. NDV NP, M, F and HN protein genes as well as the RSV G protein gene were inserted into the pCAGGS expression vector as previously described (107, 108).

NDV HN protein-RSV G protein chimera gene was constructed by ligation of PCR derived DNAs derived from pCAGGS-HN and pCAGGS-G. Primers used to generate a DNA encoding the HN cytoplasmic (CT) and transmembrane (TM) domains were GGTTATTGTGCTGTCGACTCATTTTGGC (forward primer) and CATACTATATGCCAGGGCGGCCGCAGAGATGGCTAAG (reverse primer). This product was digested with XhoI and Not I (a site introduced without changing the amino acid sequence). The primers used to generate DNA encoding the G protein ectodomain were CTTCCCTCATCATTGCAGCGGCCGCTCTTGCCTACTCTGCGAATCATAAGGTC

(forward primer which introduced a Not I site without changing the amino acid sequence) and GCCAGAAGTCAGATGGCCAAGG (reverse primer). The product was digested with Not I and Msc I. The two DNA fragments were ligated into an XhoI-MscI digested pGAGGS vector. The resulting plasmid containing the chimera protein gene was sequenced in its entirety to verify the gene junctions (illustrated in Figure 1, panel A) and to ensure that no additional changes were introduced during the PCR reactions.

Antibodies

Polyclonal rabbit anti-NDV antibody was raised against UV inactivated, purified NDV as previously described (109). Polyclonal goat anti-RSV antibody (Biodesign) and mouse monoclonal anti-G antibody (MyBiosource) were used in Western blots. Anti-RSV F monoclonal antibody (clone 131-2A, Chemicon) was used in plaque assays. Secondary antibodies utilized were anti-goat antibody (Sigma), anti-mouse antibody (Sigma), and anti-rabbit antibody (Sigma).

Transfections

Transfections were accomplished using Lipofectamine (Invitrogen), as recommended by the manufacturer. For small scale transfections, a mixture of plasmid DNA (0.5µg/35mm plate) and lipofectamine (5µl/35mm plate) in Opti-MEM media (Gibco) was incubated at room temperature for 45 minutes, and then added to cells grown in 35mm plates and previously washed with OptiMEM. Cells were incubated for 5h at 37ºC, Opti-MEM was removed, and 2ml of supplemented DMEM were added.

For quantitative preparations of VLPs, large-scale transfections of cells growing in T-150 flasks were utilized. For each T-150 flask, plasmid DNA (8μg of each plasmid) in 1.6 ml of Opti-Mem and lipofectamine (80 μl) in 3.2 ml of Opti-MEM were each incubated for 15 min at room temperature, mixed, and further incubated for 45 min at room temperature. Opti-Mem (11.2 ml) was mixed with the DNA-lipofectamine complexes and added to cells in a T-150 flask that had been twice washed with Opti-Mem. Cells and DNA-lipofectamine complexes were incubated for 5 hours at 37 C, the complexes removed, and 15 ml of complete media were added.

Polyacrylamide gel electrophoresis, Silver staining, and Western analysis

Proteins in extracts, virus, or VLPs were resolved on 8% polyacrylamide gels (SDS-PAGE) as previously described (127). Silver staining of proteins in the polyacrylamide gels was accomplished as recommended by the manufacturer (Pierce). For quantification of individual proteins in the polyacrylamide gels, different concentrations of BSA were electrophoresed on the same gel. A standard curve based on the stain of the BSA (using a Biorad densitometer to measure the intensity of staining) was used to determine the concentrations of each of the proteins in the purified VLPs or virus. For Western analysis, proteins in the polyacrylamide gels were transferred to PVDF membranes (PerkinElmer) using dry transfer (iblot from Invitrogen). Proteins were detected in the blots as previously described (91).

VLP purification

At 24 hours post-transfection, heparin was added to the cells at a final concentration of 10 μg/ml. At 72 hours post-transfection and again at 96 hours post-transfection, cell supernatants were collected and cell debris was removed by centrifugation at 5000 rpm (Sorvall GSA SLA-1500 rotor). VLPs in the supernatant were pelleted by centrifugation in a Type 19 Rotor (Beckman) at 18,000 rpm for 12 hours. The resulting pellet was resuspended in TNE buffer (25 mM Tris-HCl, pH 7.4, 150 mM NaCl, and 5 mM EDTA), dounce homogenized, and layered on top of a discontinuous sucrose gradient composed of 2 ml 65% sucrose and 4 ml 20% sucrose. The gradients were centrifuged in an SW 28 rotor (Beckman) at 24,000 rpm for 6 hours. The fluffy layer at the 20-65% sucrose interface, containing the VLPs, was collected, mixed with two volumes of 80% sucrose, and placed in top of a 1 ml layer of 80% sucrose in a SW41 Beckman centrifuge tube, and then over layered with 3.5 ml of 50% sucrose and 2ml of 10% sucrose. The gradients were centrifuged for 18 hours at 38,000 rpm. The VLPs, which float to the interface of the 50% and 10% sucrose layers, were collected and concentrated by centrifugation in an SW50.1 rotor for 16 hours at 38,000 rpm. All sucrose solutions were w/v and dissolved in TNE buffer and all centrifugations were done at 4 C.

RSV purification

RSV (moi of 0.1) in 5 ml of DMEM without serum was added to confluent Vero cells growing in T-150 flasks. Cells were incubated with virus for 2 hours at 37, and then 15 ml of DMEM with 5% fetal calf serum were added. Infected cells were incubated for

3-4 days at 37 C. The cells were then scraped into the cell supernatant; the suspended cells were frozen at -80 C, and then thawed. The resulting cell lysates were clarified by centrifugation at 3200 rpm (Sorvall) for 20 minutes. Virus in the supernatant was precipitated using PEG 8000 (50% w/v) added to the supernatant for a final concentration of 10% and incubated for 90 min with stirring at 4 C. The precipitated virus was pelleted by centrifugation at 5000 rpm for 20 min at 4 C, snap frozen, and stored at -80 C. The thawed virus pellet was resuspended in 10% sucrose in TNE, homogenized and layered on top of a discontinuous sucrose gradient composed of 1 ml of 60%, 3 ml of 45%, and 4 ml of 30% sucrose (all dissolved in TNE buffer) and the gradient was centrifuged at 35,000rpm in an SW41 rotor for 90 minutes. The visible virus band between the 30% and 45% sucrose layers was collected. The viral protein content (M, NP, F, G) of purified RSV was determined as described above using known amounts of BSA included in the same gel.

RSV UV inactivation

Purified virus was diluted in 2 ml of PBS in a 60 mm tissue culture dish and placed on a rotating platform 10 cm from a Germicidal Lamp (G15T8, Sylvania) for 20 minutes, a time previously determined to inactivate 100% of the virus as measured by plaque assay. The efficacy of UV inactivation was determined in a plaque assay.

Formaldehyde treated RSV (FI-RSV)

Formalin inactivated RSV (FI-RSV) was prepared by a modification of the method of Prince et al, (135). Virus was harvested from infected Hep-2 cells, clarified by centrifugation (1000 x g for 20 min at 4^{o} C), filtered through a 0.8 μ filter, and then formalin treated by the addition of 1/10 volume of a 1:400 dilution of 37% formaldehyde in water, and incubated for three days at 36^{o} C with gentle stirring. The formalin-treated virus was pelleted at 100,000 x g for 60 min at 10^{o} C and resuspended in 1/20 volume of HMEM, 1/10 volume SPG (2 M sucrose, 110 mM potassium phosphate, pH 7.1, 5 mM monosodium glutamate). The resuspended virus was centrifuged at 1000 x g for 15 min 4^{o}C, and the supernatant was incubated with 4 mg/ml Aluminum hydroxide (Alhydrogel) overnight at room temperature. The virus alum mixture was centrifuged at 1000 x g for 15 min and the Aluminum hydroxide pellet (adsorbed virus) was resuspended in one half volume of HMEM, 1/10 volume SPG, and stored in 0.5 ml aliquots at 4^{o}C. The amount of virus bound to the alum was estimated at 44% by measuring the amount of total protein in the formalin inactivated virus sample before and after alum adsorption. The amount of virus adsorbed to the alum was calculated to be equivalent to 6.1×10^{8} pfu/ml. This estimate was based on the known virus titer prior to formalin treatment, the volume of the virus prior to formalin inactivation; the percent protein bound to the alum, and the concentration factors for each step in the procedure.

Antibody neutralization

Mouse sera were complement inactivated and then diluted in DMEM without serum. Purified RSV virus was diluted to approximately 75 to 150 pfu in 100 μl.

Dilutions of mouse sera in 100 µl was added to the virus and incubated for 1 hour at 37^0 C. The mixture was then added to pre-washed, confluent monolayers of Vero cells growing in 24 well tissue culture dishes, and the cells were incubated at 37^0C for one hour. The antibody-virus mixture was removed and 1 ml of methylcellulose overlay was added to each well as described above. Plates were incubated for 3-4 days and plaques were stained as described above.

Animal immunization and challenge

Mice, 3-week-old BALB/c, from Jackson Laboratories or Taconic laboratories, were housed (groups of 5) under pathogen-free conditions in microisolator cages at the University of Massachusetts Medical Center animal quarters. All protocols requiring open cages were accomplished in biocontainment hoods. Mice were immunized by intraperitoneal (IP) or intramuscular (IM) inoculation of different concentrations of VLPs or UV inactivated RSV in 0.5 ml (IP) or 0.05ml (IM) of PBS containing 30% sucrose. Other groups of mice were lightly anesthetized with isoflurane and then infected by intranasal (IN) inoculation of RSV (1-3 x 10^6 pfu/mouse in 50 µl). Mice that received an immunization boost were injected IP or IM with 10 µg of VLPs or UV RSV/mouse or 1-3 x 10^6 pfu/mouse of live RSV (IN).

Mice challenged with live RSV were lightly anesthetized as described above and infected IN with 1-3 x 10^6 pfu of virus.

Detection of virus in lung tissue

Mice were anesthetized with isofluorane and exsanguinated after severing the right caudal artery. Lungs were removed aseptically, placed in 0.5 ml of 30% sucrose in PBS and stored at -80 C. Upon thawing, lungs were weighed and then homogenized using pestle (Kontes). The homogenate was centrifuged at 12,000 rpm for 15 min and the virus titer in the supernatant was determined by plaque assay as described above.

Determination of antibody titers by ELISA

Antigens used as targets in ELISA were RSV infected Vero cell extracts, extracts from 293T cells transfected with pGAGGS-G, or extracts from COS-7 cells transfected with pGAGGS-G. To prepare cell extracts, cell monolayers were washed in cold PBS and lysed in TNE buffer (25 mM Tris-HCl pH 7.4, 150 mM $NaCl_2$ and 5 mM EDTA) containing 1% Triton X-100. All antigens were placed in carbonate buffer, pH 9.6, and added to microtiter plates (Costar) and incubated overnight at 4^0C. Amounts of transfected extracts added to each well were adjusted so that the amounts of G protein were comparable as determined by Western blot.

After binding of the target antigen, wells were blocked in 50 µl PBS containing 1% BSA (bovine serum albumin) at room temperature for 1-2 hours, washed three times in PBS, and drained. Different dilutions of mouse sera were added to the microtiter wells in 50 µl of PBS-BSA and incubated for 1 hour at room temperature. After removing the mouse sera and washing wells three times, a biotinylated anti-mouse antibody (1:4000 dilution)(Sigma) in 50 µl of PBS-BSA was added and the microtiter plates were incubated for 1 hour at room temperature. The microtiter plates were then washed three

times in PBS and an HRP conjugated neutravidin (1:4000 dilution) (Pierce) was added in 50 µl of PBS-BSA (1:4000 dilution). The microtiter plates were incubated for 1 hour at room temperature and washed four times in PBS. TMB (3,3',5,5',tetramethylbenzidene) substrate (Sigma) in 50 µl was added to each well and incubated for 15-20 min. The reaction was stopped with 50 µl 1N H_2S0_4 and the OD was read in a plate reader (Molecular Devices).

Cytotoxic T cell assays

Mice were immunized via a single intramuscular dose of VLP-H/G or infected via intranasal instillation with infectious RSV A2, as described above. Spleens were harvested from mice 5 weeks after primary immunization. Single cell suspensions of splenocytes were obtained by passing cells through a 40um nylon cell strainer (BD Falcon). Cells were washed twice with RPMI (Gibco) containing 10% FBS (HyClone) and resuspended in RPMI supplemented with 10% FBS, 100u/ml Penn/Strep (Gibco), 1M HEPES (Gibco), 200mM L-Glutamine (Gibco), and 55mM 2-mercaptoethanol (Gibco) (assay medium).

For *in vitro* restimulation, single cell suspensions of naïve splenocytes harvested from unimmunized mice were generated as described above. Contaminating red blood cells were lysed using RBC lysis buffer (Sigma) and washed twice with assay medium. For use as the stimulator population, splenocytes infected for 18 hours with infectious RSV A2 (MOI 10) were irradiated with 3000 rad of ^{251}Cesium. Stimulators were washed twice with RPMI (Gibco) containing 10% FBS, resuspended in assay medium and then

mixed with primed splenocytes in a 5:1 ratio in 2ml of assay medium per one well of a 24 well tissue culture treated polystyrene plate (Costar). Cells were cultured at 37^0C and 5% CO2 for 5 days. After 5 days, splenocytes were harvested, washed 2 times with RPMI containing 10% FBS and resuspended in MEM (Gibco) containing 5% FBS.

Splenic CD8 T cell function was enumerated using a classical ^{51}chromium release assay. Briefly, P815 (H-2d) mastocytoma target cells were cultured in DMEM (Gibco) supplemented with 10% FBS, 100u/ml Penn/Strep, 1M HEPES, 200mM L-Glutamine, and 55mM 2-mercaptoethanol. P815 cells were infected with RSV A2 (MOI=10) for 18hrs then washed two times with DMEM containing 10% FBS and counted using a hemocytometer. 2×10^6 cells were incubated with 500 μCi of ^{51}Cr for 1 hour then washed 3 times with DMEM containing 10% FBS. Cells were resuspended in MEM containing 5% FBS and incubated with *in vitro* restimulated effector splenocytes at indicated effector:target ratios in 200ul total volume. 1×10^4 target cells were added in triplicate to 96 well U-bottom tissue culture plates for each condition. After 4 hours of incubation, plates were centrifuged at 400 X g for 5 minutes and 50μl of cell supernatant was added to 150μl of optiphase supermix (Wallac). Samples were enumerated using a beta-counter (Wallac). ^{51}Cr labeled target cells were incubated with 5% Triton-X 100 or medium along to measure maximum and spontaneous release. Percent specific lysis for each well was calculated as: (experimental release-spontaneous release)/(maximum release-spontaneous release) X 100.

Pulmonary histology of RSV infected mice

For histological analysis of lung tissue, mice were anesthetized with isofluorane and exsanguinated after severing the right caudal artery. The lungs were then fixed via infusion through the trachea with 4% formalin, removed, and immersed in 4% formalin for 24 hours, embedded in paraffin, sectioned, and stained with hematoxylin and eosin (H and E) or periodic acid Schiff (PAS) by the University of Massachusetts Core Facility. Six sections per mouse were obtained. Sections from each mouse were scored, blindly, for the degree of inflammation (H and E stains) of blood vessels, airways, or interstitial spaces on a scale of 0 to 3 as previously described (114). For sections stained with PAS, the percents of airways positive for PAS in 25 randomly selected airways were determined.

Statistical analysis:

Statistical significance was determined using an unpaired, two-tailed Student's t test. Values of $p<0.05$ were considered significant. Error bars are +/- SD or +/- SEM as indicated in the figure legend. Statistics were generated using Graph Pad software v4.0c (Prism).

Appendix I:

The data presented in this publication was conducted in the laboratory of Dr. Michael Clare-Salzler during my tenure as a graduate student at the University of Florida. My contributions to this publication were; performed all FACS analysis, isolated PBMC, purified Treg, presented data as an oral presentation at the 8th Immunology of Diabetes Society, Hyogo, Japan, wrote manuscript. Dr. Abdoreza Davoodi-Semiromi performed western blotting analysis.

Appendix I:

The data presented in this publication was conducted in the laboratory of Dr. Michael Clare-Salzler during my tenure as a graduate student at the University of Florida. My contributions to this publication were; performed all FACS analysis, isolated PBMC, purified Treg, presented data as an oral presentation at the 8th Immunology of Diabetes Society, Hyogo, Japan, wrote manuscript. Dr. Abdoreza Davoodi-Semiromi performed western blotting analysis.

Upregulation of Foxp3 Expression in Mouse and Human Treg Is IL-2/STAT5 Dependent Implications for the NOD STAT5B Mutation in Diabetes Pathogenesis

MATTHEW R. MURAWSKI[a] , SALLY A. LITHERLAND[a] , MICHAEL J. CLARE-SALZLER[a] , AND ABDOREZA DAVOODI-SEMIROMI[a]

a Department of Pathology, Immunology and Laboratory Medicine, College of Medicine, University of Florida, Gainesville, Florida 32610, USA

Address for correspondence: Michael J. Clare-Salzler, M.D., Department of Pathology, Immunology and Laboratory Medicine, College of Medicine, University of Florida, 1600 SW Archer Road, Gainesville, FL 32610, USA. Voice: 352-392-9886; fax: 352-392-5393. e-mail: salzler@ufl.edu

KEYWORDS
natural regulatory T cell • Foxp3 • STAT5 • IL-2 • CD25

ABSTRACT

Abstract: Regulatory T cells (Treg), characterized as CD4+/CD25+hi T cells, are critical for sustaining and promoting immune tolerance. Treg are highly dependent on IL-2 and IL-2 signaling to maintain their numbers and function and interruption of this pathway promotes autoimmunity. The transcription factor, Foxp3, is also required for Treg function as defective Foxp3 promotos autoimmunity in both mice and humans. We previously reported a point mutation in the DNA-binding domain of the NOD STAT5B gene that limits DNA binding when compared to wild-type STAT5 mice. Based on the

presence of five STAT5B consensus sequences in the Foxp3 promotor, we hypothesized a critical linkage between IL-2 signaling/STAT5B and Foxp3 expression in Treg. Our data show IL-2 activates long-form (LF) STAT5 and sustains Foxp3 expression in Treg. In contrast, CD4+/CD25- T cells do not active LF STAT5 and do not express Foxp3 under the same conditions. In addition, blocking LF STAT5 activation with a Jak inhibitor (AG-490) significantly reduced Foxp3 expression in Treg. Examination of human Treg using flow cytometry and intracellular staining for Foxp3 expression likewise demonstrates that IL-2 maintains Foxp3 expression through LF STAT5 signaling. These studies reveal a critical link between IL-2 mediated JAK-STAT5 signaling and the maintenance of Foxp3 expression in Treg of mice and humans.
DIGITAL OBJECT IDENTIFIER (DOI)
10.1196/annals.1375.031 About DOI

INTRODUCTION

Natural regulatory T cells (Treg) (CD4+/CD25+hi) are generated in both the thymus and the periphery and are essential for the promotion of immune tolerance while preventing the onset of autoimmune disease.1–3 Treg express the alpha chain of interleukin (IL)-2 receptor (CD25) and are vitally dependent on exogenous IL-2 secreted from naïve and effector T cells (Teff) for maintenance in the periphery.4 This notion is supported by experiments that demonstrate depletion of IL-2 (IL-2KO) or the IL-2 receptor-signaling pathway (IL2α-/-, IL-2β-/-) ablates Treg in mice and leads to the development of autoimmune disease.5 Treatment of these mice with IL-2 restores Treg number and function.5 It is also known that the transcription factor, Foxp3, is critical for suppressor activity of Treg because mice lacking Foxp3 succumb to severe lymphoproliferative and autoimmune disease.6 Interestingly, Van Parijs and colleagues reported that STAT5 KO mice exhibited a loss of Treg and over expression of STAT5 in IL-2 KO mice restores Treg numbers in vivo.7 These findings demonstrate that Jak/STAT5 signaling is an essential component of murine Treg. We recently reported a novel point mutation in the DNA-binding domain in the STAT5B gene in NOD mice and demonstrated that mutated STAT5B has a weaker DNA-binding affinity when compared with normal C57BL/J6 mice.8 We hypothesize that this mutation may affect the maintenance of Foxp3 in murine Treg. Our data show the Jak/STAT5-signaling pathway is utilized to maintain Foxp3 expression and blockage of this pathway completely inhibited activation of STAT5 while significantly reducing Foxp3 expression in both mouse and human natural Treg.

MATERIALS AND METHODS

Mice

C57BL/6J (B6) mice were purchased from Jackson Laboratories and housed in our mouse colony facilities in the Department of Pathology, Immunology, and Laboratory Medicine, University of Florida. All mice used in these experiments were maintained in a specific pathogen-free environment and in accordance with the University of Florida institutional animal care and use committee (IACUC). All experiments were conducted on 4- to 6-week-old female mice.

Treg Purification

Murine CD4+/CD25+ T cells were purified from the spleens of three mice. Cell suspensions were made by passing tissue through a metal mesh grid followed by a passage through a 70-μM cell strainer (BD Biosciences, Bedford, MA). The cells were pelleted, resuspended in 30 mL of RPMI-1640, counted using a hemocytometer, and assessed for viability (viability >95% as judged by Trypan Blue staining). The CD4+/CD25+ T cells were separated using mouse CD4+/CD25+ Treg cell purification kit (Miltenyi Biotech, Auburn, CA) with an AutoMACS instrument according to manufacture's instructions (Miltenyi Biotech).

Cell Culture

The purified CD4+/CD25+ Treg were cultured in RPMI-1640 plus 10% FBS (Mediatech, Inc., Herndon, VA) and PSN antibiotics (Invitrogen Co., Carlsbad, CA). For Western blotting, at the end of culture, cells were washed twice in cold PBS, pelleted, and kept frozen at -80°C until analysis.

Western Blotting

A total number of 2.0 × 105 CD4+/CD25+ T cells were cultured in the presence or absence of cytokines and inhibitor and then lysed in Laemmli sample buffer (Biorad Laboratories, Hercules, CA). The protein was denatured for 5 min in boiling water and loaded onto a 10% Tris-HCl acrylamide gel (Biorad) followed by a 1 h transfer to polyvinylidene fluoride (PVFD) membrane (Amersham Biosciences Corp., Piscataway, NJ). Tyrosine-phosphorylated STAT5 was detected using anti-STAT5A/B antibody (Cat #05-495, Upstate) and pan-STAT5A/B antibody (Cat #SC-835 and #SC-836, Santa Cruz Biotech, Santa Cruz, CA). Mouse IL-2 (Cat #1271164, Roche Applied Sciences, Indianapolis, IN) was used to stimulate T cells at a concentration range of 5–100 U/mL. Anti-mouse Foxp3 antisera was a generous gift from Dr. Alexander Rudensky (Department of Medicine, Division of Rheumatology, University of Washington, Seattle, WA). AG490 (Calbiochem, La Jolla, CA) was preincubated with cell cultures for 30 min prior to lysis at 100 μM (lane 6–7) concentration.

PBMC Isolation

Whole blood was collected from healthy controls under Institutional Review Board (IRB) approval in our lab using venupuncture. Peripheral blood mononuclear cells (PBMC) were isolated from whole blood using Ficoll Paque (Amersham Biosciences Corp., Piscataway, NJ, USA) according to manufacturer protocol. PBMC were stained with anti-CD4 and anti-CD25 antibodies (BD Biosciences) in PBS with 2% FBS and sodium azide. After surface staining, cells were intracellular stained for Foxp3 using anti-Foxp3 monoclonal antibody (E-biosciences, clone #PCH101, San Diego, CA) according to manufacturer protocol. Cells were analyzed using four-color cytometric analysis (FacsCaliber™, BD Biosciences). Appropriate isotype controls were included for all antibodies. PBMC were cultured for 24 h in RPMI-1640 plus glutamine (Mediatech, Inc.) and PSN antibiotics (Invitrogen Co.). A 2% autologous serum was added at the beginning of culture. AG-490 was diluted in DMSO as per manufacturer specifications and added to cultures 30 min prior to IL-2 stimulation. A DMSO control was included and did not affect results (data not shown).

RESULTS

Table 1 shows the position of the STAT5 consensus-binding sequences located within the first three kilobases of the murine Foxp3 promotor region. Each site has been tested for binding activity using electromobility gel shift assays and all were found to be active in binding STAT5 in Treg (data not shown). In agreement with our previous observations, mutated STAT5B in NOD Treg had a threefold weaker DNA binding when compared with normal B6 Treg (ADS and MCS manuscript in preparation). This suggests IL-2/STAT5 signaling may directly regulate Foxp3 expression in Treg.

TABLE 1. The murine Foxp3 promotor contains five STAT5B consensus binding sequences:

Position	Consensus sequence	Strand
810–828	tttcgTTCcgaGAAgtggc	Negative
1007–1025	actgtTTCttaGAAgctgt	Negative
1124–1142	cctctTTCtgaGAAtgtac	Positive
1530–1548	cacggTTCtagGAAgccag	Positive
1717–1735	gtagcTTCtgaGAAcagcc	Negative

Note: A 3-kb region of the Foxp3 promotor from the initiation of the translation codon (ATG) was searched for the presence of STAT5B consensus sequences using Genomatics software (http://www.genomatix.de). The positions are listed and the conserved binding domain, TTC(N)3GAA, in the genomic DNA is shown for each position. Negative Strand = antisense strand; Positive strand = sense strand.

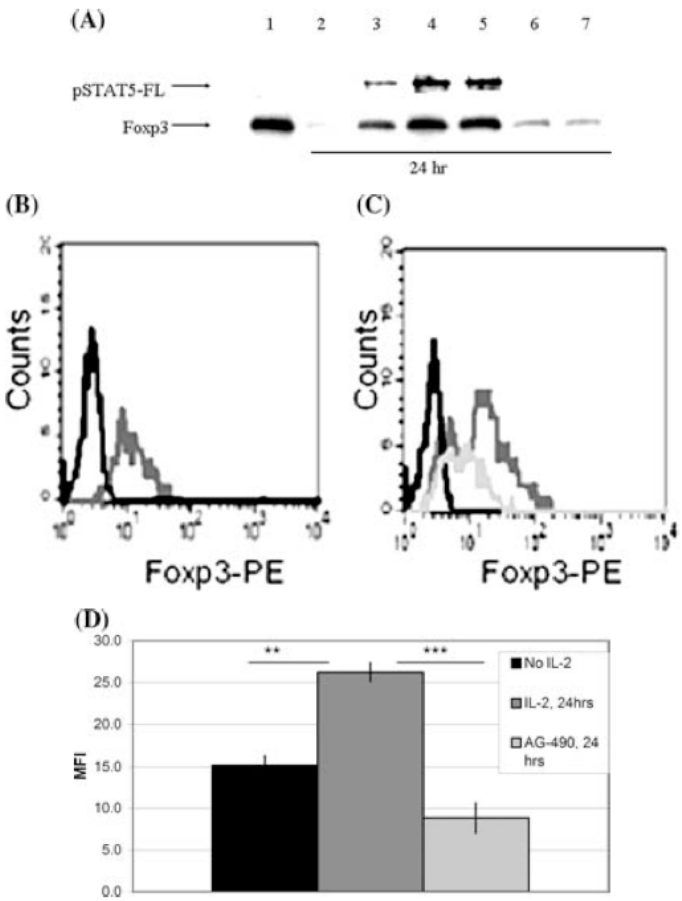

In Figure 1 A, we tested the hypothesis that IL-2/STAT5 signaling is important to maintain Foxp3 expression in murine Treg. In lane 1, freshly isolated Treg express Foxp3 and lack phosphorylated STAT5. In the absence of IL-2 for 24 h, Foxp3 expression is lost, suggesting that IL-2 is required for the maintenance of this transcription factor (lane 2). Culturing Treg in the presence of IL-2 not only maintains expression of Foxp3 but also promotes phosphorylation of LF-STAT5 (lane 3). In lanes 3–5, we demonstrate that increasing concentrations of IL-2 sustains Foxp3 expression and activates STAT5. However, culturing Treg in the presence of a selective Jak2/3 inhibitor (AG-490) and IL-2 abrogates STAT5 activation and substantially diminished the expression of Foxp3 in Treg (Fig. 1 A, lanes 6–7). We observed similar results in human Treg. As shown in Figure 1 B, freshly isolated human Treg express Foxp3 (dark gray histogram). In Figure 1 C, Foxp3 expression is upregulated by IL-2 stimulation (1000 U/mL) after 24 h, (dark gray histogram) and downregulated with the addition of AG-490 (100 μM) (light gray histogram). The isotype control for Foxp3 is shown in black for both histograms. Figure 1 D shows the statistical significance among groups (P= 0.002) using the ANOVA repeated measures (n= 3). Post hoc t-tests were used to assess significance between the groups (**= 0.001, ***= 0.0001).

FIGURE 1. (A) Murine regulatory T cells were examined via Western blot for expression of Foxp3 and FL-pSTAT5. Lane 1: freshly isolated cells without IL-2. Lane 2: cultured Treg without IL-2. Lanes 3–5: cultured Treg with different concentrations of IL-2 ranging from 5 to 100 U/mL. Lanes 6 and 7: Treg cultured with AG-490 (100 μM) in the presence of IL-2 (100 U/mL). This represents one of at least three independent experiments. (B) Human TREG were examined via flow cytometry for expression of Foxp3 using a PE-labeled monoclonal antibody. The isotype is shown in black and Foxp3 expression of freshly isolated Treg is shown in dark gray. This represents one of three independent experiments. (C) Human TREG examined via flow cytometry for expression of Foxp3 after 24 h in culture. The isotype is shown in black. Foxp3 expression after 24 h of IL-2 (1000 U/mL) stimulation is shown in dark gray. Foxp3 expression after 24 h of IL-2 (1000 U/mL) stimulation and AG-490 pretreatment (100 μM) is shown in light gray. This represents one of three independent experiments (D) Statistical significance of mean fluorescence intensity from B and C above. Error bars represent ± SD.

DISCUSSION

In this study, we attempt to identify how the IL-2 signaling pathway contributes to the maintenance of natural Treg. IL-2 has been shown to initiate a multitude of cellular events, specifically, augmentation and suppression of cytokine secretion by T lymphocytes and proliferation of naïve T cells.9 Recently, two independent studies demonstrate IL-2 is not directly required for Treg function, differentiation, or expansion of suppressor Treg in the thymus, but is required for the survival of mature Foxp3+ Treg.10,11 Our data support these findings and suggest that IL-2 signaling maintains Foxp3 expression in both murine and human Treg through the Jak/STAT5 pathway. We also demonstrate that blockade of the Jak/STAT5 pathway via AG-490, which selectively blocks Jak2/3, abrogates STAT5 activation and severely diminished Foxp3 expression. Thus, IL-2 binding to the high-affinity IL-2 receptor CD25 initiates a signaling cascade by which Foxp3 is maintained in Treg. Without IL-2, this signaling pathway is not activated and Foxp3 expression is lost, perhaps altering the suppressive capabilities of both murine and human Treg. We theorize that CD25 expression maintains Treg function even in environments of low IL-2 concentration, for example, immune homeostasis. Thus, Treg maintain Foxp3 in response to a wide spectrum of IL-2 concentrations, promoting suppression, and limiting the ability of Teff to proliferate in response to IL-2.

This study was supported by a research grant awarded to MCS (JDF 1-2004-690) and a transitional grant awarded to ADS (JDF10-2001-589) from the Juvenile Diabetes Research Foundation International (JDRFI).

REFERENCES

1. Sakaguchi , S. et al . 1995. Immunologic self-tolerance maintained by activated T cells expressing IL-2 receptor alpha-chains (CD25). Breakdown of a single mechanism of self-tolerance causes various autoimmune diseases. J. Immunol. 155 : 1151–1164. Links

2. Asano , M. et al . 1996. Autoimmune disease as a consequence of developmental abnormality of a T cell population. J. Exp. Med. 184 : 387–396. Links

3. Itoh , M. et al . 1999. Thymus and autoimmunity: production of CD25+CD4+ naturally anergic and suppressive T cells as a key function of the thymus in maintaining immunologic self-tolerance. J. Immunol. 162 : 5317–5326. Links

4. Thornton , A.M. E.M. Shevach . 1998. CD4+CD25+ immunoregulatory T cells suppress polyclonal T cell activation in vitro by inhibiting interleukin 2 production. J. Exp. Med. 188 : 287–296. Links

5. Malek , T.R. et al . 2002. CD4 regulatory T cells prevent lethal autoimmunity in IL-2Rβ-deficient mice. Implications for nonredundant function of IL-2. Immunity 17 : 167–178. Links

6. Fontenot , J.D. et al . 2003. Foxp3 programs the development and function of CD4+CD25+ T regulatory cells. Nat. Immunol. 4 : 330–336. Links

7. Van Parijs , L. et al . 2003. Essential role for STAT5 in CD25+CD4+ regulatory T cell homeostasis and the maintenance of self-tolerance. J. Immunol. 171 : 3435–3441. Links

8. Davoodi-Semiromi , A. et al . 2004. A mutant Stat5b with weaker DNA binding affinity defines a key defective pathway in nonobese diabetic mice. J. Biol. Chem. 12 : 11553–11561. Links

9. Malek , T.R. 2004. Tolerance, not immunity, crucially depends on IL-2. Nat. Rev. Immunol. 4 : 665–674. Links

10. Fontenot , J.D. et al . 2005. A function for interleukin 2 in Foxp3-expressing regulatory T cells. Nature Immunol. 11 : 1142–1151. Links

11. D'Cruz, L.M. 2005. Development and function of agonist-induced CD25+ Foxp3+ regulatory T cells in the absence of interleukin 2 signaling. Nature Immunol. 11 : 1152–1159. Links

References

1. **Aherne, W., T. Bird, S. D. Court, P. S. Gardner, and J. McQuillin.** 1970. Pathological changes in virus infections of the lower respiratory tract in children. J Clin Pathol **23:**7-18.
2. **Aikawa, T. S., S. Shimura, T. Sasaki, T. Takishima, H. Yaegashi, and T. Takahashi.** 1989. Morphometric analysis of intraluminal mucus in airways in chronic obstructive pulmonary disease. Am Rev Respir Dis **140:**477-482.
3. **Akira, S., S. Uematsu, and O. Takeuchi.** 2006. Pathogen recognition and innate immunity. Cell **124:**783-801.
4. **Alexander, D. J.** 2003. Newcastle Disease, p. 63-88. *In* Y. M. Saif, H. J. Barnes, A. M. Fadly, J. R. Glisson, L. R. McDougald, and D. E. Swayne (ed.), Diseases of poultry, 11 ed. Iowa State University Press, Ames.
5. **Alwan, W. H., F. M. Record, and P. J. Openshaw.** 1992. CD4+T cells clear virus but augment disease in mice infected with respiratory syncytial virus. Comparison with the effects of CD8+T cells. Clin. Exp. Immunol. **88:**527-536.
6. **American Academy of Pediatrics, c. o. i. d. a. c. o., and f. a. t. newborn.** 2003. Revised indications for the use of palivizumab and respiratory immune globulin intravenous for the prevention of respiratory syncytial virus infections. Pediatrics **112:**1442-1446.
7. **Anderson, L. J., P. Bingham, and J. C. Hierholzer.** 1988. Neutralization of respiratory syncytial virus by individual and mixtures of F and G protein monoclonal antibodies. J Virol **62:**4232-8.
8. **Applequist, S. E., R. P. Wallin, and H. G. Ljunggren.** 2002. Variable expression of Toll-like receptor in murine innate and adaptive immune cell lines. Int Immunol **14:**1065-74.
9. **Awomoyi, A. A., P. Rallabhandi, T. I. Pollin, E. Lorenz, M. B. Sztein, M. S. Boukhvalova, V. G. Hemming, J. C. Blanco, and S. N. Vogel.** 2007. Association of TLR4 polymorphisms with symptomatic respiratory syncytial virus infection in high-risk infants and young children. J Immunol **179:**3171-7.
10. **Barton, G. M., and R. Medzhitov.** 2002. Control of adaptive immune responses by Toll-like receptors. Curr Opin Immunol **14:**380-3.
11. **Bataki, E. L., G. S. Evans, and M. L. Everard.** 2005. Respiratory syncytial virus and neutrophil activation. Clin Exp Immunol **140:**470-7.
12. **Becker, Y.** 2006. Respiratory syncytial virus (RSV) evades the human adaptive immune system by skewing the Th1/Th2 cytokine balance toward increased levels of Th2 cytokines and IgE, markers of allergy--a review. Virus Genes **33:**235-52.
13. **Becker, Y.** 2006. Respiratory syncytial virus(RSV)-induced allergy may be controlled by IL-4 and CX3C fractalkine antagonists and CpG ODN as adjuvant: hypothesis and implications for treatment. Virus Genes **33:**253-64.
14. **Blyth, D. I., M. S. Pedrick, T. J. Savage, H. Bright, J. E. Beesley, and S. Sanjar.** 1998. Induction, duration, and resolution of airway goblet cell hyperplasia in a murine model of atopic asthma: effect of concurrent infection with respiratory syncytial virus and response to dexamethasone. Am J Respir Cell Mol Biol **19:**38-54.

15. **Blyth, D. I., M. S. Pedrick, T. J. Savage, E. M. Hessel, and D. Fattah.** 1996. Lung inflammation and epithelial changes in a murine model of atopic asthma. Am J Respir Cell Mol Biol **14:**425-438.
16. **Boukhvalova, M. S., G. A. Prince, L. Soroush, D. C. Harrigan, S. N. Vogel, and J. C. Blanco.** 2006. The TLR4 agonist, monophosphoryl lipid A, attenuates the cytokine storm associated with respiratory syncytial virus vaccine-enhanced disease. Vaccine **24:**5027-35.
17. **Briggs, J. A. G., T. Wilk, and S. D. Fuller.** 2003. Do lipid rafts mediate virus assembly and pseudotyping? J. Gen. Virol. **84:**757-768.
18. **Bukreyev, A., M. E. Serra, F. R. Laham, G. A. Melendi, S. R. Kleeberger, P. L. Collins, and F. P. Polack.** 2006. The cysteine-rich region and secreted form of the attachment G glycoprotein of respiratory syncytial virus enhance the cytotoxic T-lymphocyte response despite lacking major histocompatibility complex class I-restricted epitopes. J Virol **80:**5854-61.
19. **Bukreyev, A., L. Yang, J. Fricke, L. Cheng, J. M. Ward, B. R. Murphy, and P. L. Collins.** 2008. The secreted form of respiratory syncytial virus G glycoprotein helps the virus evade antibody-mediated restriction of replication by acting as an antigen decoy and through effects on Fc receptor-bearing leukocytes. J Virol **82:**12191-204.
20. **Buonaguro, L., L. Racioppi, M. L. Tornesello, C. Arra, M. L. Visciano, B. Biryahwaho, S. D. K. Sempala, G. Giraldo, and F. M. Buonaguro.** 2002. Induction of neutralizing antibodies and cytotoxic T lymphocytes in Balb/c mice immunized with virus-like particles presenting a gp120 molecule from a HIV-1 isolate of clade A. Antiviral Research **54:**189-201.
21. **Buonaguro, L., M. L. Tornesello, M. Tagliamonte, R. C. Gallo, L. X. Wang, R. Kamin-Lewis, S. Abdelwahab, G. K. Lewis, and F. M. Buonaguro.** 2006. Baculovirus-derived human immunodeficiency virus type 1 virus-like particles activate dendritic cells and induce ex vivo T-cell responses. J Virol **80:**9134-9143.
22. **Buonaguro, L., M. L. Visciano, M. L. Tornescello, M. Tagliamonte, B. Biryahwaho, and F. M. Guonaguro.** 2005. Induction of systemic and mucosal cross-clade neutralizing antibodies in BALB/c mice immunized with human immunodeficiency virus type 1 clade A virus-like particles administered by different routes of inoculation. Journal of Virology **79:**7059-7067.
23. **Byrd, L. G., and G. A. Prince.** 1997. Animal models of respiratory syncytial virus infection. Clin Infect Dis **25:**1363-8.
24. **Cannon, M. J., and C. R. Bangham.** 1989. Recognition of respiratory syncytial virus fusion protein by mouse cytotoxic T cell clones and a human cytotoxic T cell clone. J. Gen. Virol. **70:**79-87.
25. **Cannon, M. J., P. J. Openshaw, and B. A. Askonas.** 1988. Cytotoxic T cells clear virus but augment lung pathology in mice infected with respiratory syncytial virus. J Exp Med **168:**1163-8.

26. **Cannon, M. J., E. J. Stott, G. Taylor, and B. A. Askonas.** 1987. Clearance of persistent respiratory syncytial virus infections in immunodeficient mice following transfer of primed T cells. Immunology **62:**133-8.
27. **Chang, S., A. Dolganiuc, and G. Szabo.** 2007. Toll-like receptors 1 and 6 are involved in TLR2-mediated macrophage activation by hepatitis C virus core and NS3 proteins. J Leukoc Biol **82:**479-87.
28. **Collins, P. L., and J. E. J. Crowe.** 2007. Respiratory syncytial virus and metapneumovirus, p. 1601–1646. *In* P. M. H. In D. M. Knipe, D. E. and R. A. L. Griffin, M. A. Martin, B. Roizman, and S. E. Straus (ed.), (ed.), Fields virology, vol. 5th ed. Lippincott Williams & Wilkins, , Philadelphia, PA.
29. **Collins, P. L., and J. E. Crowe.** 2007. Respiratory syncytial virus and metapneumovirus, 5 ed, vol. 2. LippincottWilliams and Wilkins, Philadelphia.
30. **Collins, P. L., Y. T. Huang, and G. W. Wertz.** 1984. Nucleotide sequence of the gene encoding the fusion (F) glycoprotein of human respiratory syncytial virus. Proc Natl Acad Sci U S A **81:**7683-7.
31. **Collins, P. L., and G. Mottet.** 1992. Oligomerization and post-translational processing of glycoprotein G of human respiratory syncytial virus: altered O-glycosylation in the presence of brefeldin A. J Gen Virol **73 (Pt 4):**849-63.
32. **Compton, T., E. A. Kurt-Jones, K. W. Boehme, J. Belko, E. Latz, D. T. Golenbock, and R. W. Finberg.** 2003. Human cytomegalovirus activates inflammatory cytokine responses via CD14 and Toll-like receptor 2. J Virol **77:**4588-96.
33. **Connors, M.** 1992. Cotton rats previously immunized with a chimeric RSV FG glycoprotein develop enhanced pulmonary pathology when infected with RSV, a phenomenon not encountered following immunization with vaccinia-rSV recombinants or RSV. Vaccine **10:**475-484.
34. **Connors, M.** 1992. Pulmonary histopathology induced by respiratory synctial virus (RSV) challenge of formalin-inactivated RSV-immunized BALB/c mice is abrogated by depletion of CD4+T cells. J. Virol. **66:**7444-7451.
35. **Culley, F. J., A. M. Pennycook, J. S. Tregoning, T. Hussell, and P. J. Openshaw.** 2006. Differential chemokine expression following respiratory virus infection reflects Th1- or Th2-biased immunopathology. J Virol **80:**4521-7.
36. **Cyr, S. L., T. Jones, I. Stoica-Popescu, D. Burt, and B. J. Ward.** 2007. C57Bl/6 mice are protected from respiratory syncytial virus (RSV) challenge and IL-5 associated pulmonary eosinophilic infiltrates following intranasal immunization with Protollin-eRSV vaccine. Vaccine **25:**3228-32.
37. **De la Rosa, G. P., A. Monroy-Garcia, L. Mora-Garcia Mde, C. G. Pena, J. Hernandex-Montes, B. Weiss-Steider, and M. A. Lim.** 2009. An HPV 16 L1-based chimeric human papilloma virus-like particles containing a string of epitopes produced in plants is able to elicit humoral and cytoxic T cell activity in mice. Virol. J. **6:**2.
38. **De Silva, D. M., S. C. Fausch, J. S. Verbeek, and W. M. Kast.** 2007. Uptake of human papillomavirus virus-like particles by dendritic cells is mediated by

Fcgamma receptors and contributes to acquisition of T cell immunity. J. Immunol. **178:**7587-7597.

39. **De Swart, R. L., T. Kuiken, H. H. Timmerman, G. van Amerongen, G. G. Van Den Hoogen, H. W. Vos, H. J. Neijens, A. C. Andeweg, and A. D. Osterhaus.** 2002. Immunization of macaques with formalin-inactivated respiratory sncytial virus (RSV) induces interleukin-13 associated hypersensitivity to subsequent RSV infection. J. Virol. **76:**11561-11569.
40. **de Swart, R. L., B. G. van den Hoogen, T. Kuiken, S. Herfst, G. van Amerongen, S. Yuksel, L. Sprong, and A. D. Osterhaus.** 2007. Immunization of macaques with formalin-inactivated human metapneumovirus induces hypersensitivity to hMPV infection. Vaccine **25:**8518-28.
41. **Delgado, M. F., S. Coviello, A. C. Monsalvo, G. A. Melendi, J. Z. Hernandez, J. P. Batalle, L. Diaz, A. Trento, H. Y. Chang, W. Mitzner, J. Ravetch, J. A. Melero, P. M. Irusta, and F. P. Polack.** 2009. Lack of antibody affinity maturation due to poor Toll-like receptor stimulation leads to enhanced respiratory syncytial virus disease. Nat Med **15:**34-41.
42. **Demedts, I. K., K. R. Bracke, T. Maes, G. F. Joos, and G. G. Brusselle.** 2006. Different roles for human lung dendritic cell subsets in pulmonary immune defense mechanisms. Am J Respir Cell Mol Biol **35:**387-93.
43. **Dunnill, M. S., G. R. Massarella, and J. A. Anderson.** 1969. A comparison of the quantitative anatomy of the bronchi in normal subjects, in status asthmaticus, in chronic bronchitis, and in emphysema. Thorax **24:**176-179.
44. **Durbin, J. E., T. R. Johnson, R. K. Durbin, S. E. Mertz, R. A. Morotti, R. S. Peebles, and B. S. Graham.** 2002. The role of IFN in respiratory syncytial virus pathogenesis. J Immunol **168:**2944-52.
45. **Ehl, S., R. Bischoff, T. Ostler, S. Vallbracht, J. Schulte-Monting, A. Poltorak, and M. Freudenberg.** 2004. The role of Toll-like receptor 4 versus interleukin-12 in immunity to respiratory syncytial virus. Eur J Immunol **34:**1146-53.
46. **Faisca, P., D. B. Tran Anh, A. Thomas, and D. Desmecht.** 2006. Suppression of pattern-recognition receptor TLR4 sensing does not alter lung responses to pneumovirus infection. Microbes Infect **8:**621-7.
47. **Fan, C. F., and X. G. Mei.** 2005. Co-immunization of BALB/c mice with recombinant immunogens containing G protein fragment and chimeric CTL epitope of respiratory syncytial virus induces enhanced cellular immunity and high level of antibody response. Vaccine **23:**4453-4461.
48. **Fan, J., R. S. Frey, and A. B. Malik.** 2003. TLR4 signaling induces TLR2 expression in endothelial cells via neutrophil NADPH oxidase. J Clin Invest **112:**1234-43.
49. **Fisher, R. G., J. E. Johnson, S. B. Dillon, R. A. Parker, and B. S. Graham.** 1999. Prophylaxis with respiratory syncytial virus F-specific humanized monoclonal antibody delays and moderately suppressed the native antibody response but does not impair immunity to late rechallenge. J. Infect. Dis. **180:**708-713.

50. **Fritz, J. H., L. Le Bourhis, J. G. Magalhaes, and D. J. Philpott.** 2007. Innate immune recognition at the epithelial barrier drives adaptive immunity. Trends Immunol **29:**41-49.
51. **Fuentes, S., K. C. Tran, P. Luthra, M. N. Teng, and B. He.** 2007. Function of the respiratory syncytial virus small hydrophobic protein. J Virol **81:**8361-6.
52. **Garcia-Beato, R., I. Martinez, C. Franci, F. X. Real, B. Garcia-Barreno, and J. A. Melero.** 1996. Host cell effect upon glycosylation and antigenicity of human respiratory syncytial virus G glycoprotein. Virol **221:**301-309.
53. **Gatto, D., C. Ruedl, B. Odermatt, and M. F. Bachmann.** 2004. Rapid response of marginal zone B cells to viral particles. J Immunol **173:**4308-4316.
54. **Gias, E., S. U. Nielsen, L. A. Morgan, and G. L. Toms.** 2008. Purification of human respiratory syncytial virus by ultracentrifugation in iodixanol density gradient. J Virol Methods **147:**328-32.
55. **Gonzalez-Reyes, L., M. B. Ruiz-Arguello, B. Garcia-Barreno, L. Calder, J. A. Lopez, J. P. Albar, J. J. Skehel, D. C. Wiley, and J. A. Melero.** 2001. Cleavage of the human respiratory syncytial virus fusion protein at two distinct sites is required for activation of membrane fusion. Proc Natl Acad Sci U S A **98:**9859-64.
56. **Gorman, J. J., b. L. Ferguson, D. Speelman, and J. Mills.** 1997. Determination of the disulfide bond arrangement of human respiratory syncytial virus attachment (G) protein by matrix-assisted laser desorption/ionization time-of-flight mass spectrometry. Protein Sci **6:**1308-1315.
57. **Graham, B. S., L. A. Bunton, P. F. Wright, and D. T. Karzon.** 1991. Role of T lymphocyte subsets in the pathogenesis of primary infection and rechallenge with respiratory syncytial virus in mice. J Clin Invest **88:**1026-33.
58. **Graham, B. S., L. A. Bunton, P. F. Wright, and D. T. Karzon.** 1991. The role of T lymphocyte subsets in the pathogenesis of primary infection and rechallenge with respiratory syncytial virus. J. Clin. Invest **88:**1026-1033.
59. **Graham, B. S., T. R. Johnson, and R. S. Peebles.** 2000. Immune-mediated disease pathogenesis in respiratory syncytial virus infection. Immunopharmacology **48:**237-47.
60. **Gu, L., S. Tseng, R. M. Horner, C. Tam, M. Loda, and B. J. Rollins.** 2000. Control of TH2 polarization by the chemokine monocyte chemoattractant protein-1. Nature **404:**407-11.
61. **Haeberle, H. A., R. Takizawa, A. Casola, A. R. Brasier, H. J. Dieterich, N. Van Rooijen, Z. Gatalica, and R. P. Garofalo.** 2002. Respiratory syncytial virus-induced activation of nuclear factor-kappaB in the lung involves alveolar macrophages and toll-like receptor 4-dependent pathways. J Infect Dis **186:**1199-206.
62. **Hall, C. B., R. G. Douglas, Jr., K. C. Schnabel, and J. M. Geiman.** 1981. Infectivity of respiratory syncytial virus by various routes of inoculation. Infect Immun **33:**779-83.

63. **Hallak, L. K., P. L. Collins, W. Knudson, and M. E. Peeples.** 2000. Iduronic acid-containing glucosaminoglycans on target cells are required for efficient respiratory syncytial virus infection. Virology **271:**264-275.
64. **Hallak, L. K., D. Spillmann, and M. E. Peeples.** 2000. Glycosaminoglycan sulfation requirements for respiratory syncytial virus infection. Journal of Virology **74:**10508-10513.
65. **Hancock, G. E., D. J. Hahn, D. J. Speelman, S. W. Hildreth, S. Pillai, and K. McQueen.** 1994. The pulmonary immune response of Balb/c mice vaccinated with the fusion protein of respiratory syncytial virus. Vaccine **12:**267-74.
66. **Hancock, G. E., K. M. Heers, K. S. Pryharski, J. D. Smith, and L. Tiberio.** 2003. Adjuvants recognized by toll-like receptors inhibit the induction of polarized type 2 T cell responses by natural attachment (G) protein of respiratory syncytial virus. Vaccine **21:**4348-58.
67. **Hancock, G. E., D. J. Speelman, P. J. Frenchick, M. M. Mineo-Kuhn, R. B. Baggs, and D. J. Hahn.** 1995. Formulation of the purified fusion protein of respiratory syncytial virus with the saponin QS-21 induces protective immune responses in Balb/c mice that are similar to those generated by experimental infection. Vaccine **13:**391-400.
68. **Hancock, G. E., D. J. Speelman, K. Heers, E. Bortell, J. Smith, and C. Cosco.** 1996. Generation of atypical pulmonary inflammatory responses in BALB/c mice after immunization with the native attachment (G) glycoprotein of respiratory syncytial virus. J Virol **70:**7783-91.
69. **Harcourt, J., R. Alvarez, L. P. Jones, C. Henderson, L. J. Anderson, and R. A. Tripp.** 2006. Respiratory syncytial virus G protein and G protein CX3C motif adversely affect CX3CR1+ T cell responses. J Immunol **176:**1600-1608.
70. **Haynes, L. M., H. Caidi, G. U. Radu, C. Miao, J. L. Harcourt, R. A. Tripp, and L. J. Anderson.** 2009. Therapeutic Monoclonal Antibody Treatment Targeting Respiratory Syncytial Virus (RSV) G Protein Mediates Viral Clearance and Reduces the Pathogenesis of RSV Infection in BALB/c Mice. J Infect Dis.
71. **Haynes, L. M., D. D. Moore, E. A. Kurt-Jones, R. W. Finberg, L. J. Anderson, and R. A. Tripp.** 2001. Involvement of toll-like receptor 4 in innate immunity to respiratory syncytial virus. J Virol **75:**10730-7.
72. **Hendricks, D. A., K. McIntosh, and J. L. Patterson.** 1988. Further characterization of the soluble form of the G glycoprotein of respiratory syncytial virus. J Virol **62:**2228-33.
73. **Henrickson, K. J., S. Hoover, K. S. Kehl, and W. Hua.** 2004. National disease burden of respiratory viruses detected in children by polymerase chain reaction. Pediatr Infect Dis J **23:**S11-8.
74. **Iwasaki, A., and R. Medzhitov.** 2004. Toll like receptor control of adaptive immune responses. Nat Immunol **5:**987-995.
75. **Iwasaki, A., and R. Medzhitov.** 2004. Toll-like receptor control of the adaptive immune responses. Nat Immunol **5:**987-95.
76. **Janssen, R., J. Pennings, H. Hodemaekers, A. Buisman, M. van Oosten, L. de Rond, K. Ozturk, J. Dormans, T. Kimman, and B. Hoebee.** 2007. Host

transcription profiles upon primary respiratory syncytial virus infection. J Virol **81:**5958-67.

77. **Jennings, G. T., and M. F. Bachmann.** 2008. The coming of age of virus-like particles. Biol. Chem. **389:**521-536.
78. **Johnson, T. R., J. E. Johnson, S. R. Roberts, G. W. Wertz, R. A. Parker, and B. S. Graham.** 1998. Priming with secreted glycoprotein G of respiratory syncytial virus (RSV) augments interleukin-5 production and tissue eosinophilia after RSV challenge. J Virol **72:**2871-2880.
79. **Johnson, T. R., M. N. Teng, P. L. Collins, and B. S. Graham.** 2004. Respiratory syncytial virus (RSV) G glcoprotein is not necessary for vaccine-enhanced disease induced by immunization with formalin-inactivated RSV. J Virol **78:**6024-6032.
80. **Jones, A., J. M. Qui, E. Bataki, H. Elphick, S. Ritson, G. S. Evans, and M. L. Everard.** 2002. Neutrophil survival is prolonged in the airways of healthy infants and infants with RSV bronchiolitis. Eur Respir J **20:**651-7.
81. **Kahn, J. S., M. J. Schnell, L. Buonocore, and J. K. Rose.** 1999. Recombinant vesicular stomatitis virus expressing respiratory syncytial virus (RSV) glycoproteins: RSV fusion protein can mediate infection and cell fusion. Virology **254:**81-91.
82. **Kapikian, A. Z., R. H. Mitchell, R. M. Chanock, R. A. Shvedoff, and C. E. Stewart.** 1969. An epidemiologic study of altered clinical reactivity to respiratory syncytial (RS) virus infection in children previously vaccinated with an inactivated RS virus vaccine. Am J Epidemiol **89:**405-21.
83. **Kawai, T., and S. Akira.** 2006. Innate immune recognition of viral infection. Nat Immunol **7:**131-7.
84. **Kawai, T., and S. Akira.** 2007. TLR signaling. Semin Immunol **19:**24-32.
85. **Kim, H. W., and e. al.** 1969. Respiratory syncytial virus disease in infants despite prior administraion of antigenic inactivated vaccine. Am J Epidemiol **89:**422-434.
86. **Kim, H. W., J. G. Canchola, C. D. Brandt, G. Pyles, R. M. Chanock, K. Jensen, and R. H. Parrott.** 1969. Respiratory syncytial virus disease in infants despite prior administration of antigenic inactivated vaccine. Am J Epidemiol **89:**422-34.
87. **Kong, X., H. San Juan, M. Kumar, A. K. Behera, A. Mohapatra, G. R. Hellermann, S. Mane, R. F. Lockey, and S. S. Mohapatra.** 2003. Respiratory syncytial virus infection activates STAT signaling in human epithelial cells. Biochem Biophys Res Commun **306:**616-22.
88. **Kubach, J., C. Becker, E. Schmitt, K. Steinbrink, E. Huter, A. Tuettenberg, and H. Jonuleit.** 2005. Dendritic cells: sentinels of immunity and tolerance. Int J Hematol **81:**197-203.
89. **Kurt-Jones, E. A., M. Chan, S. Zhou, J. Wang, G. Reed, R. Bronson, M. M. Arnold, D. M. Knipe, and R. W. Finberg.** 2004. Herpes simplex virus 1 interaction with Toll-like receptor 2 contributes to lethal encephalitis. Proc Natl Acad Sci U S A **101:**1315-20.

90. **Kurt-Jones, E. A., L. Popova, L. Kwinn, L. M. Haynes, L. P. Jones, R. A. Tripp, E. E. Walsh, M. W. Freeman, D. T. Golenbock, L. J. Anderson, and R. W. Finberg.** 2000. Pattern recognition receptors TLR4 and CD14 mediate response to respiratory syncytial virus. Nat Immunol **1:**398-401.
91. **Laliberte, J. P., L. W. McGinnes, M. E. Peeples, and T. G. Morrison.** 2006. Integrity of membrane lipid rafts is necessary for the ordered assembly and release of infectious Newcastle disease virus particles. J Virol **80:**10652-10662.
92. **Langedijk, J. P., B. L. de Groot, H. J. Berendsen, and J. T. van Oirschot.** 1998. Structural homology of the central conserved region of the attachment protein G of respiratory syncytial virus with the fourth subdomain of 55-kDa tumor necrosis factor receptor. Virology **243:**293-302.
93. **Lanzavecchia, A., and F. Sallusto.** 2007. Toll-like receptors and innate immunity in B-cell activation and antibody responses. Current Opinion in Immunology **19:**268-274.
94. **Lechmann, M., J. Satoi, J. Vergalla, K. Murata, T. F. Baumert, and T. J. Liang.** 2001. Hepatitis C virus-like particles induce virus-specific humoral and cellular immune responses in mice. Hepatology **34:**417-423.
95. **Lee, A. H., J. H. Hong, and Y. S. Seo.** 2000. Tumour necrosis factor-alpha and interferon-gamma synergistically activate the RANTES promoter through nuclear factor kappaB and interferon regulatory factor 1 (IRF-1) transcription factors. Biochem J **350 Pt 1:**131-8.
96. **Levine, S., R. Klaiber-Franco, and P. R. Paradiso.** 1987. Demonstration that glycoprotein G is the attachment protein of respiratory syncytial virus. J Gen Virol **68 (Pt 9):**2521-4.
97. **Lichtenstein, D. L., S. R. Roberts, G. W. Wertz, and L. A. Ball.** 1996. Definition and functional analysis of the signal/anchor domain of the human respiratory syncytial virus glycoprotein G. J Gen Virol **77 (Pt 1):**109-18.
98. **Ling, Z., K. C. Tran, and M. N. Teng.** 2009. Human respiratory syncytial virus nonstructural protein NS2 antagonizes the activation of beta interferon transcription by interacting with RIG-I. J Virol **83:**3734-42.
99. **Littel-van den Hurk, S. D., J. W. Mapletoft, N. Arsic, and J. Kovacs-Nolan.** 2007. Immunopathology of RSV infection: prospects for developing vaccines without this complication. Rev Med. Virol. **17:**5-34.
100. **Liu, P., M. Jamaluddin, K. Li, R. P. Garofalo, A. Casola, and A. R. Brasier.** 2007. Retinoic acid-inducible gene I mediates early antiviral response and Toll-like receptor 3 expression in respiratory syncytial virus-infected airway epithelial cells. J Virol **81:**1401-11.
101. **Liu, X. S., W. J. Liu, K. N. Zhao, Y. H. Liu, G. Leggatt, and I. H. Frazer.** 2002. Route of administration of chimeric BPV1 VLP determines the character of the induced immune responses. Immunol Cell Biol **80:**21-29.

102. **Lo, M. S., R. M. Brazas, and M. J. Holtzman.** 2005. Respiratory syncytial virus nonstructural proteins NS1 and NS2 mediate inhibition of Stat2 expression and alpha/beta interferon responsiveness. J Virol **79:**9315-9.
103. **Lukacs, N. W., M. L. Moore, B. d. Rudd, A. A. Berlin, R. D. Collins, S. J. Olson, S. B. Ho, and R. S. Peebles.** 2006. Differential immune responses and pulmonary pathophysiology are induced by two diffferent strains of respiratory syncytial virus. Am J Pathol **169**.
104. **Matsuda, K., H. Tsutsumi, S. Sone, Y. Yoto, K. Oya, Y. Okamoto, P. L. Ogra, and S. Chiba.** 1996. Characteristics of IL-6 and TNF-alpha production by respiratory syncytial virus-infected macrophages in the neonate. J Med Virol **48:**199-203.
105. **Matsukawa, A., C. M. Hogaboam, N. W. Lukacs, P. M. Lincoln, R. M. Strieter, and S. L. Kunkel.** 1999. Endogenous monocyte chemoattractant protein-1 (MCP-1) protects mice in a model of acute septic peritonitis: cross-talk between MCP-1 and leukotriene B4. J Immunol **163:**6148-54.
106. **McGinnes, L., A. Wilde, and T. Morrison.** 1987. Nucleotide sequence of the gene encoding the Newcastle disease virus hemagglutinin-neuraminidase protein and comparisons of paramyxovirus hemagglutinin-neuraminidase sequences. Virus Res **7:**187-202.
107. **McGinnes, L. W., K. Gravel, and T. G. Morrison.** 2002. The NDV HN protein alters the conformation of F protein at cell surfaces. J Virol **73:**12622-12633.
108. **McGinnes, L. W., and T. G. Morrison.** 2006. Inhibition of receptor binding stabilizes Newcastle disease virus HN and F protein containing complexes. J Virol **80:**2894-2903.
109. **McGinnes, L. W., J. N. Reitter, K. Gravel, and T. G. Morrison.** 2003. Evidence for mixed membrane topology of the Newcastle disease virus fusion protein. J Virol **77:**1951-1963.
110. **Megiovanni, A. M., F. Sanchez, M. Robledo-Sarmiento, C. Morel, J. C. Gluckman, and S. Boudaly.** 2006. Polymorphonuclear neutrophils deliver activation signals and antigenic molecules to dendritic cells: a new link between leukocytes upstream of T lymphocytes. J Leukoc Biol **79:**977-88.
111. **Mekseepralard, C., G. L. Toms, and E. G. Routledge.** 2006. Protection of mice against Human respiratory syncytial virus by wild-type and aglycosyl mouse-human chimaeric IgG antibodies to subgroup-conserved epitopes on the G glycoprotein. J Gen Virol **87:**1267-73.
112. **Melero, J. A., B. Garcia-Barreno, I. Martinez, C. R. Pringle, and P. A. Cane.** 1997. Antigenic structure, evolution and immunobiology of human respiratory syncytial virus attachment (G) protein. J Gen Virol **78:**2411-2418.
113. **Miao, C., G. U. Radu, H. Caidi, R. A. Tripp, L. J. Anderson, and L. M. Haynes.** 2009. Treatment with respiratory syncytial virus G glycoprotein monoclonal antibody or F(ab')2 components mediates reduced pulmonary inflammation in mice. J Gen Virol **90:**1119-23.
114. **Mok, H., S. Lee, T. J. Utley, B. E. Shepherd, V. V. Polosukhin, M. L. Collier, N. L. Davis, R. E. Johnson, and J. E. Crowe.** 2007. Venezuelan equine

encephalitis virus replicon particles encoding respiratory syncytial virus surface glycoproteins induce protective mucosal responses in mice and cotton rats. J Virol **81:**13710-13722.

115. **Moore, E. C., J. Barber, and R. A. Tripp.** 2008. Respiratory syncytial virus (RSV) attachment and nonstructural proteins modify the type I interferon response associated with suppressor of cytokine signaling (SOCS) proteins and IFN-stimulated gene-15 (ISG15). Virol J **5:**116.
116. **Moron, V. G., P. Rueda, C. Sedlik, and C. Leclerc.** 2003. In vivo, dendritic cells can cross-present virus-like particles using an endosome-to-cytosol pathway. J Immunol **171:**2242-2250.
117. **Munir, S., C. Le Nouen, C. Luongo, U. J. Buchholz, P. L. Collins, and A. Bukreyev.** 2008. Nonstructural proteins 1 and 2 of respiratory syncytial virus suppress maturation of human dendritic cells. J Virol **82:**8780-96.
118. **Murawski, M. R., G. N. Bowen, A. M. Cerny, L. J. Anderson, L. M. Haynes, R. A. Tripp, E. A. Kurt-Jones, and R. W. Finberg.** 2008. Respiratory syncytial virus activates innate immunity through Toll-like receptor 2. J. Virol. **83:**1492-1500.
119. **Murphy, B. R., A. V. Sotnikov, L. A. Lawrence, S. M. Banks, and G. A. Prince.** 1990. Enhanced pulmonary histopathology is observed in cotton rats immunized with formalin-inactivated respiratory syncytial virus (RSV) or purified F glycoprotein and challenged with RSV 3-6 months after immunization. Vaccine **8:**497-502.
120. **Neilson, K. A., and E. J. Yunis.** 1990. Demonstration of respiratory syncytial virus in an autopsy series. Pediatr Pathol **10:**491-502.
121. **Noad, R., and P. Roy.** 2003. Virus-like particles as immunogens. Trends in Microbiology **11:**438-444.
122. **Ogra, P. L.** 2004. Respiratory syncytial virus: the virus, the disease and the immune response. Paediatr Respir Rev **5 Suppl A:**S119-26.
123. **Olson, M. R., and S. M. Varga.** 2007. CD8 T cells inhibit respiratory syncytial virus (RSV) vaccine-enhanced disease. J Immunol **179:**5415-24.
124. **Openshaw, P. J., S. L. Clarke, and F. M. Record.** 1992. Pulmonary eosinophilic response to respiratory syncytial virus infection in mice sensitized to the major surface glycoprotein G. Int Immunol **4:**493-500.
125. **Openshaw, P. J., F. J. Culley, and W. Olszewska.** 2001. Immunopathogenesis of vaccine-enhanced RSV disease. Vaccine **20 suppl 1:**S27-31.
126. **Paliard, X., Y. Liu, R. Wagner, H. Wold, J. Beanziger, and C. M. Walker.** 2000. Priming of strong, broad, and long-lived HIV type 1 p55 gag-specific CD8+ cytotoxic T cells after administration of a virus-like particle vaccine in rhesis macaques. AIDS Res Hum Retroviruses **16:**273-282.
127. **Pantua, H. D., L. W. McGinnes, M. E. Peeples, and T. G. Morrison.** 2006. Requirements for the assembly and release of Newcastle disease virus-like particles. J Virol **80:**11062-11073.
128. **Parnes, C., R. Guillermin, R. Habersang, P. Nicholas, V. Chawla, T. Kelly, J. Fishbein, and others.** 2003. Palivizumab prophylaxis of respiratory syncytial

virus disease in 2000-2001: results from the Palivizumab outcomes registry. Pediatr. Pulmonol. **35:**484-489.

129. **Pasare, C., and R. Medzhitov.** 2005. Control of B-cell responses by Toll-like receptors. Nature **438:**364-368.
130. **Peebles, R. S., Jr., and B. S. Graham.** 2005. Pathogenesis of respiratory syncytial virus infection in the murine model. Proc Am Thorac Soc **2:**110-5.
131. **Peebles, R. S., Jr., J. R. Sheller, R. D. Collins, K. Jarzecka, D. B. Mitchell, and B. S. Graham.** 2000. Respiratory syncytial virus (RSV)-induced airway hyperresponsiveness in allergically sensitized mice is inhibited by live RSV and exacerbated by formalin-inactivated RSV. J Infect Dis **182:**671-7.
132. **Pemberton, R. M., J. Cannon, P. J. Openshaw, L. A. Ball, G. W. Wertz, and B. A. Askonas.** 1987. Cytotoxic T cell specificity for respiratory syncytial virus proteins: fusion protein is an important target antigen. J. Gen. Virol. **68:**2177-2182.
133. **Pnnnuraj, E. M., A. R. Hayward, A. Raj, H. Wilson, and E. A. Simones.** 2001. Increased replication of respiratory syncytial virus (RSV) in pulmonary infiltrates is associated with enhance histopathological disease in bonnet monkeys (Macaca radiata) pre-immunized with a formalin-inactivated RSV vaccine. J Gen Virol **82:**2663-2674.
134. **Polack, F. P., P. M. Irusta, S. J. Hoffman, M. P. Schiatti, G. A. Melendi, M. F. Delgado, F. R. Laham, B. Thumar, R. M. Hendry, J. A. Melero, R. A. Karron, P. L. Collins, and S. R. Kleeberger.** 2005. The cysteine-rich region of respiratory syncytial virus attachment protein inhibits innate immunity elicited by the virus and endotoxin. Proc Natl Acad Sci U S A **102:**8996-9001.
135. **Prince, G. A., S. J. Curtis, K. C. Yim, and D. D. Porter.** 2001. Vaccine-enhanced respiratory syncytial virus disease in cotton rats following immunization with Lot 100 or a newly prepared reference vaccine. J Gen Virol **82:**2881-2888.
136. **Puthothu, B., M. Krueger, J. Forster, and A. Heinzmann.** 2006. Association between severe respiratory syncytial virus infection and IL13/IL4 haplotypes. J Infect Dis **193:**438-41.
137. **Rassa, J. C., J. L. Meyers, Y. Zhang, R. Kudaravalli, and S. R. Ross.** 2002. Murine retroviruses activate B cells via interaction with toll-like receptor 4. Proc Natl Acad Sci U S A **99:**2281-6.
138. **Roberts, S. R., D. Lichtenstein, L. A. Ball, and G. W. Wertz.** 1994. The membrane-associated and secreted forms of the respiratory syncytial virus attachment glycoprotein G are synthesized from alternative initiation codons. J Virol **68:**4538-46.
139. **Roman, M., W. J. Calhoun, K. L. Hinton, L. F. Avendano, V. Simon, A. M. Escobar, A. Gaggero, and P. V. Diaz.** 1997. Respiratory syncytial virus infection in infants is associated with predominant Th-2-like response. Am J Respir Crit Care Med **156:**190-5.
140. **Rudd, B. D., M. A. Schaller, J. J. Smit, S. L. Kunkel, R. Neupane, L. Kelley, A. A. Berlin, and N. W. Lukacs.** 2007. MyD88-mediated instructive signals in

dendritic cells regulate pulmonary immune responses during respiratory virus infection. J Immunol **178:**5820-7.

141. **Rudd, B. D., J. J. Smit, R. A. Flavell, L. Alexopoulou, M. A. Schaller, A. Gruber, A. A. Berlin, and N. W. Lukacs.** 2006. Deletion of TLR3 alters the pulmonary immune environment and mucus production during respiratory syncytial virus infection. J Immunol **176:**1937-42.
142. **Schlender, J., V. Hornung, S. Finke, M. Gunthner-Biller, S. Marozin, K. Brzozka, S. Moghim, S. Endres, G. Hartmann, and K. K. Conzelmann.** 2005. Inhibition of toll-like receptor 7- and 9-mediated alpha/beta interferon production in human plasmacytoid dendritic cells by respiratory syncytial virus and measles virus. J Virol **79:**5507-15.
143. **Sedlik, C., a. Dridi, E. Deriaud, M. f. Saron, P. Rueda, J. Sarrasec, J. I. Casal, and C. Leclerc.** 1999. Intranasal delivery of recombinant parvovirus-like particles elicits cytotoxic T-cell and neutralizing antibody responses. J Virol **73:**2739-2744.
144. **Shay, D. K., R. C. Holman, R. D. Newman, L. L. Liu, J. W. Stout, and L. J. Anderson.** 1999. Bronchiolitis-associated hospitalizations among US children, 1980-1996. JAMA **282:**1440-6.
145. **Shiinoff, J. J., K. L. O'Brien, B. Thumar, J. B. Shaw, R. Reid, M. Hua, M. Santosham, and R. A. Karron.** 2008. Young infants can develop protective levels of neutralizing antibody after infection with respiratory syncytial virus. J. Infect. Dis. **198:**1007-1015.
146. **Shingai, M., M. Azuma, T. Ebihara, M. Sasai, K. Funami, M. Ayata, H. Ogura, H. Tsutsummi, M. Matsumoto, and T. Seya.** 2008. Soluble G protein of respiratory syncytial virus inhibits Toll-like receptor 3/4 mediated IFN-beta induction. Int Immunol **20:**1169-1180.
147. **Sigurs, N.** 2001. Epidemiologic and clinical evidence of a respiratory syncytial virus-reactive airway disease link. Am J Respir Crit Care Med **163:**S2-6.
148. **Sioud, M.** 2006. Innate sensing of self and non-self RNAs by Toll-like receptors. Trends Mol Med **12:**167-76.
149. **Smit, J. J., B. D. Rudd, and N. W. Lukacs.** 2006. Plasmacytoid dendritic cells inhibit pulmonary immunopathology and promote clearance of respiratory syncytial virus. J Exp Med **203:**1153-9.
150. **Spann, K. M., K. C. Tran, B. Chi, R. L. Rabin, and P. L. Collins.** 2004. Suppression of the induction of alpha, beta, and lambda interferons by the NS1 and NS2 proteins of human respiratory syncytial virus in human epithelial cells and macrophages [corrected]. J Virol **78:**4363-9.
151. **Spann, K. M., K. C. Tran, and P. L. Collins.** 2005. Effects of nonstructural proteins NS1 and NS2 of human respiratory syncytial virus on interferon regulatory factor 3, NF-kappaB, and proinflammatory cytokines. J Virol **79:**5353-62.
152. **Stark, J. M., S. A. McDowell, V. Koenigsknecht, D. R. Prows, J. E. Leikauf, A. M. Le Vine, and G. D. Leikauf.** 2002. Genetic susceptibility to respiratory syncytial virus infection in inbred mice. J Med Virol **67:**92-100.

153. **Stott, E. J., L. A. Ball, K. K. Young, J. Furze, and G. W. Wertz.** 1986. Human respiratory syncytial virus glycoprotein G expressed from a recombinant vaccinia virus vector protects mice against live-virus challenge. J Virol **60:**607-13.
154. **Sukkar, M. B., S. Xie, N. M. Khorasani, O. M. Kon, R. Stanbridge, R. Issa, and K. F. Chung.** 2006. Toll-like receptor 2, 3, and 4 expression and function in human airway smooth muscle. J Allergy Clin Immunol **118:**641-8.
155. **Suzuki, K., T. Suda, T. Naito, K. Ide, K. Chida, and H. Nakamura.** 2005. Impaired toll-like receptor 9 expression in alveolar macrophages with no sensitivity to CpG DNA. Am J Respir Crit Care Med **171:**707-13.
156. **Swenson, D. L., K. L. Warfield, D. L. Negley, A. Schmaljohn, M. J. Aman, and S. Bavari.** 2005. Virus-like particles exhibit potential as a pan-filovirus vaccine for both Ebola and Marburg virus infections. Vaccine **23:**3033-3042.
157. **Syed, M. M., N. K. Phulwani, and T. Kielian.** 2007. Tumor necrosis factor-alpha (TNF-alpha) regulates Toll-like receptor 2 (TLR2) expression in microglia. J Neurochem **103:**1461-71.
158. **Takeda, K., T. Kaisho, and S. Akira.** 2003. Toll-like receptors. Annu Rev Immunol **21:**335-76.
159. **Taylor, G., E. J. Stott, J. Furze, J. Ford, and P. Sopp.** 1992. Protective epitopes on the fusion protein of respiratory syncytial virus recognized by murine and bovine monoclonal antibodies. J. Gen. Virol. **73:**2217-2223.
160. **Taylor, G., E. J. Stott, M. Hughes, and A. P. Collins.** 1984. Respiratory syncytial virus infection in mice. Infect Immun **43:**649-55.
161. **Tekkanat, K. K., H. Maassab, A. Miller, A. A. Berlin, S. L. Kunkel, and N. W. Lukacs.** 2002. RANTES (CCL5) production during primary respiratory syncytial virus infection exacerbates airway disease. Eur J Immunol **32:**3276-84.
162. **Teng, M. N., and P. L. Collins.** 1998. Identification of respiratory syncytial virus proteins required for formation and passage of helper dependent infectious particles. J Virol **72:**5707-5716.
163. **Teng, M. N., S. S. Whitehead, and P. L. Collins.** 2001. Contribution of the respiratory syncytial virus G glycoprotein and its secreted and membrane-bound forms to virus replication in vitro and in vivo. Virology **289:**283-96.
164. **Thompson, W. W., D. K. Shay, E. Weintraub, L. Brammer, N. Cox, L. J. Anderson, and K. Fukuda.** 2003. Mortality associated with influenza and respiratory syncytial virus in the United States. JAMA **289:**179-86.
165. **Tulic, M. K., R. J. Hurrelbrink, C. M. Prele, I. A. Laing, J. W. Upham, P. Le Souef, P. D. Sly, and P. G. Holt.** 2007. TLR4 polymorphisms mediate impaired responses to respiratory syncytial virus and lipopolysaccharide. J Immunol **179:**132-40.
166. **van der Sluijs, K. F., L. van Elden, M. Nijhuis, R. Schuurman, S. Florquin, H. M. Jansen, R. Lutter, and T. van der Poll.** 2003. Toll-like receptor 4 is not involved in host defense against respiratory tract infection with Sendai virus. Immunol Lett **89:**201-6.
167. **Wang, S. Z., and K. D. Forsyth.** 2000. The interaction of neutrophils with respiratory epithelial cells in viral infection. Respirology **5:**1-10.

168. **Wang, S. Z., H. Xu, A. Wraith, J. J. Bowden, J. H. Alpers, and K. D. Forsyth.** 1998. Neutrophils induce damage to respiratory epithelial cells infected with respiratory syncytial virus. Eur Respir J **12:**612-8.
169. **Waris, M. E., C. Tsou, D. D. Erdman, S. R. Zaki, and L. J. Anderson.** 1996. Respiratory synctial virus infection in BALB/c mice previously immunized with formalin-inactivated virus induces enhanced pulmonary inflammatory response with a predominant Th2-like cytokine pattern. J Virol **70:**2852-60.
170. **Welliver, R. C.** 2003. Review of epidemiology and clinical risk factors for severe respiratory syncytial virus (RSV) infection. J Pediatr **143:**S112-7.
171. **Welliver, T. P., R. P. Garofalo, Y. Hosakote, K. H. Hintz, L. Avendano, K. Sanchez, L. Velozo, H. Jafri, S. Chavez-Bueno, P. L. Ogra, L. McKinney, J. L. Reed, and R. C. Welliver, Sr.** 2007. Severe human lower respiratory tract illness caused by respiratory syncytial virus and influenza virus is characterized by the absence of pulmonary cytotoxic lymphocyte responses. J Infect Dis **195:**1126-36.
172. **Wertz, G. W., P. L. Collins, Y. Huang, C. Gruber, S. Levine, and L. A. Ball.** 1985. Nucleotide sequence of the G protein of human respiratory syncytial virus reveals an unusual type of viral membrane. Proc Natl Acad Sci U S A **82:**4075-4079.
173. **Wertz, G. W., M. Krieger, and L. A. Ball.** 1989. Structure and cell surface maturation of the attachment glycoprotein of human respiratory syncytial virus in a cell line deficient in O glycosylation. J Virol **63:**4767-76.
174. **Wu, Q., R. J. Martin, S. Lafasto, B. J. Efaw, J. G. Rino, R. J. Harbeck, and H. W. Chu.** 2008. Toll-like Receptor 2 Down-regulation in Mouse Allergic Lungs Decreases Mycoplasma Clearance. Am J Respir Crit Care Med.
175. **Yamamoto, M., S. Sato, K. Mori, K. Hoshino, O. Takeuchi, K. Takeda, and S. Akira.** 2002. Cutting edge: a novel Toll/IL-1 receptor domain-containing adapter that preferentially activates the IFN-beta promoter in the Toll-like receptor signaling. J Immunol **169:**6668-72.
176. **Zhang, L., M. E. Peeples, R. C. Boucher, P. L. Collins, and R. J. Pickles.** 2002. Respiratory syncytial virus infection of human airway epithelial cells is polarized, specific to ciliated cells, and without obvious cytopathology. J Virol **76:**5654-66.
177. **Zhou, S., E. A. Kurt-Jones, L. Mandell, A. Cerny, M. Chan, D. T. Golenbock, and R. W. Finberg.** 2005. MyD88 is critical for the development of innate and adaptive immunity during acute lymphocytic choriomeningitis virus infection. Eur J Immunol **35:**822-30.
178. **Zhu, J., J. Martinez, X. Huang, and Y. Yang.** 2007. Innate immunity against vaccinia virus is mediated by TLR2 and requires TLR-independent production of IFN-beta. Blood **109:**619-25.
179. **Zimmer, G., M. Rohn, G. P. McGregor, M. Schemann, K. K. Conzelmann, and G. Herrler.** 2003. Virokinin, a bioactive peptide of the tachykinin family, is released from the fusion protein of bovine respiratory syncytial virus. J Biol Chem **278:**46854-61.